

October 25, 1996
B-B600-15828-ASI

Boeing Commercial Airplane Group
P.O. Box 3707
Seattle, WA 98124-2207

Mr. Tom Jacky, RE-60
National Transportation Safety Board
490 L'Enfant Plaza SW
Washington D.C. 20594

Subject: Derivation of Lateral and Directional Control Positions for the
USAir 737-300 Accident, N513AU near Pittsburgh, September 8,
1994

Dear Mr. Jacky:

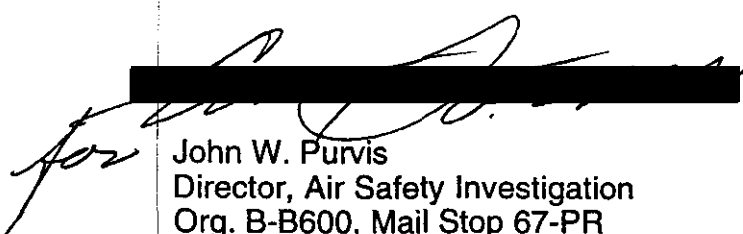
BOEING

In the course of the USAir 427 accident investigation, much emphasis has been placed on understanding the encounter with a Delta 727 wake and the subsequent response of the flight crew. As part of this investigation, a significant effort has been undertaken to understand wake behavior and wake effects on the 737 flight characteristics, as well as to understand specifically how the Delta 727 wake affected USAir 427. Initial estimates of USAir 427 lateral and directional control positions that accounted for the wake effects were presented at the NTSB all party meeting in Seattle in May 1995. Since that time the modelling techniques have been refined and validated using data from the 727/737 wake encounter flight test accomplished by the parties in September 1995.

The enclosed documentation presents the results of the analysis that followed that testing and provides a final estimate of the lateral and directional control positions for USAir 427. The video tape mentioned in the document will be hand carried and delivered during the meeting in Pittsburgh on October 31, 1996.

If you have any questions, please contact me.

Very truly yours,


[Redacted]
John W. Purvis
Director, Air Safety Investigation
Org. B-B600, Mail Stop 67-PR
Telex 32-9430. STA DIR PURVIS
[Redacted]

Enclosure: As noted

cc: Tom Haueter, AS-10
Keakini Kaulia- ALPA
Bob McCullough- USAir
Steve O'Neal- FAA

Table of Contents

Introduction	1
Flight Kinematics Analysis Process	1
Wake Encounter Derivation Process	2
Review of Previous Work	3
Overview of 727 / 737 Wake Encounter Flight Test	4
Flight Data Analysis	5
Wake Encounter Model Updates	6
Refinement of May 1995 Wake Encounter Scenario	7
Heading Interpolation Analysis	8
Resulting USAir 427 Lateral and Directional Control Positions	9
Synopsis of USAir 427 Wake Encounter Scenario	9
Conclusions	11
References	13
Appendix A. Chronology of Events Related to Derivation of Flight Controls for USAir 427 Accident Investigation.	A1
Appendix B. Description of the Wake Encounter Simulation Math Model	B1
Appendix C. Update to Simulator Rudder Hinge Moments and Aerodynamic Coefficients	C1
Appendix D. Validation of Wake Encounter Derivation Process	D1
Appendix E. Methodology for Correcting for the Effects of Low Sample Rate	E1
Appendix F. Parametric Study of Wake Position and Characteristics	F1
Appendix G. Parametric Study of Derived Rudder Input	G1

Introduction

In the course of the USAir 427 accident investigation, much emphasis has been placed on understanding the encounter with a Delta 727 wake and the subsequent response of the flight crew. As a part of this investigation, a significant effort has been undertaken to understand wake behavior and wake effects on 737 flight characteristics, as well as to understand specifically how the Delta 727 wake affected USAir 427. Initial estimates of USAir 427's lateral and directional control positions that accounted for wake effects were presented at the National Transportation Safety Board (NTSB) all-parties meeting in Seattle in May, 1995. Since that time the modeling techniques have been refined and validated using data from the 727 / 737 Wake Encounter Flight Test accomplished by the parties of the investigation in September 1995. This document presents the results of the analysis that followed that testing and provides a final estimate of the lateral and directional control positions for USAir 427.

Flight Kinematics Analysis Process

References 1 and 2 describe the work accomplished previously by the USAir 427 Performance Group towards the end of deriving as much information as possible about the accident from the Flight Data Recorder (FDR), including wake encounter effects and estimates for the unrecorded lateral and directional control surface positions. The work documented here is a continuation of the work described in these references using a flight-test-validated modeling of airplane response to a wake. A chronology of the entire FDR analysis history for the USAir 427 accident is presented in Appendix A.

Figure 1 presents an overview of the process used to derive the unrecorded lateral and directional control positions as a function of time. Starting with the basic 11 parameters recorded on the FDR, the data set was expanded by deriving angular rates and accelerations from the Euler angles and integrating the linear accelerations to determine a flight trajectory. Comparisons of derived data and measured speed and altitude data were performed to achieve a final converged solution, from which angle-of-attack and sideslip angle were derived. This process is described in detail in Reference 1.

The next step was to determine the total aerodynamic forces and moments which acted on the aircraft to result in the recorded trajectory; these were obtained from Newton's second law as applied to the derived and measured angular and linear accelerations. Next, the aerodynamic forces arising from known or derived effects (such as those due to angle-of-attack, sideslip, elevator position, throttle position, etc.) were computed using the 737-300 engineering simulator database. These effects were then subtracted from the total, leaving behind the sum of all unknown aerodynamic effects. These include the effects of wake turbulence, lateral and directional control surface deflections, FDR processing errors, possible structural damage and deficiencies in the simulator aerodynamics math model.

The magnitude of any FDR processing errors was shown to be very small at the $\bar{I}RU$ platform testing undertaken by the Performance Group in February of 1995 at the Honeywell facility in Clearwater, FL. Furthermore, the 737-300 engineering simulator aerodynamic math model is a proven, valid model of the aircraft with a very small magnitude of error in the aerodynamic data throughout the normal flight envelope, as demonstrated in Reference 3. Furthermore, this model was updated to an even higher degree of accuracy following flight testing performed in conjunction with the wake encounter testing. This work is described in a later section.

Thus, as noted in Reference 2, once the possibility of structural damage was eliminated only the effects of wake turbulence and the lateral and directional control surface positions were of a magnitude significant for further consideration.

Wake Encounter Derivation Process

Upon identifying the total effect of wake turbulence and lateral and directional control positions, it was postulated that if the wake effects could be independently determined and removed, the remaining unknown forces and moments would represent the unrecorded control positions. These wake effects would be calculated using a wake model developed by the Performance Group. A detailed description of this model is provided in Appendix B.

The method developed by the Performance Group to determine the wake encounter scenario for USAir 427 was based upon the understanding that wake-induced lift and pitch characteristics are closely coupled to wake-induced roll and yaw effects. Since the major inputs to the longitudinal axis (angle-of-attack, elevator position, flaps, gear, thrust and sideslip angle) are known for USAir 427 either by measurement or derivation from the FDR, their effects could be removed from the total longitudinal forces and moments; the remaining unknown longitudinal forces and moments are due to the wake and to the longitudinal effects of the unknown lateral and directional flight controls. Since the latter effects are small even for maximum lateral and directional control deflections, the remaining unknown forces and moments can be attributed almost entirely to the wake.

The working principle was to position the wake model relative to the USAir 427 derived flight path in such a way as to generate wake-induced lift and pitch signatures which matched as closely as possible those derived from the FDR data. In this way the corresponding rolling and yawing moments generated by the wake model would be representative of the wake-induced rolling and yawing moments which acted on USAir 427. These roll and yaw effects could then be removed from the total lateral and directional unknowns, and the remaining unknown lateral and directional forces and moments would then be the control effects.

Review of Previous Work

An initial attempt to isolate the control positions using the method described above is documented in detail in Reference 2. An overview of that analysis is presented here.

Figures 2, 3 and 4 present the May 1995 version of the derived USAir 427 wake scenario presented in Reference 2. At the time of this scenario's development the wake was assumed to follow a fairly straight, uniform path through space while maintaining an even separation of the cores. Figure 2 shows the Delta 727 flight path as it descended on a shallow glideslope, and the USAir 737 as it made a turn onto the heading of the 727 at the moment of intersecting the wake. From this it is clear that the 737 encountered the 727 wake nearly parallel to the cores. Figure 3 shows the simulator match of lift and pitch characteristics resulting from this wake encounter, and the corresponding rolling and yawing moments attributed to the wake.

Figure 4 shows the derived wheel and rudder inputs for this encounter, after the predicted wake rolling and yawing moments presented in Figure 3 were removed from the total unknown rolling and yawing moments derived from the FDR. In this case the wheel first deflects to the left, in the direction of the first roll upset at time 135, and then deflects back rapidly to the right. At the same time, left rudder deflects rapidly to the blowdown limit at time 136, holds level, then jumps again to the blowdown limit (now increased as a result of hinge moment relief due to sideslip angle) at time 141. Examination of the flight path in Figure 2 and the coefficients in Figure 3 provides insight into this anomalous behavior.

First, the rolling moment generated by the wake as placed was not sufficient to entirely account for the initial left roll response at time 134-135; therefore, some left wheel input was required. This occurred because in the envisioned encounter the 737 passed significantly below the right wake core during this time segment. Under the plausible assumption that the wake was completely responsible for the first roll upset at time 134, the 737 would have had to pass much closer to the right core to experience the required level of rolling moment. However, this would have also placed the 737 nearer to the *left* core at time 133, because it was assumed that the wake path was fairly straight and uniform. This would have generated a roll to the right from the left wake core around time 133 which was not evident on the FDR.

Similarly, the rudder derivation results from the fact that the yawing moment generated by the wake model during this scenario was a strong, sustained yaw to the right, opposing the measured direction of heading change. This yaw resulted because, in the scenario, the 737 passed over the right wake core from time 136-142. This location was a direct result of the assumption that the wake path was fairly straight and uniform.

At this location the theoretical model, which did not at the time account for wing, body or horizontal tail interference effects, induced a velocity field on the vertical tail which resulted in a nose-right yaw. However, the FDR data indicates that the 737 was yawing

to the left during this time segment. As a result, a strong left rudder was required in order to overcome the predicted nose-right wake yaw and match the flight path. As explained in the following sections, this nose-right yawing moment is not observed in the vicinity of the right wake core in actual wake encounters.

Since the time of this initial analysis, a flight test has been accomplished which has provided much valuable data on wake encounter characteristics. Thus, the analysis has been refined and repeated, using an updated wake encounter model validated with flight test data. The results of this analysis are discussed in the following sections.

Overview of 727 / 737 Wake Encounter Flight Test

Because of the heavy reliance on the wake encounter simulation to provide accurate predictions of wake behavior, it was deemed necessary to validate the wake model with flight test data and update the model as necessary. The NTSB thus tasked the USAir 427 Performance Group to carry out a flight test in which a 737-300 would be instrumented and flown into the wake of a 727 to quantitatively measure wake response characteristics.

The test was directed by the Performance Group, led by the NTSB, and involved participation by the Boeing Company, the Federal Aviation Administration (FAA), USAir Airlines, the Air Line Pilots Association (ALPA), and the National Aeronautics and Space Administration (NASA). The test was held at the FAA Technical Center in Atlantic City, NJ, in late September, 1995. The Performance Group developed and oversaw the test planning, instrumentation requirements and data reduction. The 737-300 test aircraft was provided by USAir, the wake-generating 727-100 was provided by the FAA, and the T-33 chase aircraft was provided by Boeing. Pilots from Boeing, the FAA, USAir and ALPA participated in flying the test maneuvers. NASA provided their OV-10 atmospheric data testbed aircraft to gather atmospheric data and to measure wake velocities. The 737 also flew a number of lateral-directional maneuvers for basic simulation validation, about 150 measured wake encounter responses, and an additional 50 wake encounters performed to gather sound signatures on the test Cockpit Voice Recorder (CVR).

The data were recorded simultaneously on a specialized FDR installed specifically for the test program and on a standard Boeing Portable Airborne Digital Data System (PADDS), an onboard data analysis station. Data reduction was performed initially on-site by downloading the FDR after each flight and processing the data into engineering units. Preliminary data conditioning, coefficient extraction and plotting were also performed on-site. Final data reduction was performed in Seattle, WA by Boeing. For the final data set, parameters from the FDR and PADDS systems were properly time-correlated and merged into a single coherent data set. Reference 4 provides a final list of the conditions.

Flight Data Analysis

The primary use of the data from the Wake Encounter Flight Test was to validate and update the 737-300 wake encounter simulation model. An update of the basic flaps I lateral-directional characteristics was also performed using the simulation validation maneuvers flown in Seattle before the wake encounter testing in Atlantic City. The validation showed that the basic model was very good in the normal flight envelope and only required some minor adjustments to the modeling of rudder hinge moments and high sideslip, high angle-of-attack aerodynamics. The changes resulting from these updates are presented in Appendix C.

Validation of the wake modeling began with the task of performing open loop simulator wake intercepts in a manner similar to those performed in flight, and then comparing the characteristics. Figures 5 and 6 present examples of the results. It can be seen that the wake-induced lift, roll and pitch characteristics were accurately predicted by the model. However, yawing moment characteristics were not modeled correctly. In the case where the 737 flew over the wake, the simulation predicted yawing moment responses which are absent in the flight test data. On the other hand, when the 737 flew just below the wake, the simulator did predict the yawing moment response measured in flight test, although to a lesser magnitude.

Additional validation was accomplished by performing closed-loop matches of several flight test wake encounters. This was done by observing video footage of the wake as it passed over the test aircraft, and then recreating the encounter in the simulation and driving the simulator controls with those from flight test. Figure 7 shows an example of the results. Again the simulator does a satisfactory job of predicting the wake lift, roll and pitch characteristics, but once again, the predicted yaw responses were not observed when the aircraft passed over the wake.

Close examination of the video for these and other cases in the flight test revealed that as the aircraft passed over or directly through the wake, the wake was disrupted by interference with the wing, body and horizontal tail, and thus did not produce any yawing moment. Only when the aircraft's vertical tail passed cleanly through the wake was a sharp yaw response recorded in the flight test data.

In addition, analysis was performed in correlating observed wake lift and wake rolling moment characteristics. Examination of the data showed that the location between the cores where the maximum lift loss occurs is a function of the airplane's bank angle; in other words, the maximum lift loss does not necessarily occur at the midpoint between the cores. As bank angle increases, the point for maximum lift loss occurs off center. Understanding this behavior was key in the ensuing wake analysis when attempting to place the wake to achieve maximum lift loss.

It was also noted that the maximum lift loss generally occurred at the point where rolling moment between the wake cores was close to zero. Peak rolling moments were observed to occur when the aircraft was just inside of each core.

Other effects attributable to wake encounters, such as rapid airspeed fluctuations and low level turbulence, were observed in abundance in the flight test data. Airspeed fluctuations were observed to occur before, during and after the wake encounter, leading to the understanding that this kind of fluctuation was somewhat random. Low level turbulence on the order of ± 0.1 g's was also noted, mostly when the aircraft was level with or slightly below the wake cores.

Besides the Crow instability and wake span characteristics described earlier, other wake characteristics were also noted. Wake core size appeared to be 2-3 ft in radius, though this may have only been the region where the smoke was concentrating near the center of the cores. Wake strength was calculated by estimating the velocity profile needed to generate the lift loss observed when the aircraft was level with and between the cores; these strength values tended to range from $800 \text{ ft}^2 / \text{sec}$ to $1500 \text{ ft}^2 / \text{sec}$. Numerous examples of vortex breakup and linking were observed as well in the video footage of the wake encounters.

Wake Encounter Model Updates

As noted above, during wake model validation testing, the yawing moment characteristics predicted for an airplane flying above or in the wake were not present in flight test. In flight test significant yawing moments were detected only when the wake core passed above the fuselage and cleanly impacted the vertical tail. In this case a substantial, short duration yaw spike was recorded. Figure 8 presents an example of this type of measurement. In all other cases measured yawing moment was essentially nonexistent.

As a result, it was necessary to update the simulation of yawing moment induced by the wake. The strip theory approach for the yawing moment calculations was set aside in favor of an empirical model based on flight test data. The empirical model was developed by careful observation of wake yawing moment as a function of vertical tail position relative to the wake cores (see Appendix B for description). The resulting model predicts yawing moment much more accurately, as shown in Figures 9 and 10 (which are repetitions of Figures 5 and 6 with the new tail yawing moment model added).

Furthermore, it became apparent during validation of the wake simulation that placing the wake relative to the aircraft CG in such a manner as to match lift characteristics made it nearly impossible to also consistently predict pitching moment characteristics. The cause of this incompatibility was believed to be the distortion introduced into the wake by the aircraft flow field. It was observed in flight test that the wake was shifted significantly when it passed over the wing and body of the airplane. However, the wake as modeled was still a straight line. The wake could be located relative to the wing to match lift

characteristics, but then the wake's location was fixed relative to the tail because it was assumed to be straight. Figure 11 demonstrates this situation.

To rectify this, a provision was made to locate the wake separately for the wing and the tail. Using this capability, the analysis strategy was expanded so that the wake would be located relative to the CG and wing in such a way as to match lift as closely as possible, and then the resulting wake roll effects would be considered representative of those experienced by USAir 427. Similarly, the wake would be independently located relative to the tail in such a way as to match pitching moment as closely as possible, and then the resulting wake yaw effects would be considered representative of those experienced by USAir 427. Figure 12 presents how this new model is implemented. The final exercise would be to "close the loop" by comparing the wake location relative to the CG to the wake location relative to the tail and determining that any differences are small enough to be accounted for by flow field distortion.

A final refinement to the model was the addition of the ability to vary the location of the cores along the wake path to model the Crow instability tendencies of a more mature wake.

Refinement of May 1995 Wake Encounter Scenario

The flight test and subsequent analysis of the resulting data has led to significant refining of the analysis. These refinements have led to changes in both the modeling methods and the analysis assumptions. Thus the analysis was repeated with the validated and updated simulation.

First, the Cockpit Voice Recorder (CVR) soundings taken during the flight testing confirmed that the "thump" recorded on the USAir 427 CVR at time 135.2 matched the noise profile of a wake core hitting the forward fuselage of the aircraft. Thus it was realized that the wake in the USAir accident scenario must be impacting the body of the airplane at that time, and that it could not be as far away from the fuselage as the previous analysis assumed.

Secondly, it became obvious early in the flight testing that the assumption that the wake would follow a straight and uniform path was inaccurate, especially in the case where the wake-generating aircraft was in a descent. Large fluctuations in the vertical position of the cores was noted, sometimes as much as 100 feet over short distances. This observation supported a hypothesis that the USAir aircraft may have initially passed beneath one of these fluctuations as the wake was rising, experiencing relatively little effect from the left wake core. The wake then dropped again in the manner observed in the testing, resulting in the right wake core impacting the fuselage at time 135.2 and producing the thump recorded on the CVR.

Figures 13, 14 and 15 present the current best wake scenario derived from the USAir 427 data. Figure 13 presents the wake location relative to the airplane CG in the same format

as Figure 2, showing the relative wake and aircraft trajectories throughout the encounter. Comparison of Figure 13 to Figure 2 shows the small but significant changes made to the wake path in order to match *lift* characteristics. This is the wake position relative to the wing and forward body, which results in most of the lift and rolling moment due to the wake.

Likewise, Figure 14 presents the wake location relative to the airplane empennage in the same format as Figure 2. Comparison of Figure 14 to Figure 2 shows the small but significant changes made to the wake path in order to match *pitch* characteristics. This is the wake position in the vicinity of the aft body, which is primarily responsible for the pitching and yawing moments due to the wake.

Figure 15 shows the final coefficient matches of lift and pitching moment that result from this encounter, and the resulting predictions of wake-induced rolling and yawing moments. Before presenting the manner in which these predicted coefficients affect the USAir 427 derived wheel and rudder inputs, it is necessary to discuss some additional kinematic analysis of the heading data which was done in parallel with the wake scenario derivation for the USAir 427 accident.

To validate the techniques described here, several wake encounters from the flight test were evaluated. This validation process is described in detail in Appendix D.

Heading Interpolation Analysis

During the course of the wake scenario development, a parallel effort was undertaken to eliminate signal noise generated by numerical processing techniques from the derivation of rudder position. Specifically, when the sample rate of heading data is below 2 samples-per-second (as in the case of USAir 427), the rudder position derived using kinematics becomes contaminated with an overlying “noise” signal produced by the digital filter used to process the data. This noise signal shows up as an oscillation in derived rudder, with a period of about 0.75 seconds and a peak-to-peak amplitude which can exceed ten degrees. The rudder position derivations presented in References 1 and 2 show ample evidence of this signal noise, in many cases exceeding the rudder blowdown limit.

In regions of a flight maneuver where rudder position is known or can be inferred (such as when the rudder is believed to be at its blowdown limit), it is possible to derive a continuous heading trace between the low-sample rate data points that are known from measurement. This heading trace accurately represents the airplane heading during the period of time where rudder position is known or can be inferred.

The process used to accomplish this is an iterative one. Starting with a linear interpolation of heading between the known data points, small modifications are made to the heading data between the known points and then rudder position is re-derived until the artificial oscillations in the derived rudder position are minimized around the known

or inferred rudder position. The following constraints are observed in the process of deriving the airplane heading trace:

- 1) ~~Only the interpolated regions between known, recorded data points may be~~ changed.
- 2) The resulting heading curve must be smooth and continuous and go through all the known, recorded data points.

The end result of this effort is an improved knowledge of the boundary conditions (i.e., characteristics) of the heading trace at the edges of the adjoining regions where rudder position is not known or cannot be inferred (e.g., when the airplane is in the influence of a wake). Applying these new boundary conditions under the above constraints to the USAir 427 data resulted in an improved representation of the airplane's heading from FDR time 133 to 140, when the airplane was in the influence of the wake. This new heading interpolation (presented in Figure 16) was then used, along with the derived wake-induced yawing moment presented in Figure 15, to derive a final, best estimate of rudder position. A more detailed description and validation of this methodology is presented in Appendix E.

Resulting USAir 427 Lateral and Directional Control Positions

Figure 17 presents the current best derivation of the USAir 427 lateral and directional control positions. The left side of Figure 17 presents the extracted rolling and yawing moment coefficients derived from the USAir 427 FDR using the latest interpolation of heading presented in Figure 16. The rolling and yawing moment coefficients due to the 727 wake, calculated using the wake model updated with the flight test data from the Atlantic City testing and presented in Figure 15, are also shown on the left side Figure 17. The right side of Figure 17 shows the wheel and rudder required to compensate for the difference in the coefficients extracted from the FDR and those produced by the 727 wake. These control positions represent the best estimate of rudder and wheel that can be derived from the available FDR data.

Two parametric studies were conducted to provide confidence in the derived solutions. A parametric study of the effects of varying wake position on the derived control positions is presented in Appendix F. In addition, a parametric study to demonstrate the effects of small changes in the derived rudder time history on the flight path is documented in Appendix G.

Synopsis of USAir 427 Wake Encounter Scenario

The derived wake encounter presented in Figures 13-15 and the resulting derived controls presented in Figure 17 represent the current best estimate of these data given the available FDR data set. As shown in Appendix D, the methods used to derive the data give accurate predictions of wheel and rudder position when applied to the wake encounter flight test data. Assuming the data in Figure 17 is accurate, it is possible to integrate this

derived data with the other kinematic parameters measured and derived from the FDR and hypothesize a scenario. Figures 18-20 present this integrated data set. The yaw damper command in Figure 20 was calculated based on body axes yaw rate derived from the FDR Euler angles.

The wake encounter began at time 132.5 with some low-level load factor fluctuations. At time 133 a jump in airspeed occurred as a result of pressure field changes on the pitot static sensors. At time 134 USAir 427 experienced a sharp left roll acceleration due to the wake, peaking at 20 deg/sec^2 , to which the autopilot responded with its full right roll authority of 25° of wheel. Moments later the wake core passed across the fuselage, causing the thumping sound recorded at time 135.2. At that point the crew put in full right wheel, overriding the autopilot and causing it to drop into the Control Wheel Steering (CWS) mode.

The large right wheel deflection was more than enough to overcome the wake's left roll influence, and the aircraft rolled back toward the right, experiencing a sharp right roll acceleration peaking at 35 deg/sec^2 . Nose-left rudder pedal was deflected briefly to about 3/4 of full travel in a direction to slow the large right roll acceleration, and then reduced to about 1/4 of full travel. During this time the right wheel input was also reduced significantly; both actions would be understandable responses to the large right roll acceleration. However, the aircraft was still in the influence of the right wake core, which, along with the left roll acceleration caused by the rudder-induced sideslip, began to roll the aircraft back to the left with a large acceleration peaking at nearly 40 deg/sec^2 .

At this point the wheel was put in again to full right, which would be a proper response to stop the left roll acceleration; at the same time, rudder deflection increased again to full nose-left. At time 136 the pitch attitude began to drop, and the crew began applying nose-up column in response. Another large right roll acceleration resulted, peaking at 40 deg/sec^2 . The right wheel was reduced again at time 139 in response to the large right roll acceleration, while full left rudder remained applied. The result was an increasing left roll, and the aircraft was now banked at nearly 40° left wing down.

The crew disconnected the autopilot, and wheel was again put in back to the right, at a slower rate than before. During this time interval, the crew continued to pull back on the column, resulting in an increase in load factor and in angle-of-attack. Wheel remained constant at about 2/3 of full authority for a few seconds, which at the recorded airspeed of 190 KCAS was about the right level required to balance the rolling moment generated by the rudder-induced sideslip. As a result of the positions of the wheel and rudder, the roll acceleration went to zero, but the wheel input was not large enough to cancel the established left roll rate of about 10 deg/sec . The aircraft continued to roll left until a time of about 143, when full right wheel was again applied, arresting the left roll.

The airplane was then balanced at a left bank angle of over 70° , and the column was near its aft limit. Angle-of-attack was approaching that for stall. At time 144 the column was pulled to its full aft limit; this in turn caused the aircraft to pitch up quickly through the

angle-of-attack for stick shaker and into stall. At this pitch rate the airplane entered stall before the slats, which were commanded to the gapped position by the autoslat system, could be fully extended. The control column was recorded to have remained near the full aft limit until just before impact. The stick shaker also continued until impact, indicating that the aircraft was stalled for the remainder of the maneuver.

As a result of the nose-left sideslip induced by the left rudder, the left wing stalled first, resulting in yet another left roll acceleration. The aircraft rolled further over to the left and pitched nose down to a nearly vertical attitude. It appears from the analysis that the control wheel probably remained at full right deflection, and rudder at full left deflection to the blowdown limit. However, the dynamic, post-stall nature of the aircraft motion after time 145 makes it difficult to be completely certain of the rudder and wheel positions after that time.

For additional clarity in presenting the scenario, a VHS video tape, which shows a computer-generated visual representation of the USAir 427 accident accompanies this document. The accident is seen from two different viewpoints. The representations of the flight path, aircraft orientation and instrument readings are based upon the aircraft's FDR; the captions and cockpit area sound recreations are based on the CVR transcript. The wake derived for the accident and presented in Figures 13-14 is highlighted over the time interval where it is considered to be known, and the effect of the airplane flow field in disrupting the wake has also been added. The motion of the elevator and control column represent the data recorded on the FDR; the motion of the lateral controls, the rudder, the control wheel and rudder pedals represent the position derived for the encounter and presented in Figure 17. The video also contains representations of the validation cases discussed in Appendix D.

Conclusions

The derivation of lateral and directional control positions in the USAir 427 accident is highly desired as information needed to help investigators understand the sequence of events that contributed to the accident. Because of the limited number of parameters on the FDR and the involvement of the wake turbulence, any derivation of the lateral and directional controls will not be precise.

However, the methods established and validated during this investigation for determining wake effects give accurate results, and the resulting extractions of the lateral and directional control positions for flight test validation cases agree well with the actual measured control positions. This validation provides confidence in the methods used to derive the lateral and directional controls for the USAir 427 accident.

The control positions derived and presented here provide the best approximation of the lateral and directional control inputs during the accident sequence, given the available data from the FDR. All the parties involved in the investigation are encouraged to examine the derived control positions and their correlation with the measured and derived

aircraft motion in order to better understand the role of the wake and the control \bar{s} system in the USAir 427 accident sequence.

REFERENCES

1. Boeing Letter B-U01B-15081-ASI, January 10, 1995
2. Boeing Letter B-U01B-15291-ASI, June 20, 1995
3. D6-37912, "Flight-Test-Resource and Simulator Validation Data for the 737-300 Flight Simulator", Revision NEW, July 1, 1992
4. Boeing Letter B-XK01-15405-ASI, November 1, 1995
5. D6-37908, "Aerodynamic Data and Control System Description for the 737-300 Flight Simulator", Revision C, January 30, 1992

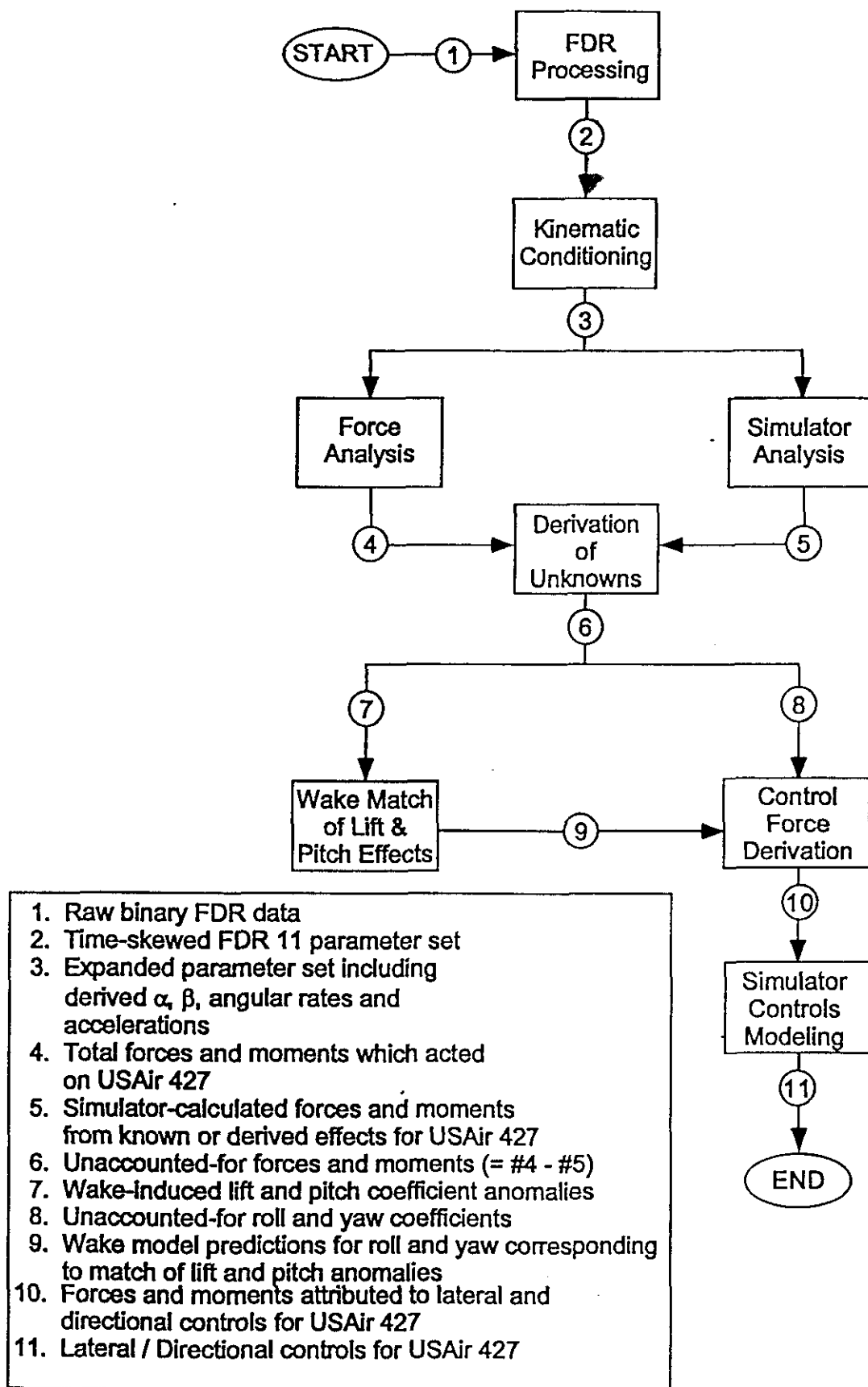


Figure 1. Process for Deriving Flight Control Positions for USAir 427 Accident from Flight Data Recorder Information

BOEING

WAKE LOCATION
DERIVED RELATIVE
TO THE C.G.

ESTIMATED USAIR 427 WAKE ENCOUNTER SCENARIO

MAY 1995 SCENARIO

ALTITUDE
(FT)

DISPLACEMENT
NORTH-SOUTH
(FT)

SIDE VIEW

TOP VIEW

ELAPSED TIME - SEC

WAKE FROM DAL1083

USAIR 427

USAIR 427

LEFT VORTEX CORE

RIGHT VORTEX CORE

DAL1083

MAY 1995 KINEMATIC ANALYSIS
ESTIMATED USAIR 427 WAKE ENCOUNTER
WAKE LOCATION RELATIVE TO AIRCRAFT CG

REV	CALC	CHECK	APPD	APPD
	J. Wilborn			
	17OCT96			
	REVISED	DATE		

731-300

FIGURE

PAGE 2

MAY 1995 WAKE SCENARIO

— EXTRACTED COEFFICIENTS FROM USAIR 427 FDR
 - - - WAKE ENCOUNTER SIMULATION COEFFICIENTS

LIFT
 COEFFICIENT

ROLLING
 MOMENT
 COEFFICIENT

LEFT WING DOWN

PITCHING
 MOMENT
 COEFFICIENT

YAWING
 MOMENT
 COEFFICIENT

NOSE LEFT

NOSE RIGHT

FDR TIME (SEC)

FDR TIME (SEC)

BOEING

MAY 1995 KINEMATIC ANALYSIS
 USAIR 427 EXTRACTED COEFFICIENTS
 VS. WAKE MODEL PREDICTED COEFFICIENTS

737-300
 FIGURE
 3

REV

PAGE

CALC	J. WILBORN	17OCT95
CHECK		
APPD		
APPD		
APPD		
REVISED		
DATE		

REV

PAGE

MAY 1995 WAKE SCENARIO

— EXTRACTED COEFFICIENTS FROM USAIR 427 FDR
- - - WAKE ENCOUNTER SIMULATION COEFFICIENTS
- - - DERIVED CONTROL POSITIONS

ROLLING
MOMENT
COEFFICIENT

LEFT WING DOWN

DERIVED
WHEEL
POSITION
(DEG)

LEFT WING DOWN

RIGHT WING DOWN

RIGHT WING DOWN

YAWING
MOMENT
COEFFICIENT

NOSE LEFT

DERIVED
RUDDER
POSITION
(DEG)

NOSE LEFT

NOSE RIGHT

NOSE RIGHT

FDR TIME (SEC)

FDR TIME (SEC)

MAY 1995 KINEMATIC ANALYSIS
USAIR 427 EXTRACTED VS PREDICTED
COEFFICIENTS AND DERIVED CONTROLS

737-300

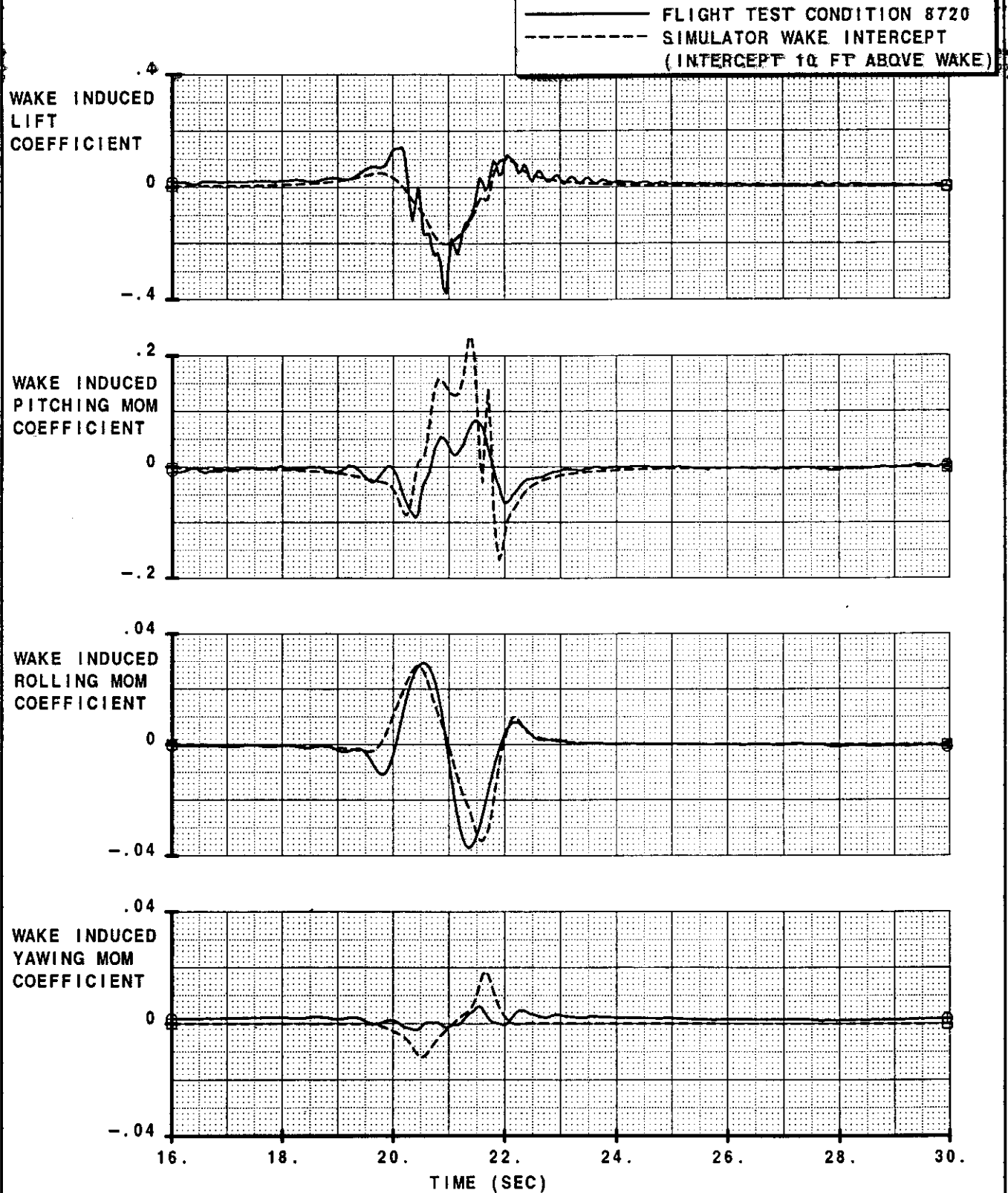
FIGURE

4

BOEING

**WAKE MODEL VALIDATION
INTERCEPT COMPARISON**

MAY 1995 WAKE
ENCOUNTER MODEL
(DBNEW26)



CALC	J. WILBORN	18OCT96	REVISED	DATE
CHECK				
APPD				
APPD				

WAKE ENCOUNTER FLIGHT TEST SEQ. NO. 8720
MAY 1995 WAKE ENCOUNTER MODEL (DBNEW26)
FLIGHT-TO-SIMULATOR COMPARISON

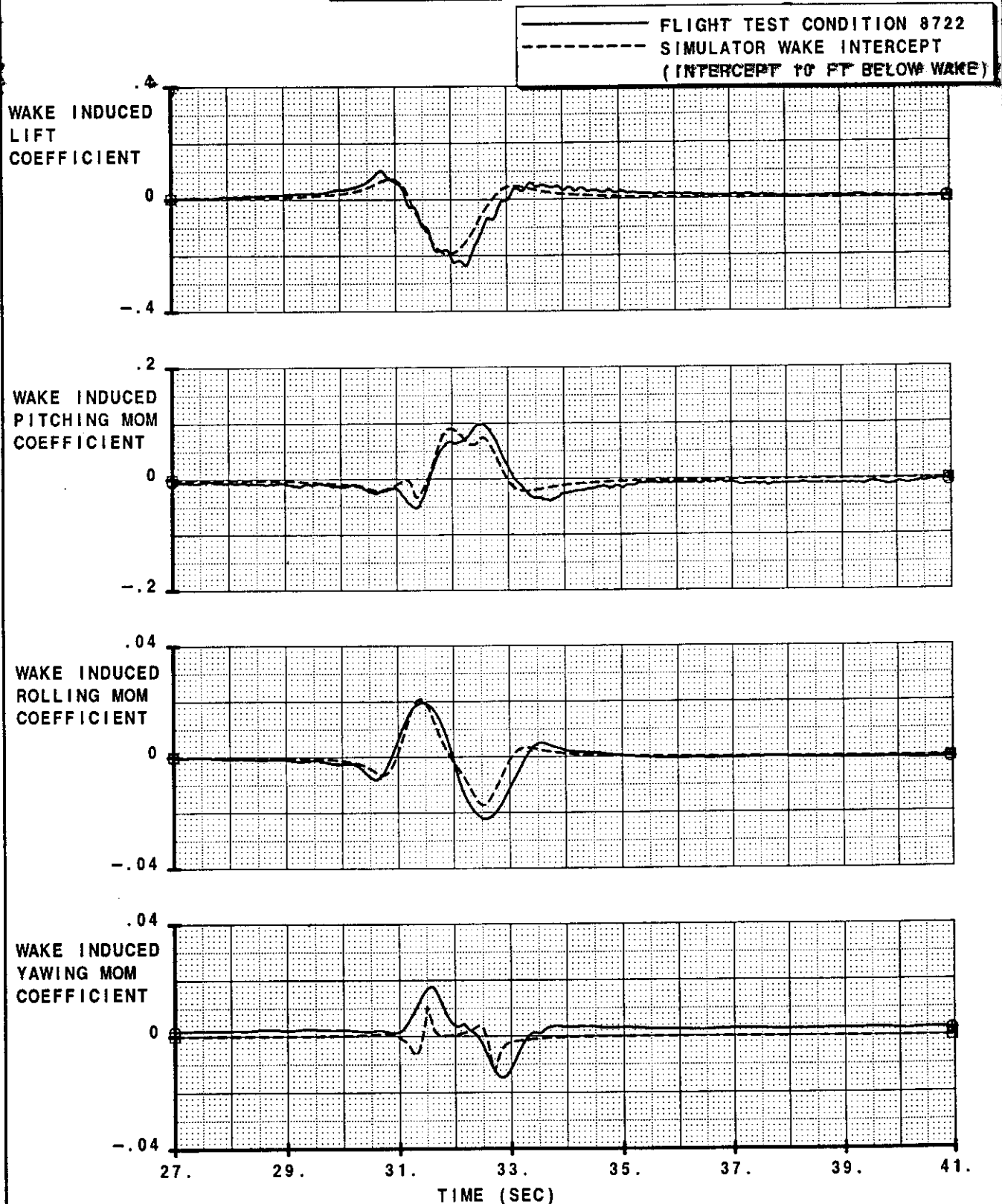
PP053

FIGURE

5

**WAKE MODEL VALIDATION
INTERCEPT COMPARISON**

MAY 1995 WAKE
ENCOUNTER MODEL
(DBNEW26)



CALC	J. WILBORN	18OCT96	REVISED	DATE
CHECK				
APPD				
APPD				
DEV				

WAKE ENCOUNTER FLIGHT TEST SEQ. NO 8722
MAY 1995 WAKE ENCOUNTER MODEL (DBNEW26)
FLIGHT-TO-SIMULATOR COMPARISON

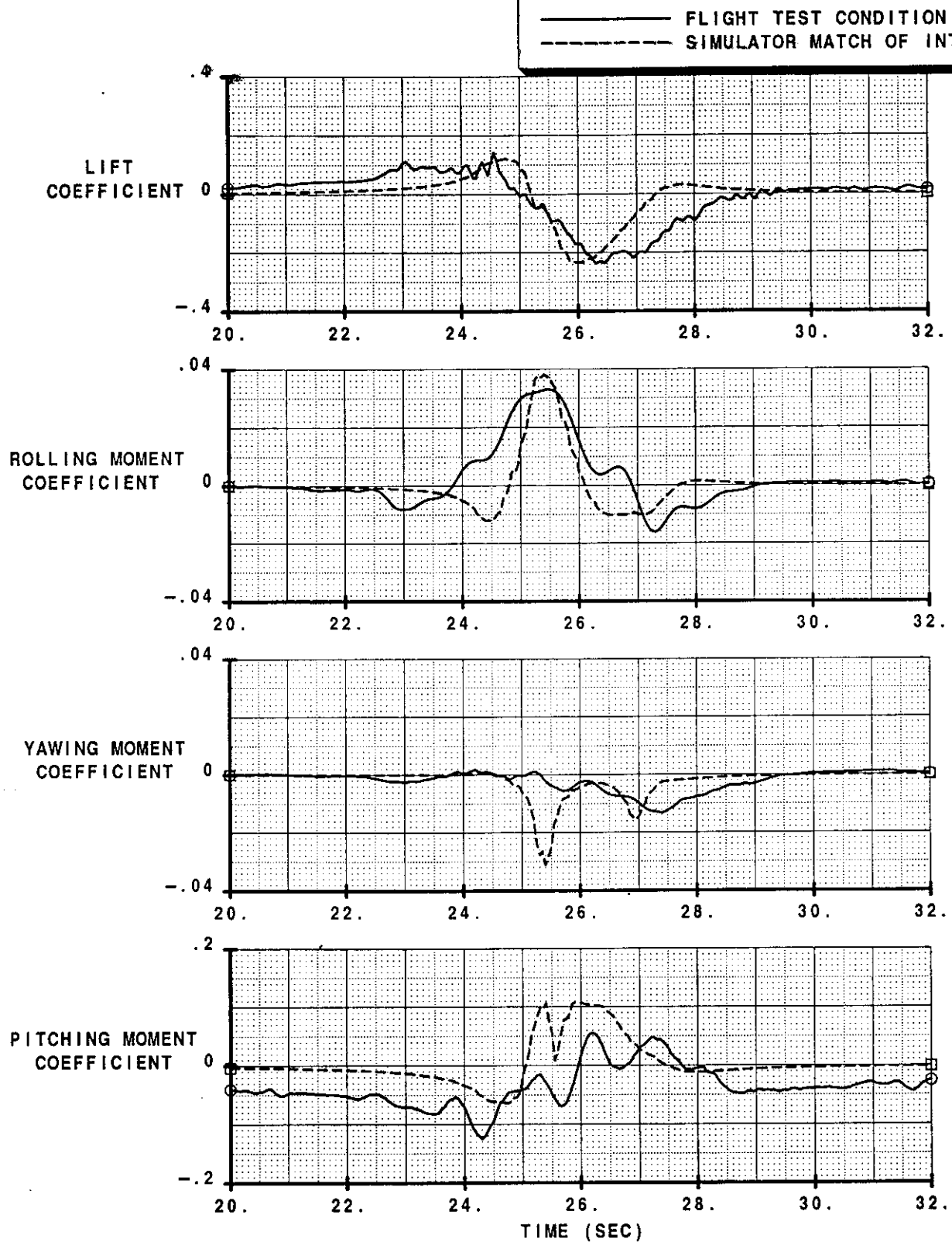
PP053

FIGURE

6

PAGE

**WAKE MODEL VALIDATION
SIMULATOR MATCH**

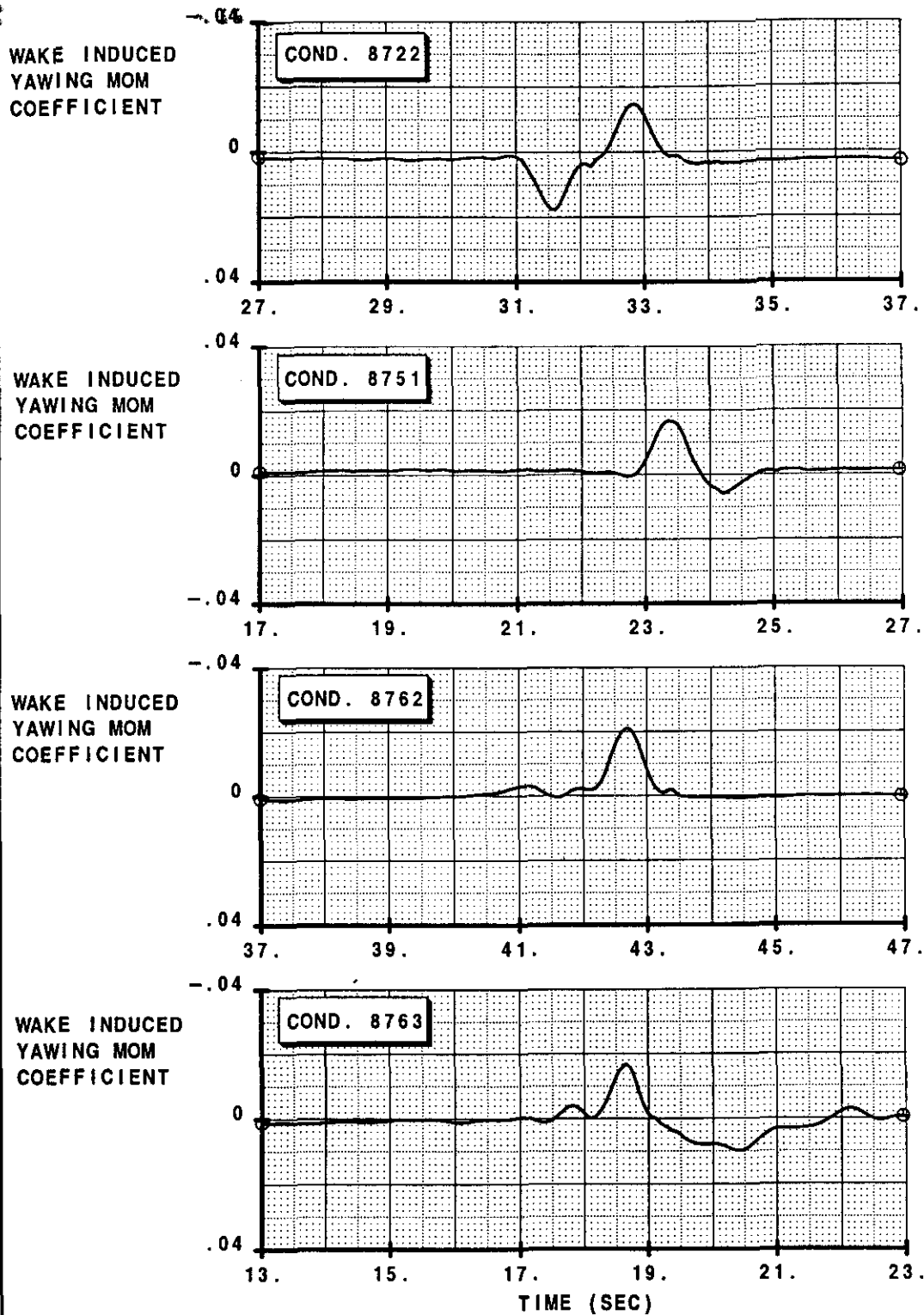


CALC	J. WILBORN	17OCT96	REVISED	DATE
CHECK				
APPD				
APPD				
REV				

WAKE ENCOUNTER FLIGHT TEST
SEQ. NO. 8851
FLIGHT-TO-SIMULATOR COMPARISON

PP053
FIGURE
7

**WAKE ENCOUNTER FLIGHT TEST
YAWING MOMENT CHARACTERISTICS**



CALC	J. WILBORN	17OCT96	REVISED	DATE
CHECK				
APPD				
APPD				

WAKE ENCOUNTER FLIGHT TEST
YAWING MOMENT COEFFICIENTS

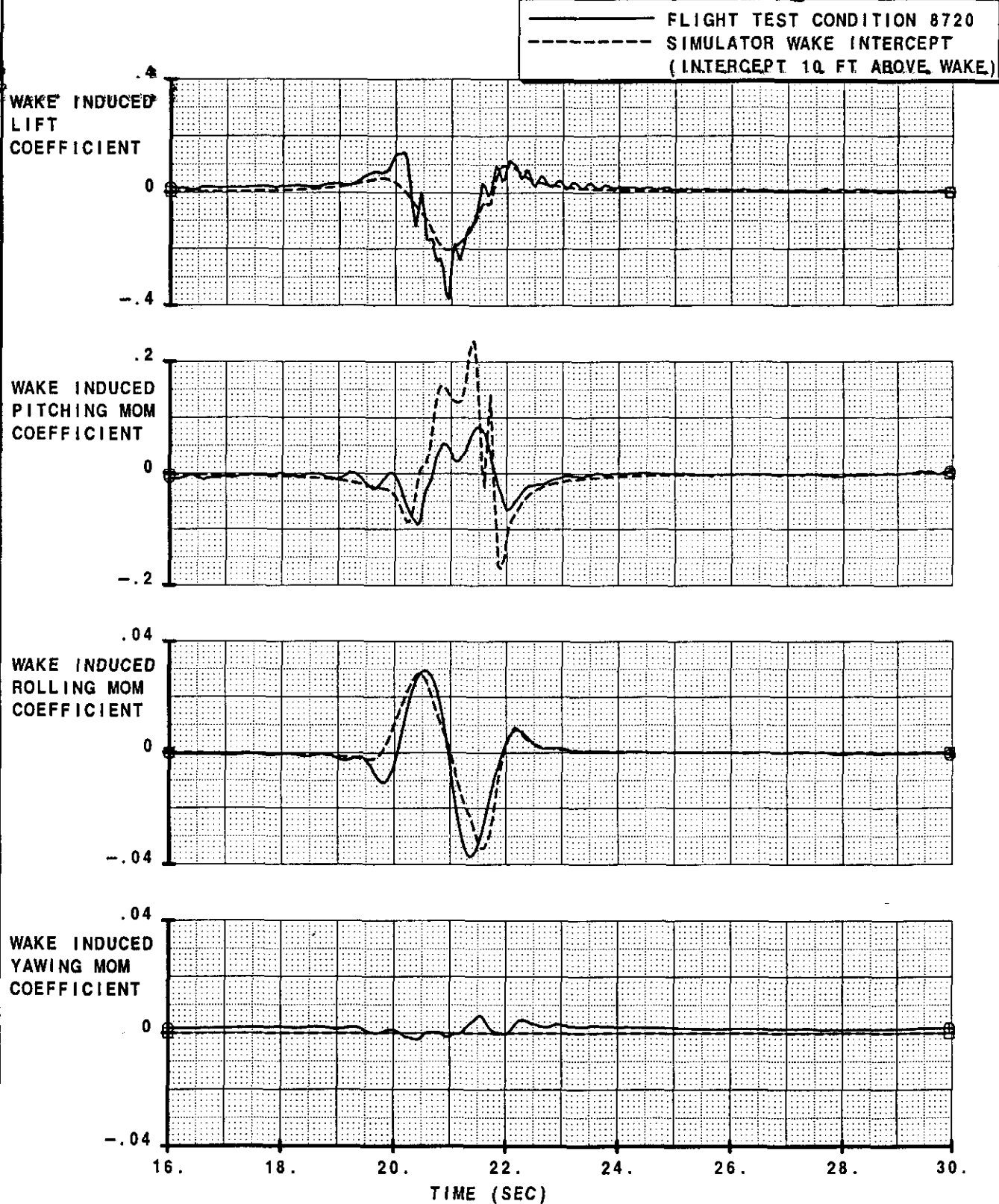
PP053

FIGURE

8

**WAKE MODEL VALIDATION
INTERCEPT COMPARISON**

JULY 1996 WAKE
ENCOUNTER MODEL
(DBNEW32)



CALC	J. WILBORN	18OCT96	REVISED	DATE
CHECK				
APPD				
APPD				

WAKE ENCOUNTER FLIGHT TEST SEQ. NO. 8720
JULY 1996 WAKE ENCOUNTER MODEL (DBNEW32)
FLIGHT-TO-SIMULATOR COMPARISON

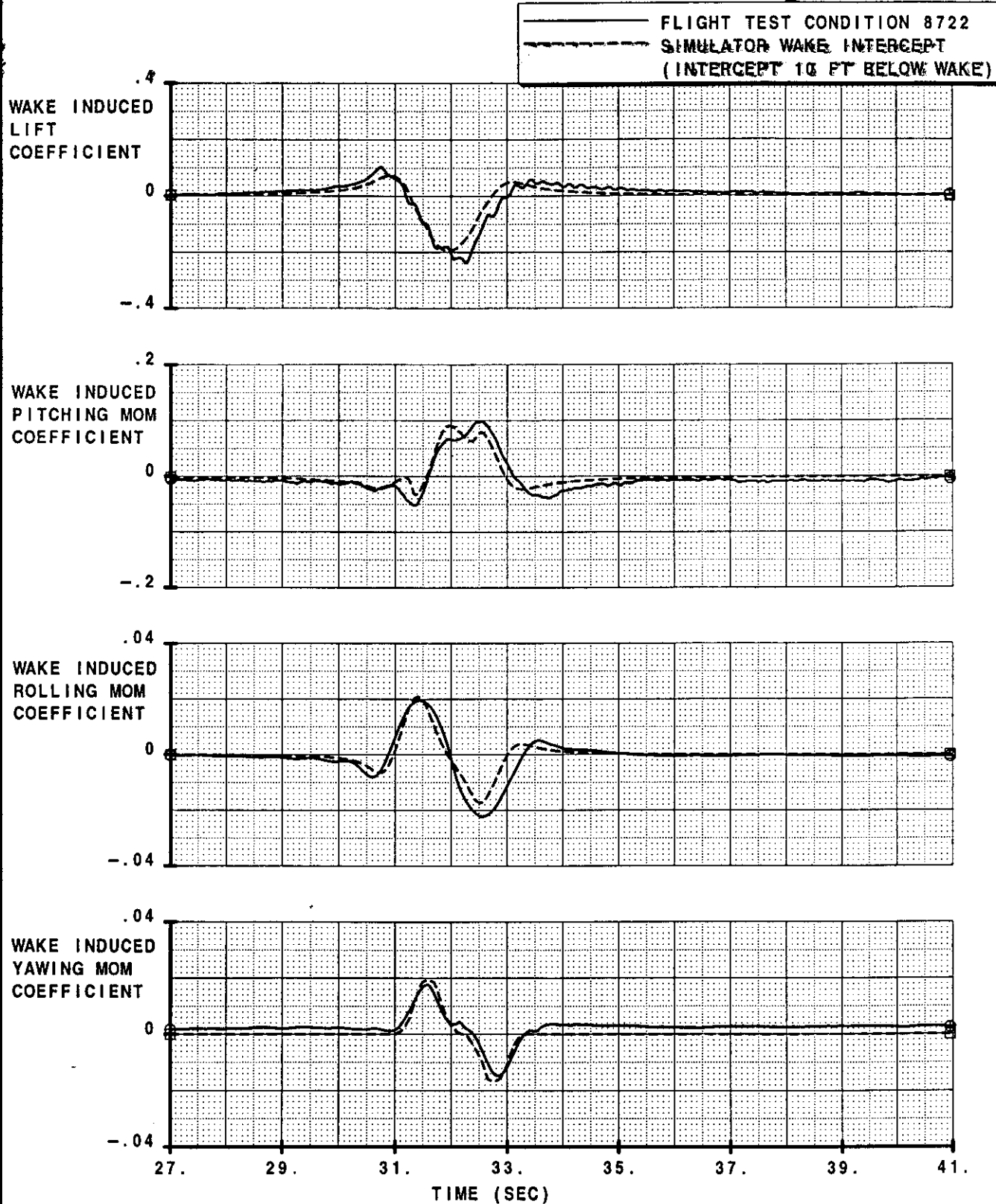
PP053

FIGURE

9

**WAKE MODEL VALIDATION
INTERCEPT COMPARISON**

JULY 1996 WAKE
ENCOUNTER MODEL
(DBNEW32)



CALC	J. WILBORN	18OCT96	REVISED	DATE
CHECK				
APPD				
APPD				

WAKE ENCOUNTER FLIGHT TEST SEQ. NO 8722
JULY 1996 WAKE ENCOUNTER MODEL (DBNEW32)
FLIGHT-TO-SIMULATOR COMPARISON

PP053

FIGURE
10

Single Wake Structure Model (May 1995)

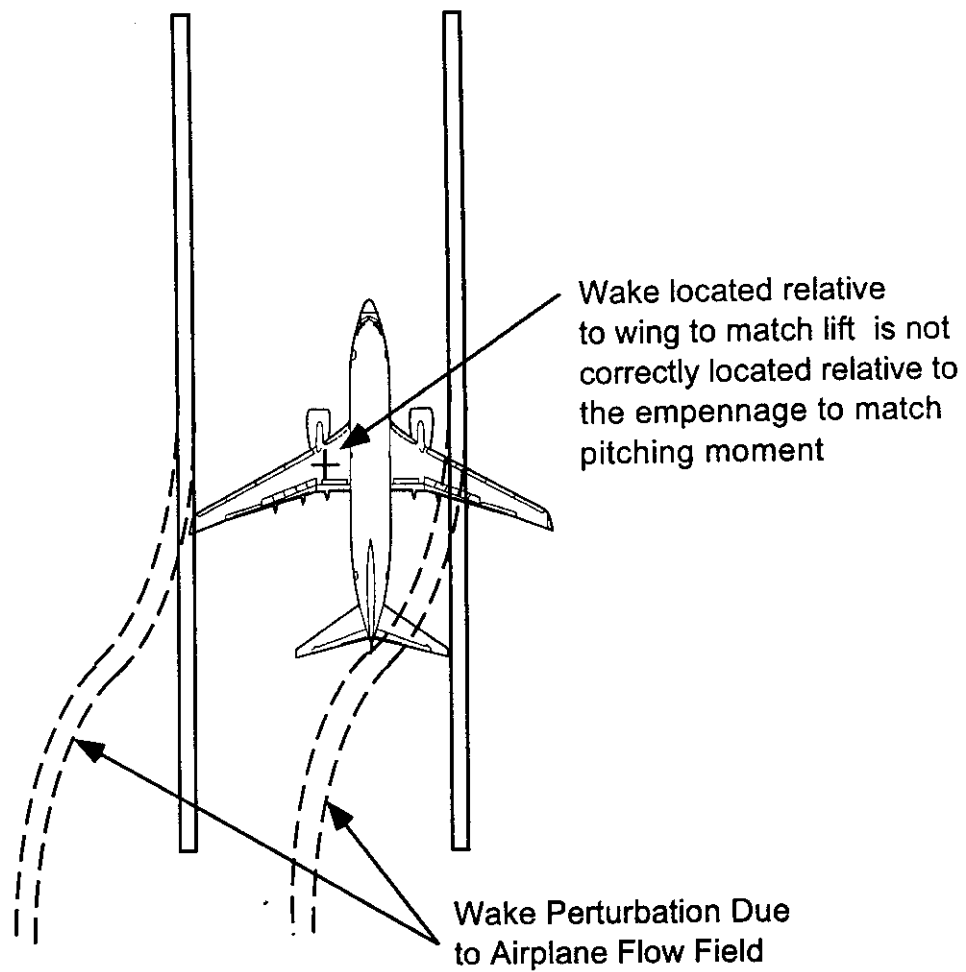


Figure 11. Single Wake Structure in May 1995 Model.

Dual Wake Structure Model (September 1996)

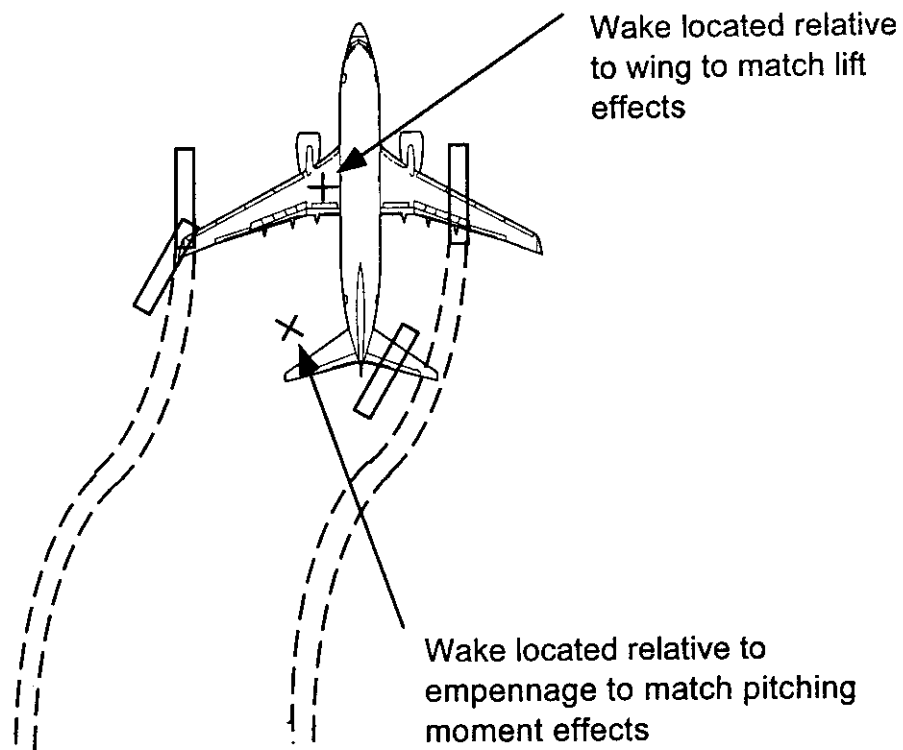


Figure 12. Dual Wake Structure in July 1996 Model.

REV

PAGE

JULY 1996 SCENARIO

ESTIMATED USAIR 427 WAKE ENCOUNTER SCENARIO

WAKE LOCATION
DERIVED RELATIVE
TO THE C.G.ALTITUDE
(FT)DISPLACEMENT
NORTH-SOUTH
(FT)

WAKE FROM DAL1083

USAIR 427

SIDE VIEW

USAIR 427

TOP VIEW

LEFT VORTEX CORE

RIGHT VORTEX CORE

DAL1083

ELAPSED TIME - SEC

JULY 1996 KINEMATIC ANALYSIS
ESTIMATED USAIR 427 WAKE ENCOUNTER
WAKE LOCATION RELATIVE TO AIRCRAFT CG

737-300

FIGURE

13

CALC J. WILBOBN 170C196 REVISED DATE

CHECK

APPD

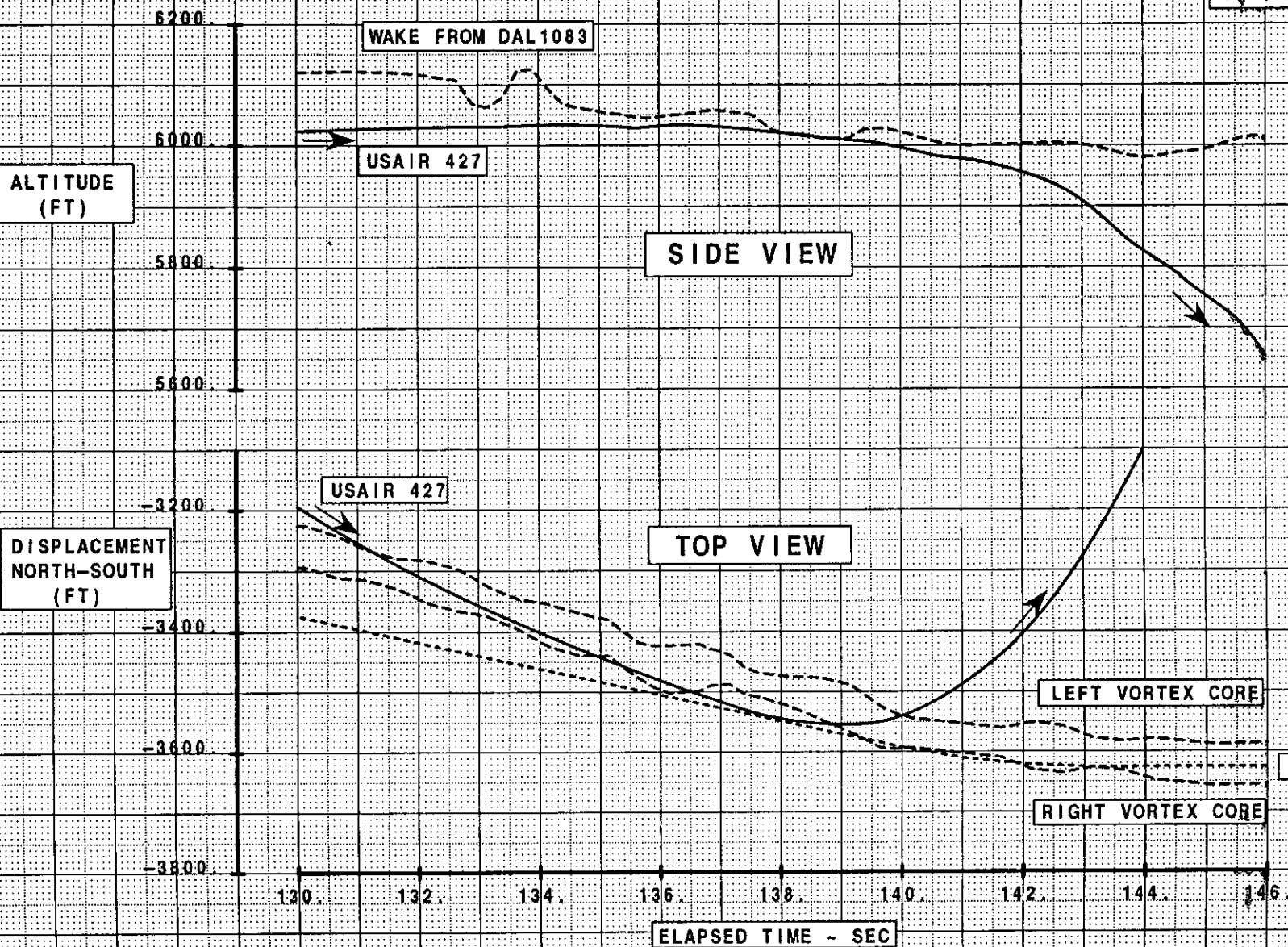
APPD

REV

PAGE

JULY 1996 SCENARIO

ESTIMATED USAIR 427 WAKE ENCOUNTER SCENARIO

WAKE LOCATION
DERIVED RELATIVE
TO THE TAIL

BOEING

JULY 1996 KINEMATIC ANALYSIS

ESTIMATED USAIR 427 WAKE ENCOUNTER
WAKE LOCATION RELATIVE TO TAIL MAC

737-300

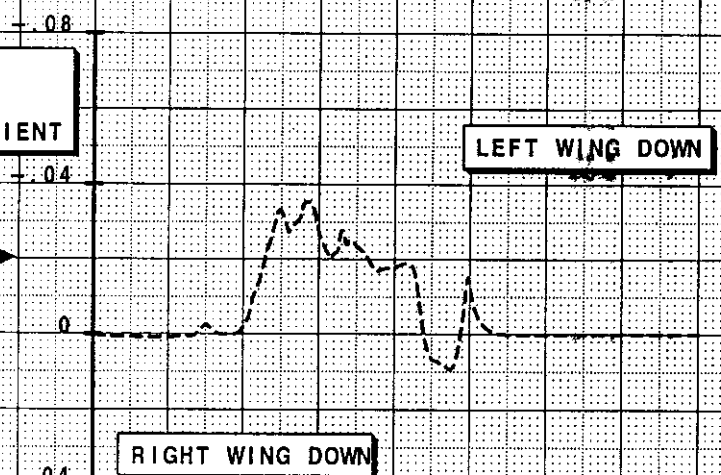
FIGURE

14

REV

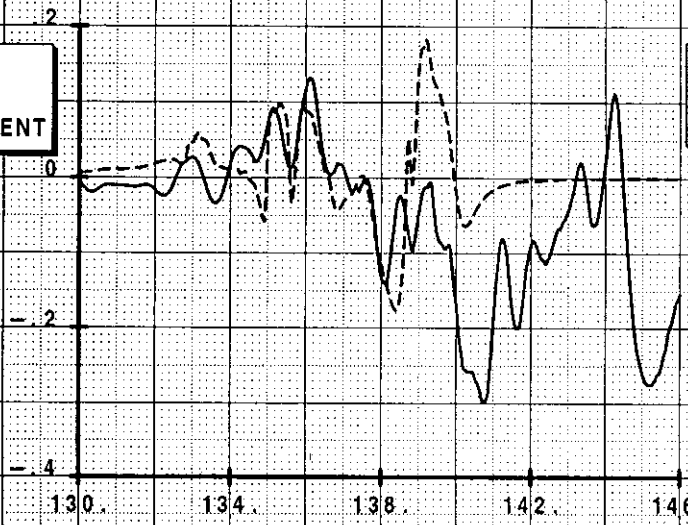
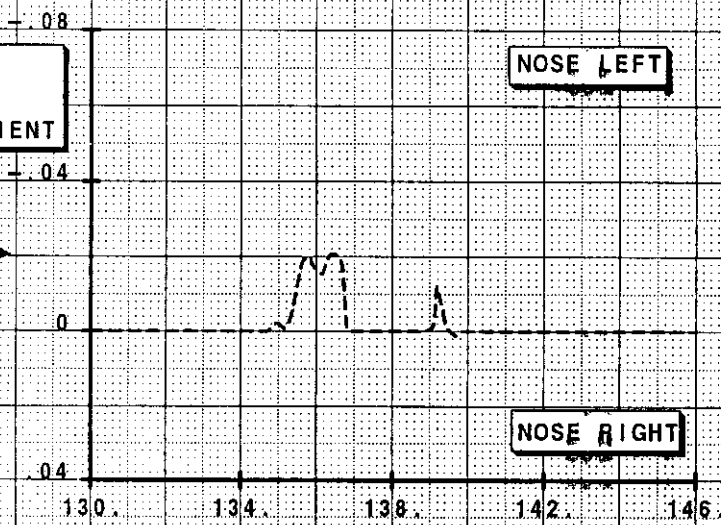
PAGE

JULY 1996 WAKE SCENARIO

LIFT
COEFFICIENTROLLING
MOMENT
COEFFICIENT

LEFT WING DOWN

RIGHT WING DOWN

PITCHING
MOMENT
COEFFICIENTYAWING
MOMENT
COEFFICIENT

NOSE LEFT

NOSE RIGHT

FDR TIME (SEC)

FDR TIME (SEC)

BOEING

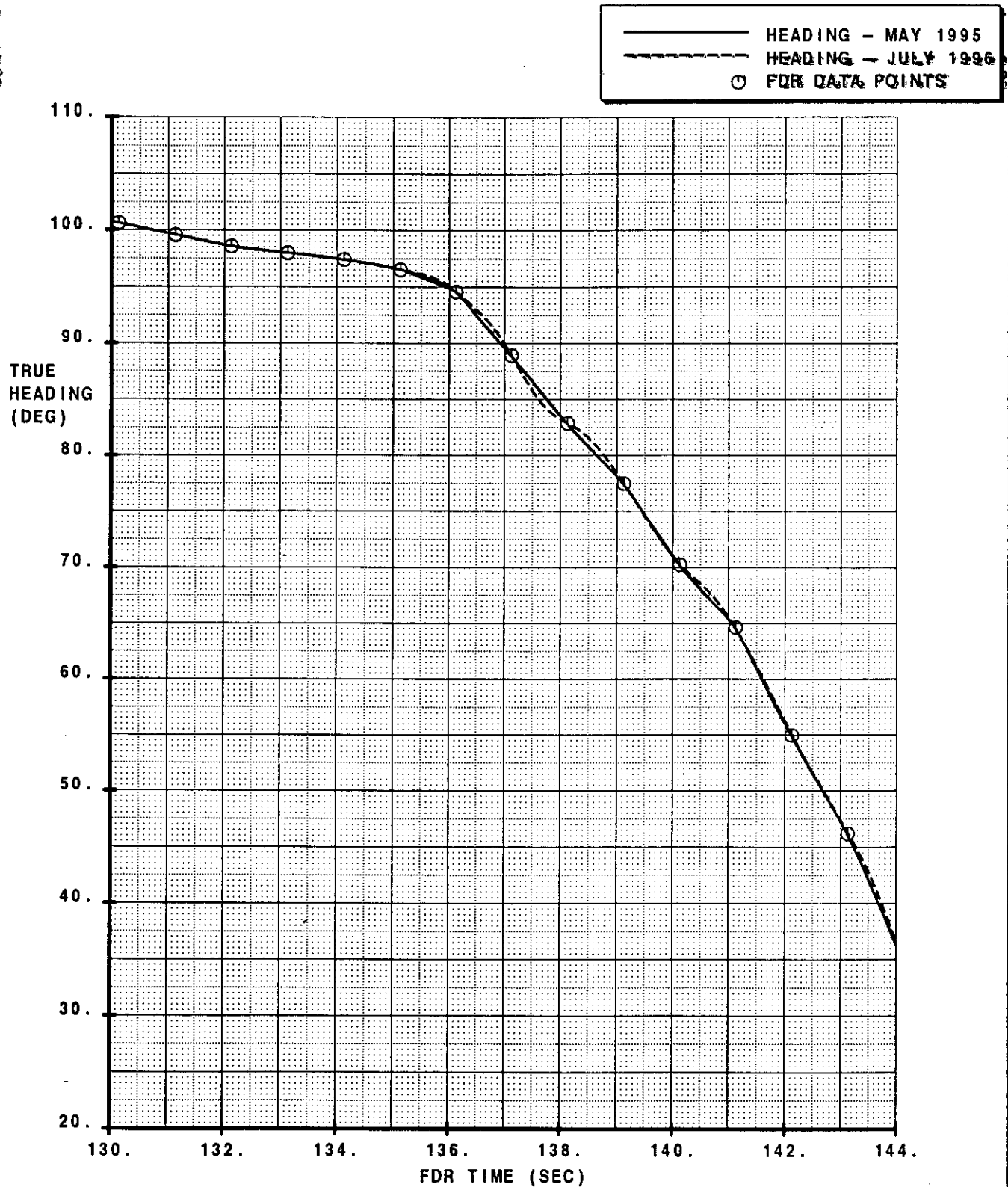
JUNE 1996 KINEMATIC ANALYSIS
USAIR 427 EXTRACTED COEFFICIENTS
VS. WAKE MODEL PREDICTED COEFFICIENTS

737-300

FIGURE

15

**HEADING INTERPOLATION
PARAMETRIC ANALYSIS**



CALC	J. WILBORN	17OCT96	REVISED	DATE
CHECK				
APPD				
APPD				
REV				

USAIR 427 HEADING INTERPOLATION
PARAMETRIC ANALYSIS

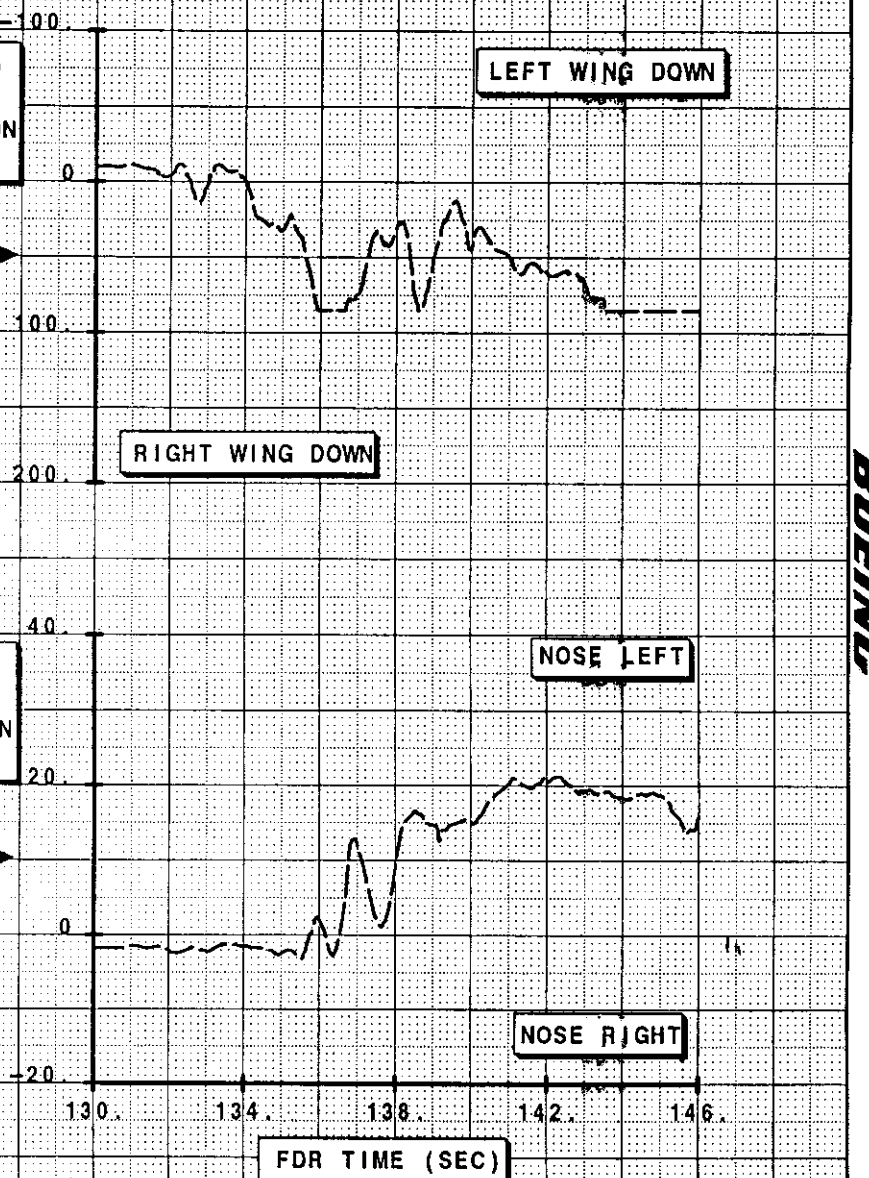
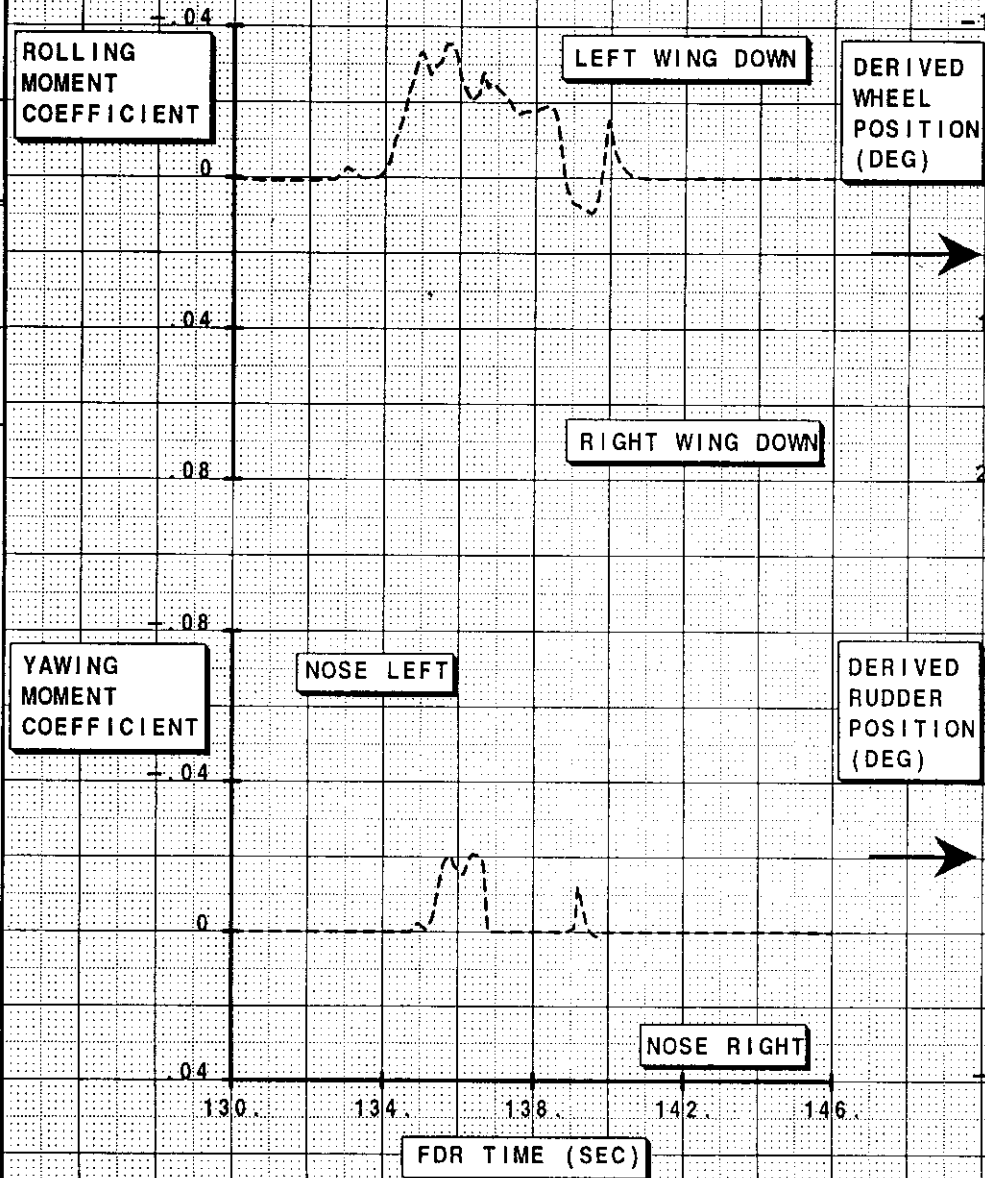
PP053

FIGURE

16

JULY 1996 WAKE SCENARIO

----- WAKE ENCOUNTER SIMULATION COEFFICIENTS
 ----- DERIVED CONTROL POSITIONS



BOEING

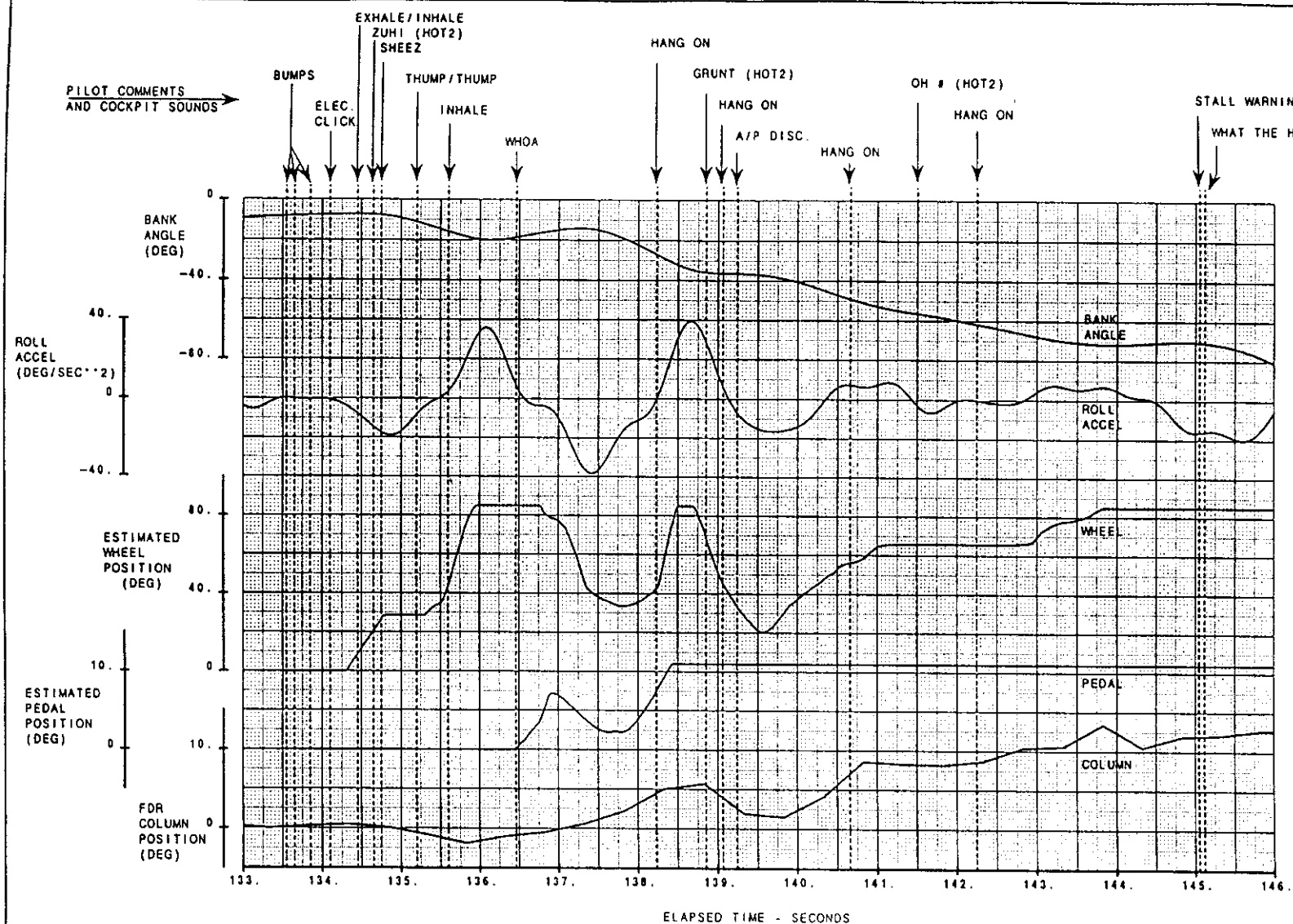
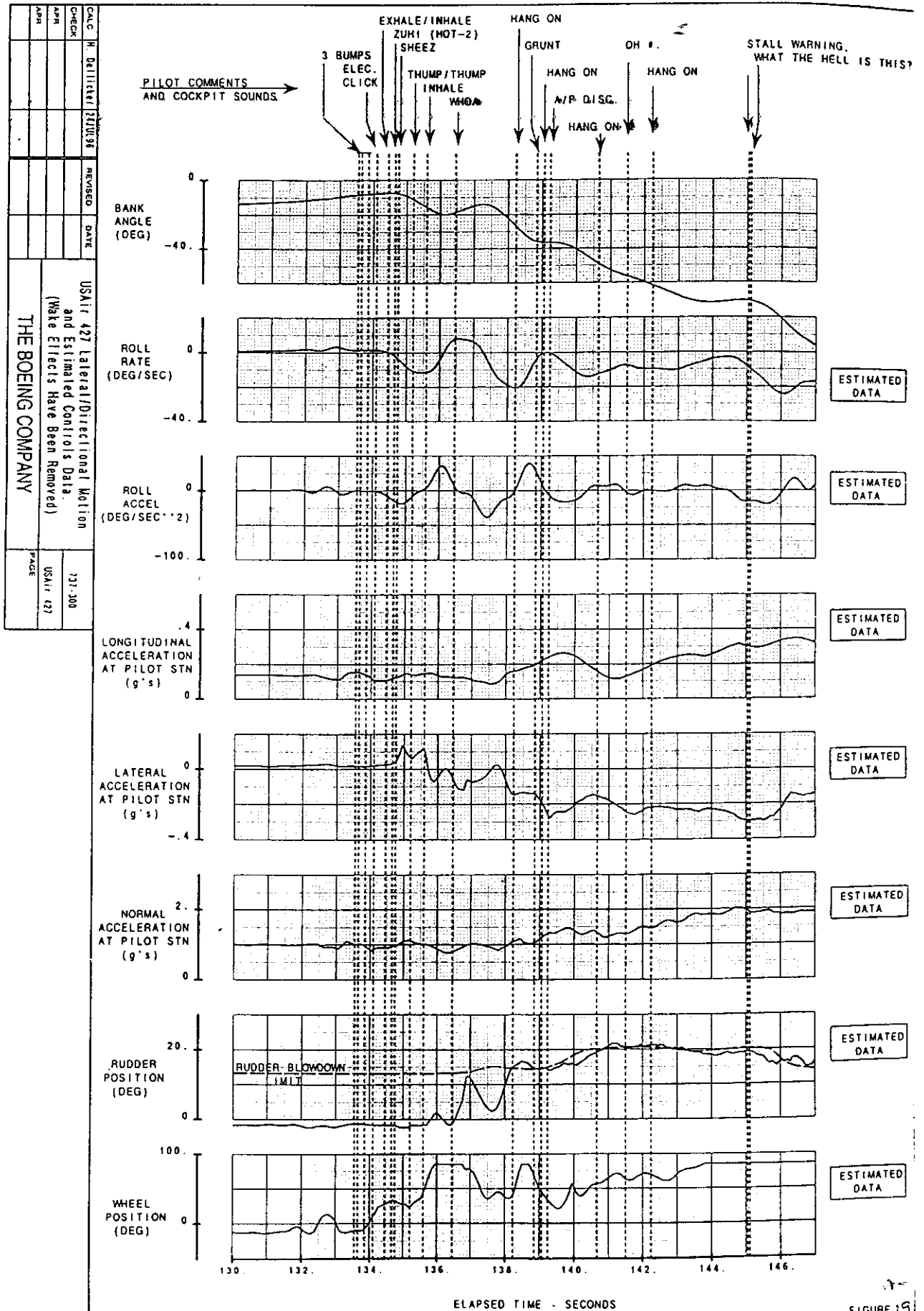


FIGURE 16.1

CALC	H. Dellicker	01AUG96	REVISED	DATE	USAir 427 FDR and Estimated Control Position Data, Based on Currently Estimated Wake Effects	737-300
CHECK						USAir 427
APR						PAGE
APR					THE BOEING COMPANY	



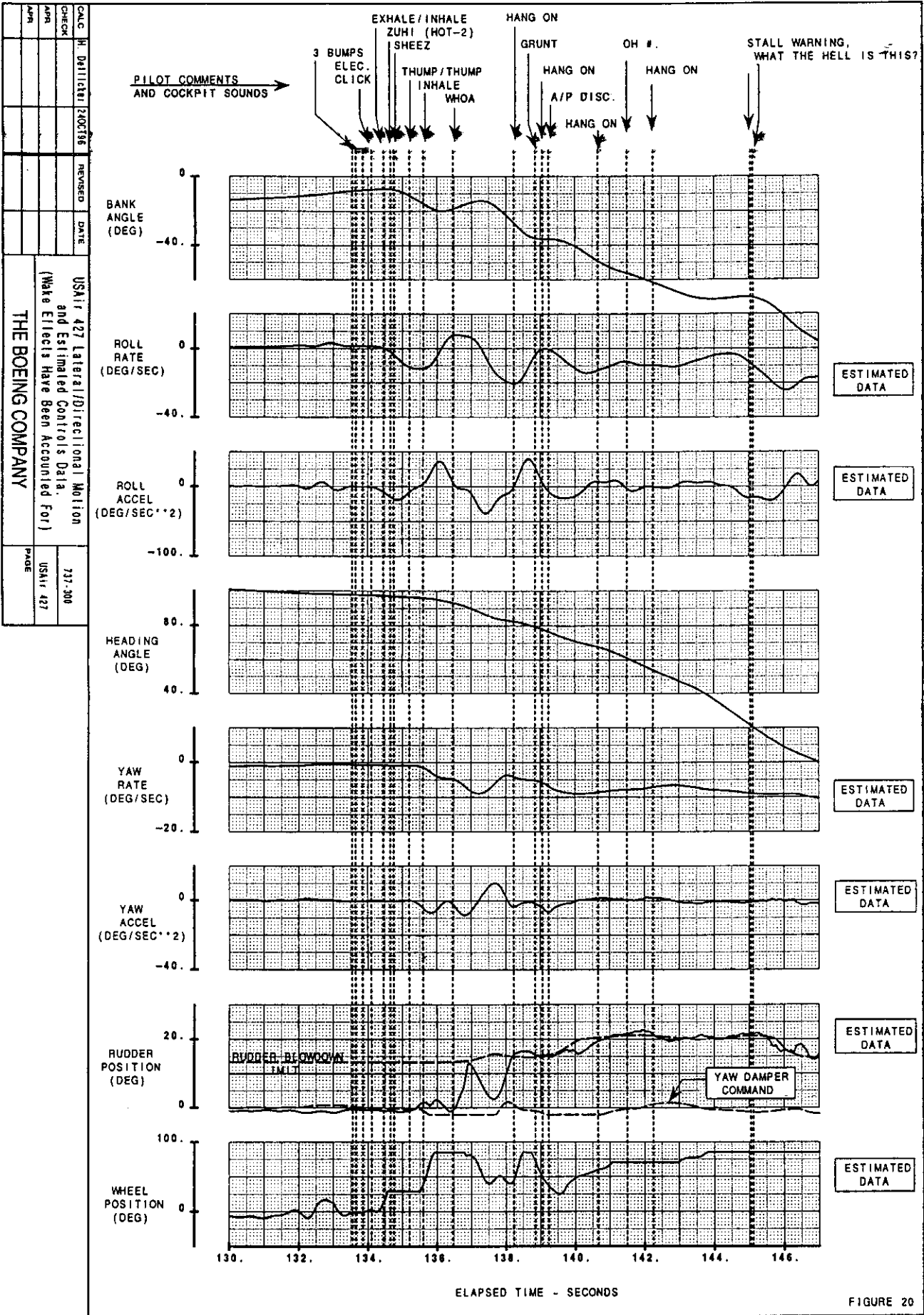


FIGURE 20

APPENDIX A. Chronology of Events Related to Derivation of Flight Controls for USAir 427 Accident Investigation.

9/94	Accident occurs on 9/8/94 near Aliquippa, PA; parameters retrieved from Flight Data Recorder; kinematic corrections made to FDR data; wake encounter simulation development begins; preliminary roll and lift model is finished by 9/30/94
10/94	Kinematic processing of FDR data begins; angular rates and accelerations, angle-of-attack, sideslip and flight path are initially derived; tail effects added to wake encounter simulation model
12/94	All-parties meeting in Seattle; wake model with lift, roll and yaw characteristics is demonstrated for investigation parties
1/95	Coefficient extractions yield first estimate of flight control positions which do not account for wake effects; Public hearing in Pittsburgh; wake encounter flight test is requested by Safety Board
2/95	Preliminary body effects added to wake encounter model
3/95	First coefficient extractions are performed which attempt to account for wake effects in flight control derivations
4/95	Wake encounter simulation updated to include effects of wake-induced sideslip and sideforce
5/95	All-parties meeting in Seattle; estimate of flight control positions which attempt to account for wake effects based on "final theoretical" wake encounter simulation is presented and documented; wake flight test is approved by parties to gather flight test data to verify wake model
6/95	Wake encounter flight test planning begins
7/95	Proof-of-concept flight test of 727 smoke generators in Seattle is successful in demonstrating that the wake cores can be marked with smoke
8/95	Flight test plans are finalized and aircraft for test are identified
9/95	Flight test occurs in Atlantic City, NJ

10/95-11/95	Reduction of flight test data and preliminary validation of simulation; second public hearing occurs in Washington, DC.
12/95-2/96	Validation of wake encounter model using flight test data; analysis of yawing moment characteristics leads to development of new yaw model
3/96	All-parties meeting in Washington, DC; wake model validation results presented to investigation team, along with ramifications of yawing moment analysis of flight test data
4/96-5/96	Final derivation of wake position, wake effects, and subsequent derivation of lateral and directional control positions
6/96	Final documentation begins

APPENDIX B. Description of the Wake Encounter Simulation Math Model

The basic 737-300 simulation math model, described in reference 5, is essentially a point-mass model; that is, all forces and moments (from aerodynamics, thrust, and gear) are resolved at the aircraft center-of-gravity (CG). The kinematic equations of motion are then applied at this point to calculate the trajectory and orientation of the aircraft. All aerodynamic forces are thus functions of the angle-of-attack and sideslip as defined at the aircraft CG. For flight in a uniform wind field, this assumption is accurate because the angle-of-attack and sideslip angle are the same nearly everywhere on the aircraft body, and the few locations where they do vary (such as in the wing downwash field) can be measured and modeled as functions of angle-of-attack or sideslip at the CG.

However, in the case where it is desired to model the effects of a wake flow field, the angle-of-attack and sideslip can vary considerably at different locations on the aircraft. Thus, to model a wake encounter effectively, it becomes necessary to expand the basic model to account for this variation in angle-of-attack and sideslip. To do this, two basic modeling elements are needed.

The first element is a mathematical description of the wake-induced velocity field as a function of position relative to the wake. In the USAir 427 wake analysis the velocity field was modeled using two counter-rotating Rankine vortices. Rankine vortices were used because they are simple to model and have been shown in the past to provide a reasonable prediction of vortex velocity distribution.

The second element is a method to translate the wake flow field velocities into local angles-of-attack and local sideslip angles at various points on the airplane. This is done using aerodynamic strip theory. In this method the aerodynamic surfaces of the aircraft are divided into thin strips which run in the chordwise direction (see Figure B-1). For the case of a wing or tail, the strip represents a nearly two-dimensional airfoil section. The midspan chord of the strip is chosen as a representative airfoil section, and then the quarter-chord position along this section is chosen as a representative point for the entire strip; that is, the angle-of-attack and sideslip at that point are considered to hold constant over the strip.

The location of this point is known in body axes. A simple transformation to the airplane's ground axes position through its Euler angles (pitch attitude, roll attitude and heading) is applied to determine the point's location in the ground axes system. Next, the point must be transformed to the wake axes system. In this model the wake is defined about a central point, considered the wake axes system origin. This point has a ground axes location, and the wake axes system has an Euler angle (pitch, roll and heading) orientation relative to the ground axes system. A transformation of the point's ground axes position through this set of wake Euler angles locates the point in the wake axes system.

The wake axes system is defined so that the wake x-axis runs parallel to the wake cores, and the wake y-axis is normal to the cores and in the plane of the lines defining the wake core centers. The wake z-axis is normal to the wake x and y-axes and is positive up. This last definition actually causes the wake axes system to be left-handed, but this was considered acceptable because the wake effects are identical for positive or negative values of x in wake axes and the definition of the wake z-axis as positive upward was more intuitive. Figure B-2 shows the wake axes system definition.

As previously noted, the wake vortices are modeled by two counterrotating 2-D Rankine vortices. The horizontal and vertical velocity components (denoted v_{wake} and w_{wake} , respectively) of a single Rankine vortex are:

Given:

$$r^2 = \Delta y^2 + \Delta z^2$$

for $r > c_{wake}$:

$$v_{wake} = (\Gamma * \Delta z) / (2 * \pi * r^2)$$

$$w_{wake} = (\Gamma * \Delta y) / (2 * \pi * r^2)$$

for $r \leq c_{wake}$:

$$v_{wake} = (\Gamma * \Delta z) / (2 * \pi * c_{wake}^2)$$

$$w_{wake} = (\Gamma * \Delta y) / (2 * \pi * c_{wake}^2)$$

where Γ = wake circulation (ft² / sec)
 Γ = $k_{diss} W / \rho V_T b'$, positive counterclockwise
 k_{diss} = dissipation factor
 W = weight of wake-generating aircraft (lbs)
 ρ = air density (slugs / ft³)
 V_T = true airspeed of wake-generating aircraft (ft / sec)
 b' = wake generational span of generating aircraft (ft)
 b' = $(\pi / 4) * \text{span}$
 Δy = horizontal distance from center of vortex to point of interest (ft), positive to the right
 Δz = vertical distance from center of vortex to point of interest (ft), positive up
 c_{wake} = wake core radius (ft)

The velocity at a given point in the whole wake system is computed by applying this equation twice, once for each core. The distances for each core are computed as the horizontal and vertical distances between the point of interest and each core's center, taking careful note of the sign convention. The circulation value is positive for the right core and negative for the left core. The value of the dissipation factor can vary between 0 and 1 and can be calculated using several theoretical models of wake strength dissipation as a function of distance behind the trailing aircraft. Once the velocities from each core have been calculated the total wake-induced velocity at the point of interest is simply the sum of the velocities contributed by each core.

The velocity at each point is transformed back through ground axes to the airplane body axes system, where it is resolved into local incremental u , v , and w velocities. These velocities translate into incremental angles-of-attack and sideslip angles by the following:

$$\Delta\alpha_i = \tan^{-1} (w_i / (u_i + U))$$

$$\Delta\beta_i = \tan^{-1} (v_i / (u_i + U))$$

where $\Delta\alpha_i$ = incremental wake-induced angle-of-attack at point i (deg)
 $\Delta\beta_i$ = incremental wake-induced sideslip angle at point i (deg)
 u_i = incremental wake-induced x-axis velocity at point i (ft/sec)
 v_i = incremental wake-induced y-axis velocity at point i (ft/sec)
 w_i = incremental wake-induced z-axis velocity at point i (ft/sec)
 U = total aircraft x-axis velocity (ft/sec)

Incremental aerodynamic lift and drag forces on the wings are then computed from these local angles-of-attack and sideslip angles using 2-D airfoil aerodynamics:

$$L_{wi} = K_{wi} * [Cl_{wi}(\alpha_w + \Delta\alpha_i + 2 * \Gamma \sin(\Delta\beta_i)) - Cl_{wi}(\alpha_w)] * q * S_i$$

where L_{wi} = wing lift for section i (lbs)
 K_{wi} = spanwise wing lift distribution factor
 Cl_{wi} = sectional wing lift coefficient for section i
 α_w = wing angle-of-attack (deg)
 $\Delta\alpha_i$ = incremental angle-of-attack induced by wake velocity field for section i (deg)
 Γ = wing dihedral angle (deg)
 $\Delta\beta_i$ = incremental sideslip induced by wake velocity field for section i (deg)
 q = dynamic pressure (lbs / ft²)
 S_i = sectional strip area for section i (ft²)

Note that at each point the lift coefficient is first evaluated at the total angle-of-attack. In the case of the wing, this is the sum of the wing basic angle-of-attack, the incremental angle-of-attack due to the wake, and the incremental angle-of-attack due to wake-induced incremental sideslip angle. The lift coefficient due to just the wing basic angle-of-attack is then subtracted from the total, leaving the increment due to the wake only. By using this method it is possible to incorporate 2-D stall characteristics of the wing airfoil section into the equation.

An equation to that used for the calculation of wing lift coefficient is used to compute incremental drag along the *wing only* for purposes of computing the wake-induced yawing moment on the wing:

$$D_{wi} = K_{wi} * [C_{dwi}(\alpha_w + \Delta\alpha_i + 2 * \Gamma \sin(\Delta\beta_i)) - C_{dwi}(\alpha_w)] * q * S_i$$

$$\begin{aligned} \text{where } D_{wi} &= \text{wing drag for section } i \text{ (lbs)} \\ C_{dwi} &= \text{sectional drag coefficient for section } i \end{aligned}$$

Incremental aerodynamic lift forces on the horizontal tail are computed in similar manner as those for the wing:

$$L_{HTi} = K_{Hi} * [C_{LHTi}(\alpha_H + \Delta\alpha_i) - C_{LHTi}(\alpha_H)] * q * S_i$$

$$\begin{aligned} \text{where } L_{HTi} &= \text{horizontal tail lift for section } i \text{ (lbs)} \\ K_{Hi} &= \text{spanwise horizontal tail lift distribution factor} \\ C_{LHTi} &= \text{sectional horizontal tail lift coefficient for section } i \\ \alpha_H &= \text{horizontal tail angle-of-attack (deg)} \end{aligned}$$

The calculation of lift over the horizontal tail is simpler than for the wing because sideslip angle effects are neglected for the horizontal tail. The lift coefficient is again first evaluated at the total angle-of-attack, which in this case is the sum of the horizontal tail angle-of-attack and the incremental angle-of-attack due to the wake. The lift coefficient due to just the horizontal tail angle-of-attack is then subtracted from the total, leaving the increment due to the wake only. This allows for the incorporation of 2-D stall characteristics of the horizontal tail airfoil into the equation.

The vertical tail is modeled in the same manner except that a sideforce is computed from incremental sideslip effects:

$$Y_{VTi} = K_{Vi} * [C_{yVTi}(\beta + \Delta\beta_i) - C_{yVTi}(\beta)] * q * S_i$$

$$\begin{aligned} \text{where } C_{yVTi} &= \text{sectional vertical tail lift coefficient for section } i \\ \beta &= \text{airplane sideslip angle (deg)} \\ K_{Vi} &= \text{spanwise vertical tail lift distribution factor} \end{aligned}$$

As in the wing and horizontal tail calculations, the coefficient is computed for the total surface angle-of-attack (which is the sideslip angle in the case of the vertical tail) and then the coefficient due to the basic surface angle-of-attack is subtracted to leave only the increment due to the wake, preserving the ability to model stall characteristics of the tail surface.

The drag terms for the tail surfaces are neglected because the yawing and pitching moment increments due to drag changes along the tail are negligibly small.

The wake effects on the forebody are modeled in a slightly different fashion from the lifting surfaces. The body section is divided into rings, each five feet long. The velocities for each ring are calculated at the center point of the circular section and resolved into local angles-of-attack and sideslip angles using the same equations presented above for the lifting surfaces. The incremental lift and sideforce on each body section are then computed using the following:

$$L_{BDY_i} = [C_{f_{bdy}}(\Delta\alpha_i)] * q * S * l_i$$

$$Y_{BDY_i} = [C_{f_{bdy}}(\Delta\beta_i)] * q * S * l_i$$

where

$$\begin{aligned} L_{BDY_i} &= \text{lift force for body section } i \text{ (lbs)} \\ Y_{BDY_i} &= \text{side force for body section } i \text{ (lbs)} \\ C_{f_{bdy}} &= \text{body force coefficient per unit body length (ft}^{-1}\text{)} \\ S &= \text{wing area (ft}^2\text{)} \\ l_i &= \text{body sectional length for section } i \text{ (ft)} \end{aligned}$$

The body force coefficient function was derived from tail-off 757 wind tunnel data which was scaled to represent the 737, and is considered to be the same for lift and sideforce, since the body is a cylinder. The wind tunnel coefficients were normalized by airplane wing area and then divided by body length to represent a body force per unit length; hence the multiplication by both wing area and body sectional length. Note that only the incremental angles-of-attack and sideslip are used to evaluate the function; this approximation was made because stall characteristics for the wing-body only were not readily available.

In order to determine the total wake effects on the airframe, it is necessary to integrate the incremental wake forces over all surfaces. The lift and side forces are summed directly over each surface to obtain total wake forces:

$$L_{wake} = \sum_{i=1}^{N_{WING}} L_{w_i} + \sum_{i=1}^{N_{HT}} L_{HT_i} + \sum_{i=1}^{N_{BDY}} L_{BDY_i}$$

$$Y_{wake} = \sum_{i=1}^{N_{VT}} Y_{VT_i} + \sum_{i=1}^{N_{BDY}} Y_{BDY_i}$$

The rolling, pitching and yawing moments (ℓ , M and N, respectively) are computed by multiplying the incremental forces by their respective moment arms and then summing over each surface:

$$\begin{aligned}\ell_{\text{wake}} &= \sum_{i=1}^{\text{NWING}} (Lw_i * \Delta y_i) + \sum_{i=1}^{\text{NHT}} (LHT_i * \Delta y_i) + \sum_{i=1}^{\text{NVT}} (YVT_i * \Delta z_i) \\ M_{\text{wake}} &= \sum_{i=1}^{\text{NWING}} (Lw_i * \Delta x_i) + \sum_{i=1}^{\text{NHT}} (LHT_i * \Delta x_i) + \sum_{i=1}^{\text{NBDY}} (LBDY_i * \Delta x_i) \\ N_{\text{wake}} &= \sum_{i=1}^{\text{NVT}} (YVT_i * \Delta x_i) + \sum_{i=1}^{\text{NWING}} (Dw_i * \Delta y_i) + \sum_{i=1}^{\text{NBDY}} (YBDY_i * \Delta x_i)\end{aligned}$$

Finally, these forces and moments are normalized into coefficient form and converted to stability axes:

$$\begin{aligned}C_{L_{\text{wake}}} &= (L_{\text{wake}} / qS) * \cos(\alpha_w) \\ C_{Y_{\text{wake}}} &= Y_{\text{wake}} / qS \\ C_{\ell_{\text{wake}}} &= (\ell_{\text{wake}} / qSb) * \cos(\alpha_w) + (N_{\text{wake}} / qSb) * \sin(\alpha_w) \\ C_{N_{\text{wake}}} &= (N_{\text{wake}} / qSb) * \cos(\alpha_w) + (\ell_{\text{wake}} / qSb) * \sin(\alpha_w) \\ C_{M_{\text{wake}}} &= (M_{\text{wake}} / qSc) * \cos(\alpha_w) \\ \text{where } b &= \text{aircraft span (ft)} \\ c &= \text{aircraft mean aerodynamic chord (ft)}\end{aligned}$$

These coefficients are then added to the basic aerodynamic coefficient buildup to represent the total aerodynamic force and moment effects on the aircraft.

Revisions to Model Resulting From Wake Encounter Flight Test

As a result of the Wake Encounter Flight Test performed in Atlantic City, NJ, in September 1995, a significant change was made to the yawing moment calculation in the wake encounter simulation. Specifically, it was clear that significant yawing moments were only observed in flight test when the wake cores would pass cleanly above the aircraft body and impact the vertical tail. In all other cases the interference of the wake velocity field with the aircraft's own flow field would disrupt the wake and break it apart.

The simulation was updated by replacing the strip theory calculations for the vertical tail with an empirical yawing moment model. The model was developed by observing video footage of the wake encounters and correlating wake yawing moment (derived from measured kinematic data) with the location of the wake core relative to the vertical tail. Also, since no notable yawing moments were observed in flight test when the wake cores were near the forebody or over the wings, no modeling of the body and wing contributions to yawing moment was implemented.

The total wake yawing moment is the product of two functions. The first function, denoted C_{NWKFTD} , is the wake-yawing moment as a function of normalized lateral location in the wake axes system and wake circulation strength:

$$C_{NWKFTD} = f(y_{norm_w}, \Gamma)$$

$$\begin{aligned} \text{where } y_{norm_w} &= \text{Normalized lateral position in wake axes system} \\ &= y_w / b_{wake} \\ y_w &= \text{Lateral location in wake axes system (ft)} \\ b_{wake} &= \text{Distance between wake cores (ft)} \\ \Gamma &= \text{Wake circulation strength, (ft}^2\text{/sec)} \end{aligned}$$

The second function, K_{NWKFTD} , is a shaping factor which varies from 0 to 1 and is a function of normalized vertical location in the wake axes system:

$$K_{NWKFTD} = f(z_{norm_w})$$

$$\begin{aligned} \text{where } z_{norm_w} &= \text{Normalized vertical position in wake axes system} \\ &= z_w / b_{wake} \\ z_w &= \text{Vertical location in wake axes system (ft)} \end{aligned}$$

It is this factor which is used to apply interference effects of the airplane on the wake flow field. The factor is zero for vertical positions of the wake relative to the body where interference was observed to disrupt the wake effects. This is observed when the wake cores are located at or below the level of the airplane aft body. As the wake moves upward relative to the vertical tail, the shaping factor increases to a maximum value of 1 at a location approximately equal to the 3/4 span location on the vertical tail. The factor then decreases back to zero as the wake moves above the vertical to the point where the wake flow field no longer influences the aircraft. This position where the wake no longer affects the vertical occurs when the wake core is approximately 30-40 feet above the tip of the vertical tail.

The total wake yawing moment is calculated as follows:

$$C_{N_{wake}} = C_{NWKFTD} * K_{NWKFTD}$$

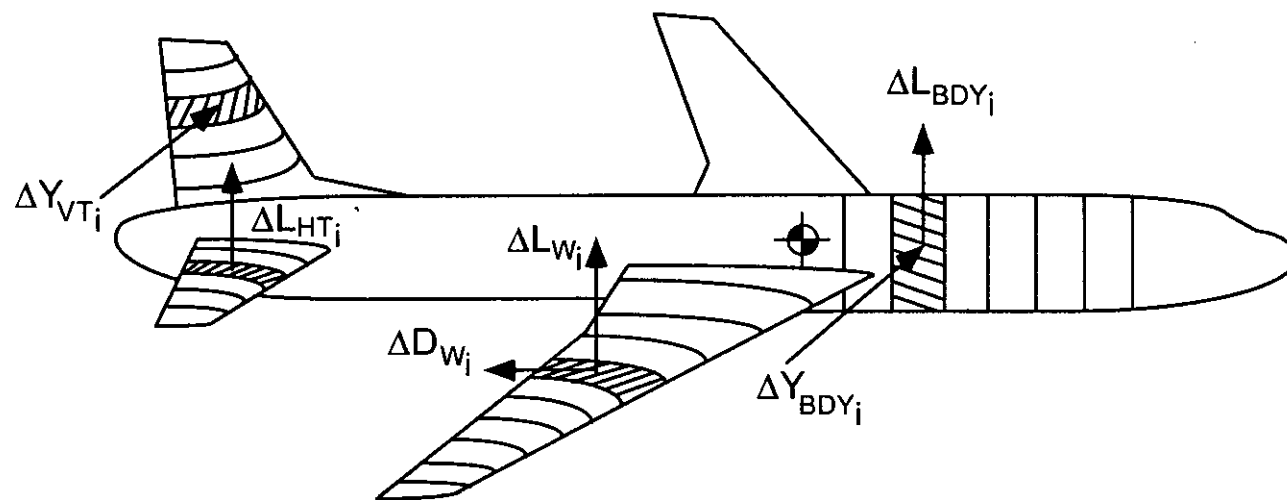


Figure B1. General Distributed Lift Model.

Vertical velocity profile along line cut
through center of wake cores

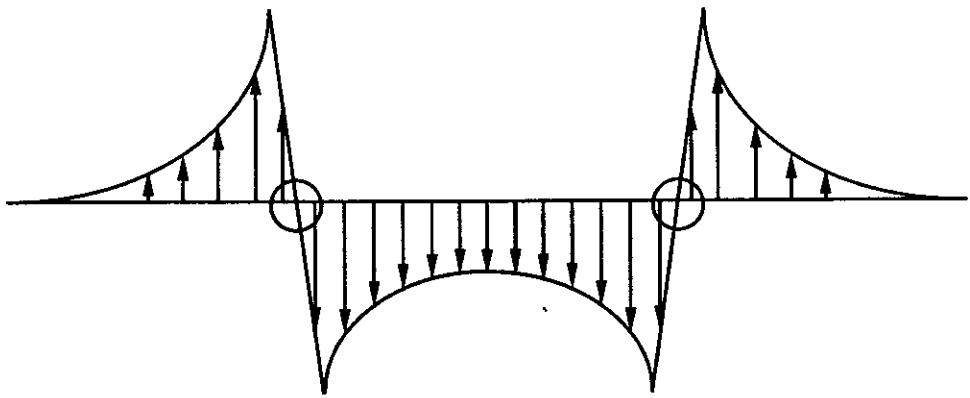


Figure B2a.

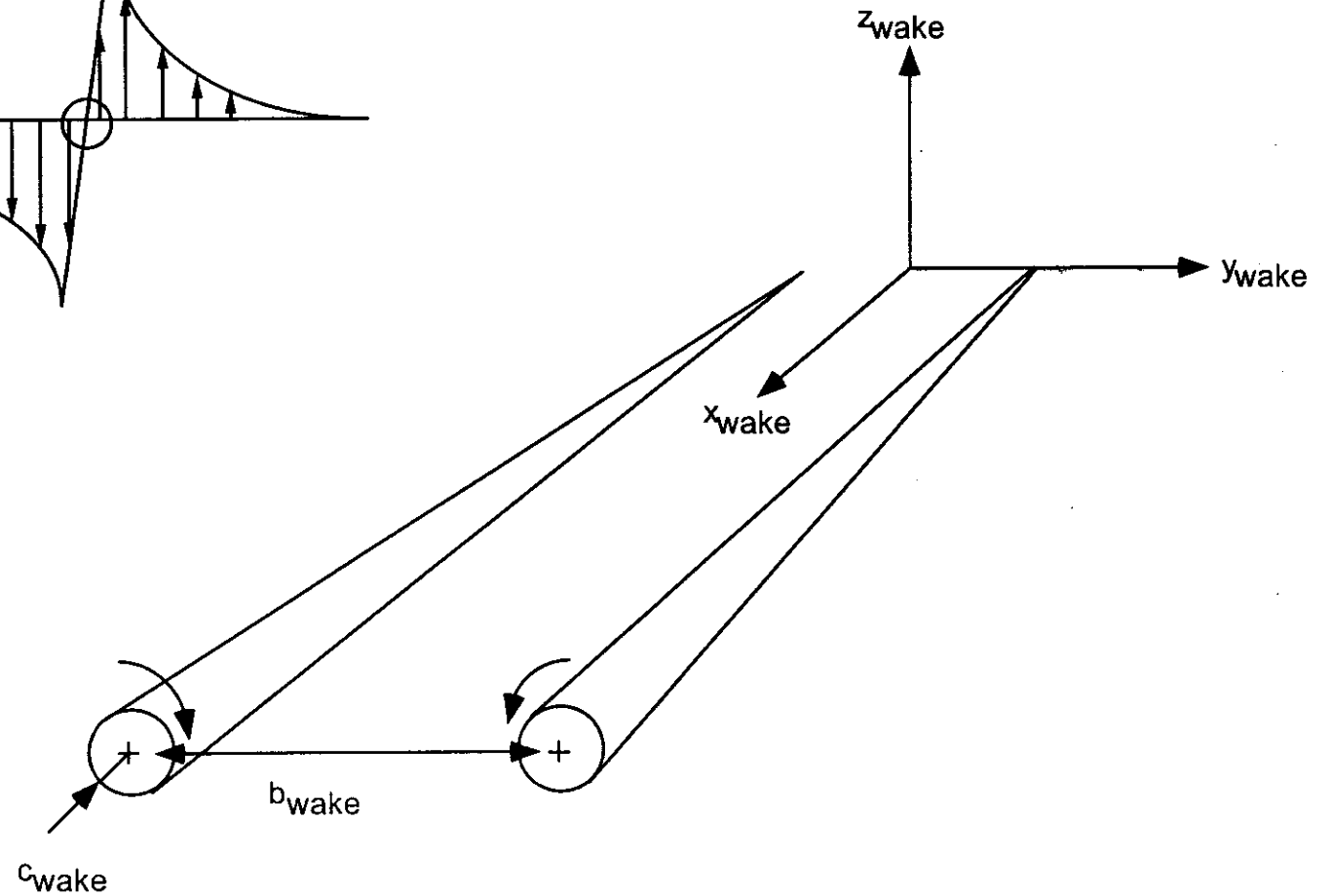


Figure B2b.

Figure B2. Wake-induced velocity field (a) and wake axes system(b).

APPENDIX C. Update to the 737-300 Aerodynamic Simulator Model

The data collected during the 1995 Seattle and Atlantic City flight testing on the USAir 737-300 PP053 was used to update the aerodynamic model documented in Reference 5. The flight test results validated the accuracy of the simulator model in the normal flight envelope. They also provided the basis for minor adjustments to the modeling of rudder hinge moments and to the high sideslip, high angle-of-attack aerodynamic data. The validation of the model in the normal flight envelope was given to the NTSB performance group during the meeting in Seattle on 12/18/95 and is not repeated here.

The new hinge moment model is based on all relevant data from the 737-300, -400, and -500 flight test data bases as well as the data flown in the 1995 flight testing. This includes flight testing conducted before, during and after the certification of these models. The data covered the maximum range of sideslip and rudder angles predicted for the USAir 427 accident. The data show increased sensitivity to sideslip angle in the 8 to 12 degree range of sideslip. The new model significantly improves the correlation between predicted rudder and rudder blowdown as shown in figure C-1.

The new aerodynamic model incorporates "high angle-of-attack" sideslip data from the 1995 flight testing for angles of attack up to about 14-15 degrees, for angles of sideslip up to about 12 degrees and for rudder angles up to about 15 degrees. Above 15 degrees angle-of-attack, the aerodynamic data is weighted mid-way between pure wind tunnel data and a rational extrapolation of the flight data available below 15 degrees. Incorporation of this new model further improves the correlation between predicted rudder and rudder blowdown as shown in figure C-2.

The revisions to the model at high sideslip and high angles-of-attack resulted in changes that were only significant during full rudder sideslips. Figure C-3 shows the effect of the noted changes in the rudder hinge moment and aerodynamic coefficient models, in terms of their effect on the full rudder / full wheel crossover speed.

COMPARISON OF USAIR 427 ESTIMATED RUDDER POSITION VS. ESTIMATED RUDDER BLOWDOWN LIMIT

(BASED ON ORIGINAL AERO MODEL AND LINEAR INTERPOLATION OF HEADING)
(WAKE EFFECTS NOT ACCOUNTED FOR)

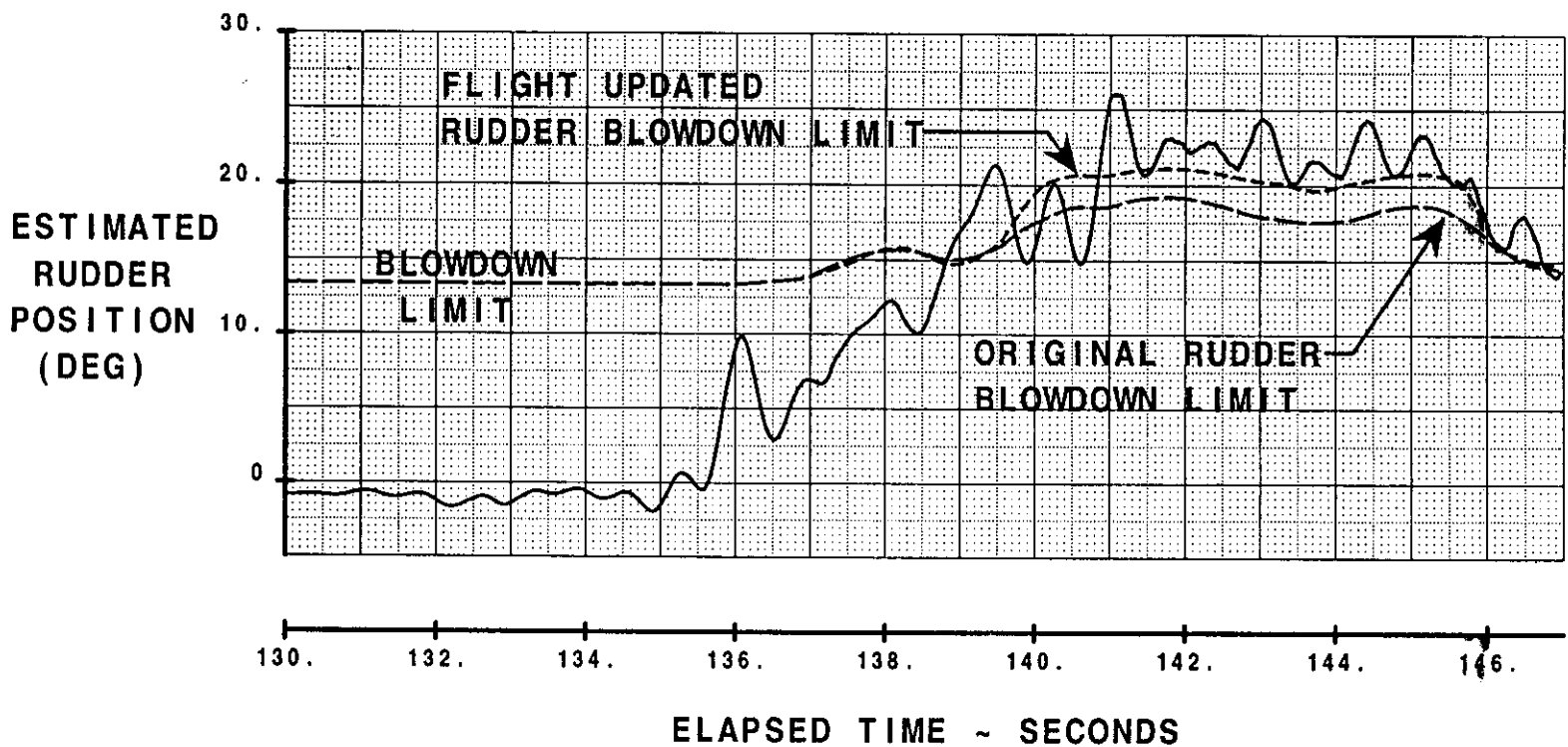


FIGURE C1

CALC	H. Dellicker	18SEP96	REVISED	DATE	Comparison of Estimated Rudder Position Vs. Estimated Rudder Blowdown Limit	THE BOEING COMPANY	PAGE
CHECK							
APR							
APR							
					737-300	USAIR 427	
					USAIR 427		

Fig. C-1

EFFECT OF AERO MODEL UPDATE ON USAIR 427 ESTIMATED RUDDER POSITION

(BASED ON LINEAR INTERPOLATION OF HEADING)
(WAKE EFFECTS INCLUDED)

ESTIMATED
RUDDER
POSITION
(DEG)

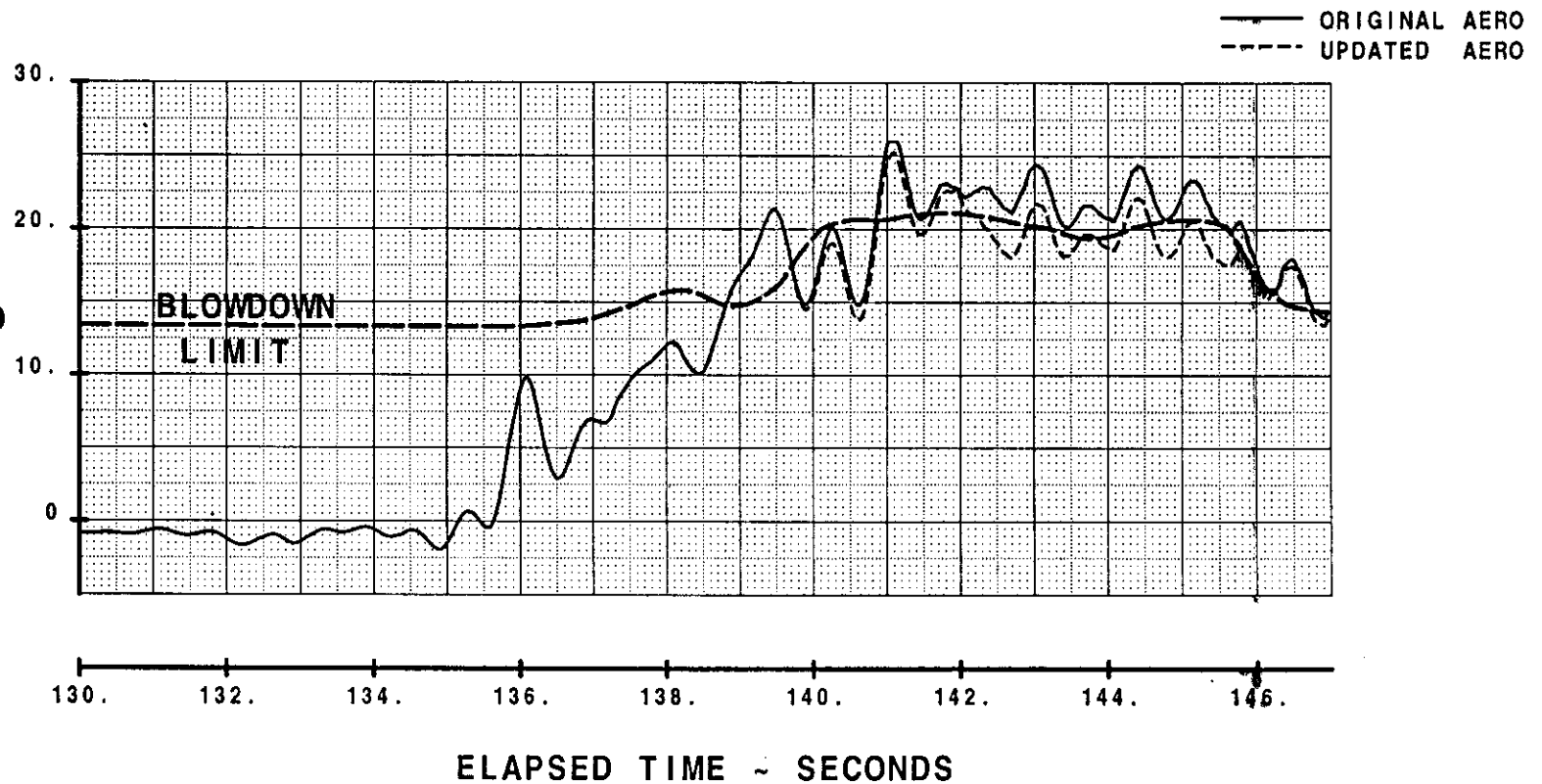


FIGURE C2

CAC	H. Dellicker	18SEP96	REVISED	DATE	Effect of Aero Model Update on USAir 427 Estimated Rudder Position (Linear Interpolated Heading)	
CHECK						
APR						
APR						
					THE BOEING COMPANY	
					PAGE	737-300
					USAir 427	

FIG. C-2

737-300

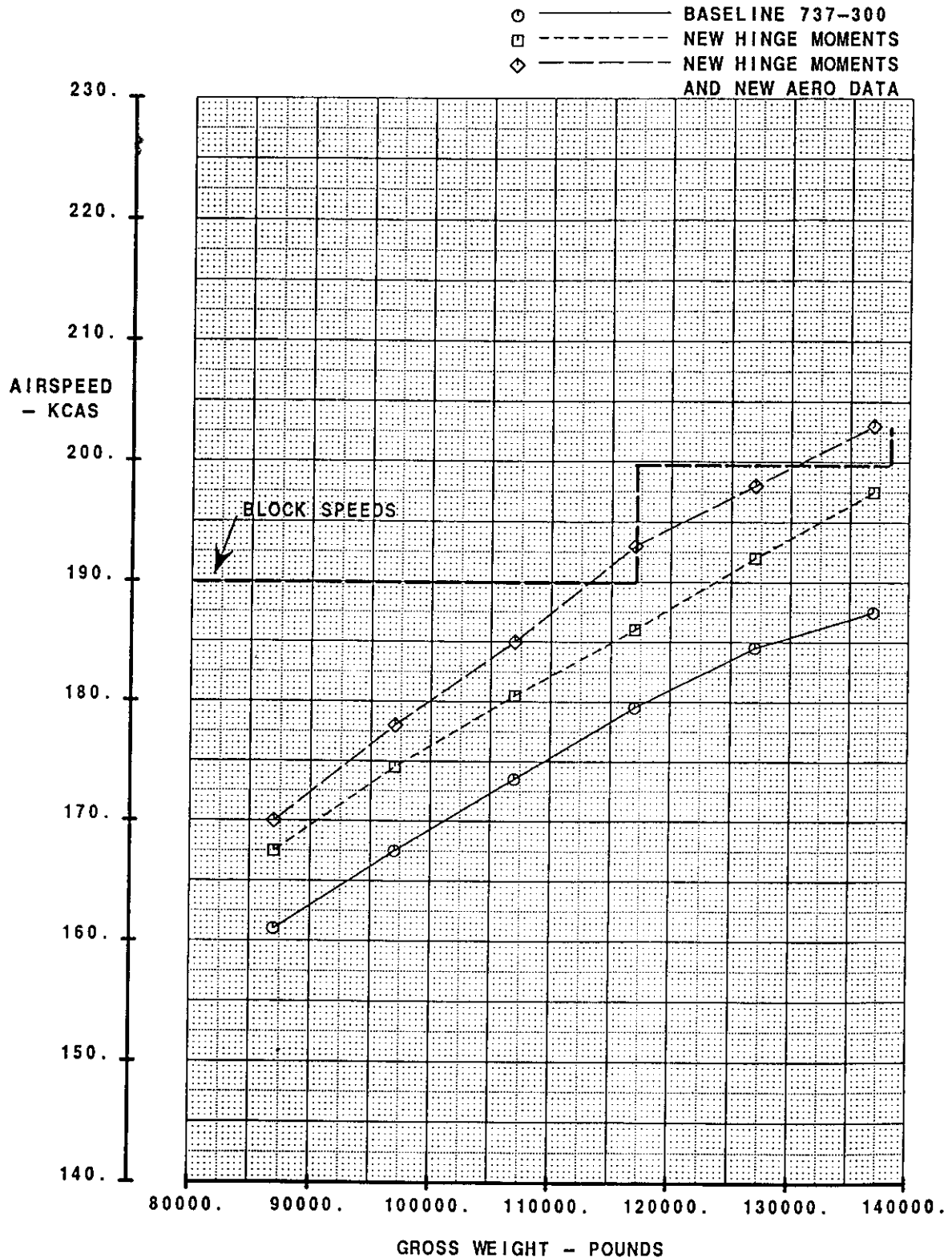


FIG. C-3

CALC	S. LEWIS	15OCT96	REVISED	DATE	CONTROL OF FULL RUDDER WITH FULL WHEEL FLAPS 1 EFFECT OF SIMULATOR DATA REVISIONS THE BOEING COMPANY	737-300
CHECK						
APR						
APR						
						PAGE

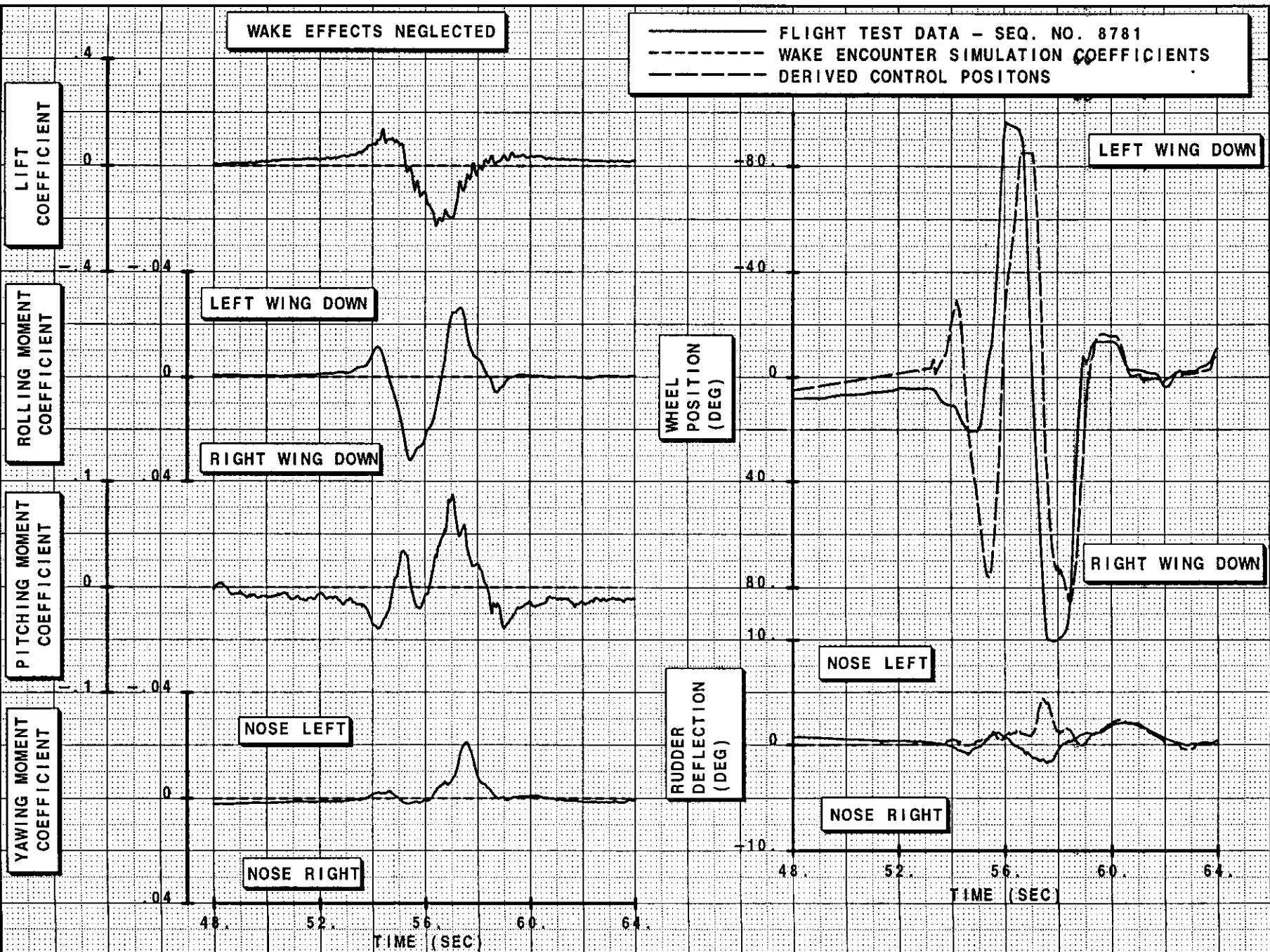
Appendix D. Validation of Wake Encounter Derivation Process

To validate the techniques used to derive the control inputs from the FDR data, several wake encounters from the flight test were evaluated. The validation was performed by placing the wake in each case in such a way as to match the derived flight test lift and pitching moment characteristics due to the wake, and using the resulting wake rolling and yawing moment characteristics to predict the wheel and rudder positions during the encounter. These predicted control positions were then compared to the actual recorded controls as a measure of the accuracy of the process.

Three validation cases are presented here. All three are from flight test number 19-08. The condition numbers are B1.41.0065.002.1, B1.41.0065.006 and B1.41.0065.006.1. Figures D-1 to D-6 show the results.

Figures D-1 and D-2 present the results for condition B1.41.0065.006, Figures D-3 and D-4 present the results for condition B1.41.0065.006.1, and Figures D-5 and D-6 present the results for condition B1.41.0065.002.1. In each case the match of the derived flight controls to the actual measured flight controls is shown with and without accounting for wake effects. In each case the match of wheel and rudder is improved when wake effects are included, and the overall match of control position magnitudes and characteristics is very good. This good agreement between estimated and measured control positions demonstrates the validity of the method used to derive the lateral and directional control positions for USAir 427.

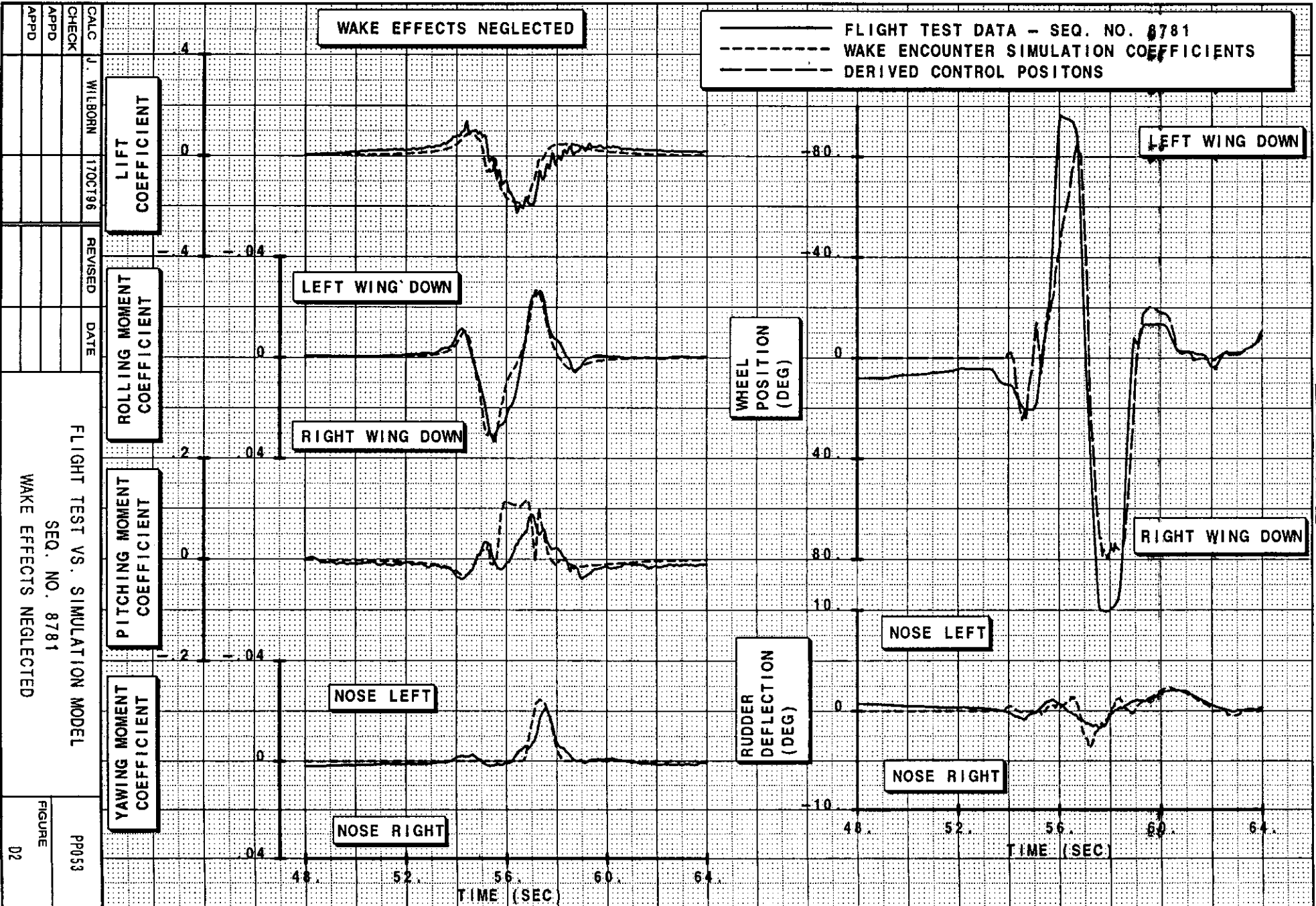
CALC	J. WILBORN	17OCT96	REVISED	DATE
CHECK				
APPD				
APPD				
FLIGHT TEST VS. SIMULATION MODEL				
SEQ. NO. 8781				
WAKE EFFECTS NEGLECTED				
FIGURE				
01				
PP053				



BOEING

_____ FLIGHT TEST DATA - SEQ. NO. 8781
 - - - - - WAKE ENCOUNTER SIMULATION COEFFICIENTS
 - - - - - DERIVED CONTROL POSITIONS

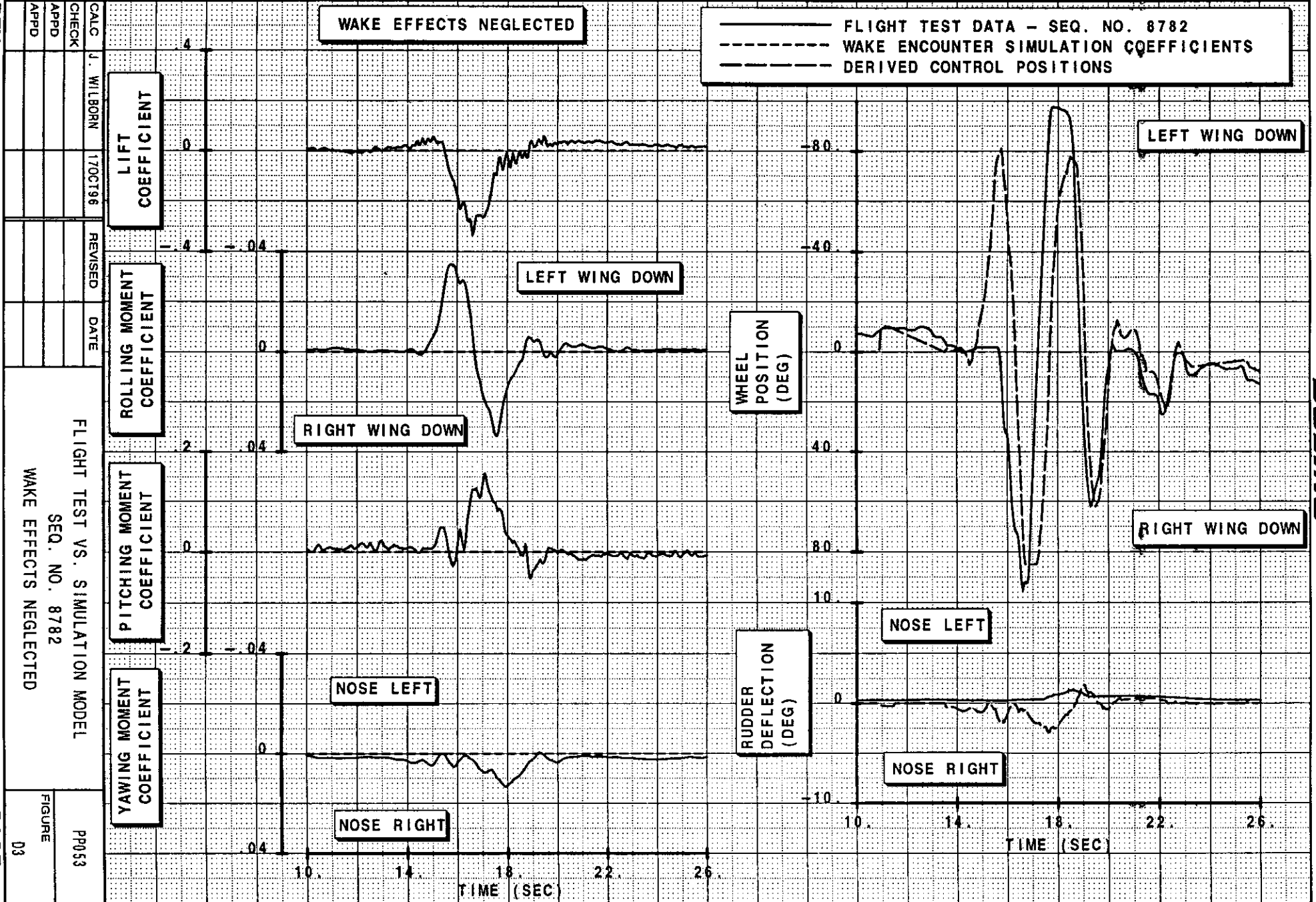
WAKE EFFECTS NEGLECTED



REV	CALC	J. WILBORN	17OCT196	REVISED	DATE	FLIGHT TEST VS. SIMULATION MODEL	PP053
	CHECK					SEQ. NO. 8781	FIGURE
	APPD					WAKE EFFECTS NEGLECTED	02
	APPD						
	APPD						

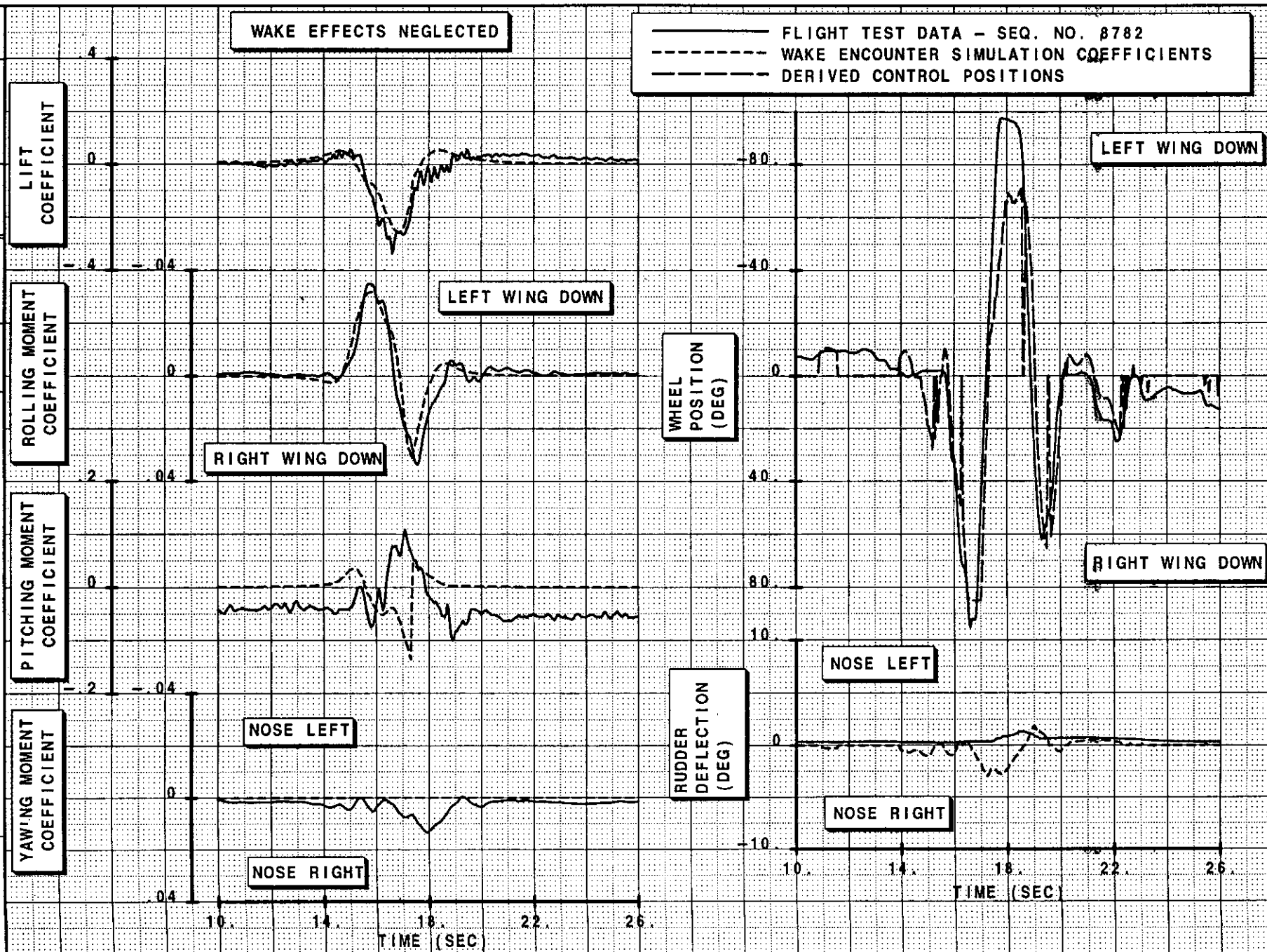
REV

PAGE



BOEING

CALC	J. WILBORN	170CT96	REVISED	DATE	FLIGHT TEST VS. SIMULATION MODEL SEQ. NO. 8782 WAKE EFFECTS NEGLECTED	PP053
CHECK						FIGURE
APPD						04
APPD						



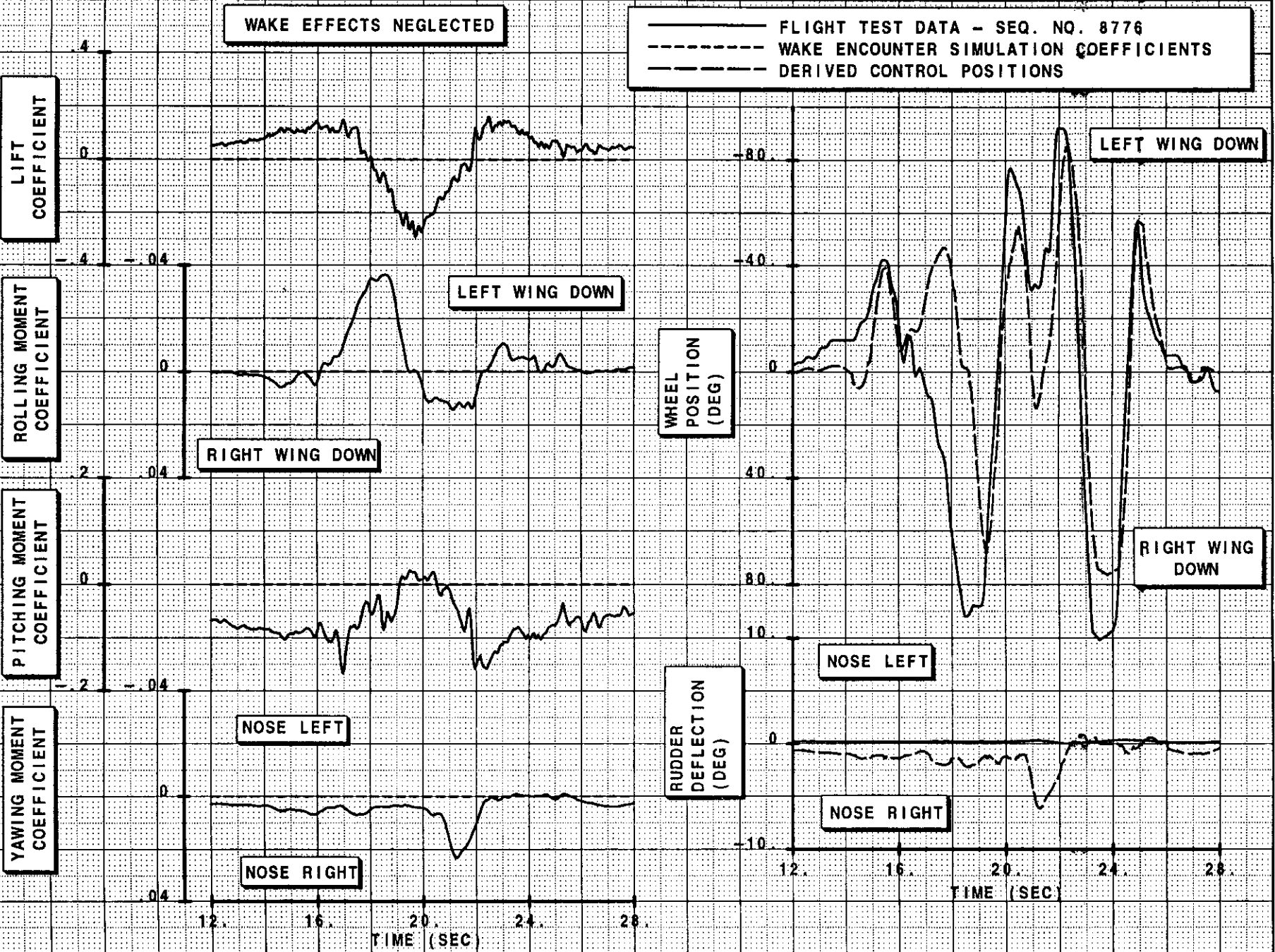
CALC	S. LEWIS	17OCT196	REVISED	DATE
CHECK				
APPO				
APPO				

FLIGHT TEST VS. SIMULATION MODEL
SEQ. NO. 8776
WAKE EFFECTS NEGLECTED

PPO53

FIGURE

05



REV

APPD

APPD

CHECK

CALC

S. LEWIS

17OCT96

REVISED

DATE

WAKE EFFECTS INCLUDED

SEQ. NO. 8776

FLIGHT TEST VS. SIMULATION MODEL

PAGE

D6

FIGURE

PP053

WAKE EFFECTS INCLUDED

— FLIGHT TEST DATA - SEQ. NO. 8776
 --- WAKE ENCOUNTER SIMULATION COEFFICIENTS
 - - - DERIVED CONTROL POSITIONS

LIFT
COEFFICIENTROLLING MOMENT
COEFFICIENTPITCHING MOMENT
COEFFICIENTYAWING MOMENT
COEFFICIENT

LEFT WING DOWN

RIGHT WING DOWN

WHEEL
POSITION
(DEG)RUDDER
DEFLECTION
(DEG)

LEFT WING DOWN

RIGHT WING
DOWN

NOSE LEFT

NOSE RIGHT

NOSE RIGHT

NOSE LEFT

TIME (SEC)

BOEING

APPENDIX E. Methodology for Correcting for the Effects of Low Sample Rate

Given airplane heading at a rate of at least two samples per second, along with roll and pitch attitude, vertical and longitudinal acceleration, and airspeed and altitude, it is possible to derive a detailed representation of rudder position to within an accuracy of about one degree. Figure E-1 shows a comparison of measured and derived rudder position for a series of five flight test rudder-step conditions. These conditions were flown in the simulator validation flight test prior to the wake effects testing in Atlantic City.

Figure E-2 shows the effect of airplane heading sample rate on the accuracy of derived rudder position. As previously stated, derived rudder position is generally accurate to within about one degree when heading sample rate is at least two per second. When the sample rate is less than two per second, however, the rudder position estimate becomes contaminated with noise produced by the digital filter used to process the data. The effect of this contamination is seen as an oscillation in the rudder estimate, with a period of about 0.75 seconds and a peak-to-peak amplitude that can exceed ten degrees.

In regions of a flight maneuver where rudder position is known or can be inferred from other information (such as when rudder reaches its blowdown limit), it is possible to derive a continuous heading trace between the low-sample rate data points that are known from measurement. This heading trace accurately represents the airplane heading during the period of time where rudder position is known or can be inferred.

The process used to accomplish this is an iterative one. Starting with a linear interpolation of heading between the known data points, small modifications are made to the heading data between the known points and then rudder position is re-derived until the artificial oscillations in the derived rudder position are minimized around the known or inferred rudder position. The following constraints are observed in the process of deriving the continuous heading trace:

- 1) Only the interpolated regions between known data points may be changed.
- 2) The resulting curve must be smooth and continuous through each data point.

Figure E-3 illustrates the improvement that can be gained in derivation of rudder and heading with this methodology, using an example from the Atlantic City flight test. The top half of Figure E-3 present derived rudder position using airplane heading data at a sample rate of once per second, compared to the actual measured rudder position. The derived rudder position shows the effect of sample-rate induced noise, as described above, with a maximum peak-to-peak amplitude of about six degrees. The bottom half of Figure E-3 presents the results of using the above process of to derive a heading between the known points during the interval where rudder position is known. The derived heading is nearly an exact re-creation of the measured heading trace.

Furthermore, the derived rudder shows a significant reduction in signal noise, and is a much more accurate representation of the measured rudder position.

The end result of this effort is an improved knowledge of the boundary conditions (i.e., characteristics) of the heading trace at the edge of adjoining regions where rudder position is not known. Applying these new boundary conditions, along with the requirement that the data be smooth and continuous, it is then possible to create an accurate representation of the actual airplane heading during those periods of unknown rudder deflection. The new heading data are then used to derive a final, more accurate rudder position with minimum artificial signal noise during the time intervals where rudder is not known or cannot be inferred.

Figures E-4 and E-5 illustrate the application of this methodology to the USAir 427 accident data in the region where the rudder is believed to be deflected to the blowdown limit. The resulting heading trace is smooth, continuous, goes through all the known data points, and is consistent with expected airplane behavior.

The resultant slopes of the heading trace at times of 135 and 138.2 provide the boundary conditions needed for re-interpolating heading in the interval between 135 and 138.2, where the rudder position is unknown and cannot be inferred because the airplane is in the influence of the wake. The heading derived for this time interval and the corresponding derived rudder are presented in Figure E-6. Note that this rudder was not derived with wake effects taken into account, and therefore represents the total effect of wake-induced yaw and actual rudder deflection.

Figure E-7 shows a comparison between the predicted rudder blowdown limit and the derived rudder position (with and without predicted wake effects.) It appears that the rudder is generally against the blowdown limit after an elapsed time of 138.2 seconds, with the exception of the 1.5 second period from 139.5 to 141.

The depression of rudder position below the blowdown limit line, from 139.5 to 141, may indicate that the rudder is lagging behind, momentarily, as the blowdown limit increases with increasing sideslip angle. Similarity in the shape of the predicted rudder and blowdown limit, however, tends to suggest that the rudder is actually up against the real blowdown limit. This would indicate that the rudder hinge moment model may need further refinement in that range of sideslip angles.

CALC.	H. D. 11/11/11	2/00/78	REVISED	DATE
CHECK	APR			
APR				
APR				
Rudder-Step Proof of Match Conditions				
THE BOEING COMPANY				
PAGE				737-300

RUDDER-STEP PROOF OF MATCH CONDITIONS

— FDR DATA
 ---- KINEMATIC ANALYSIS

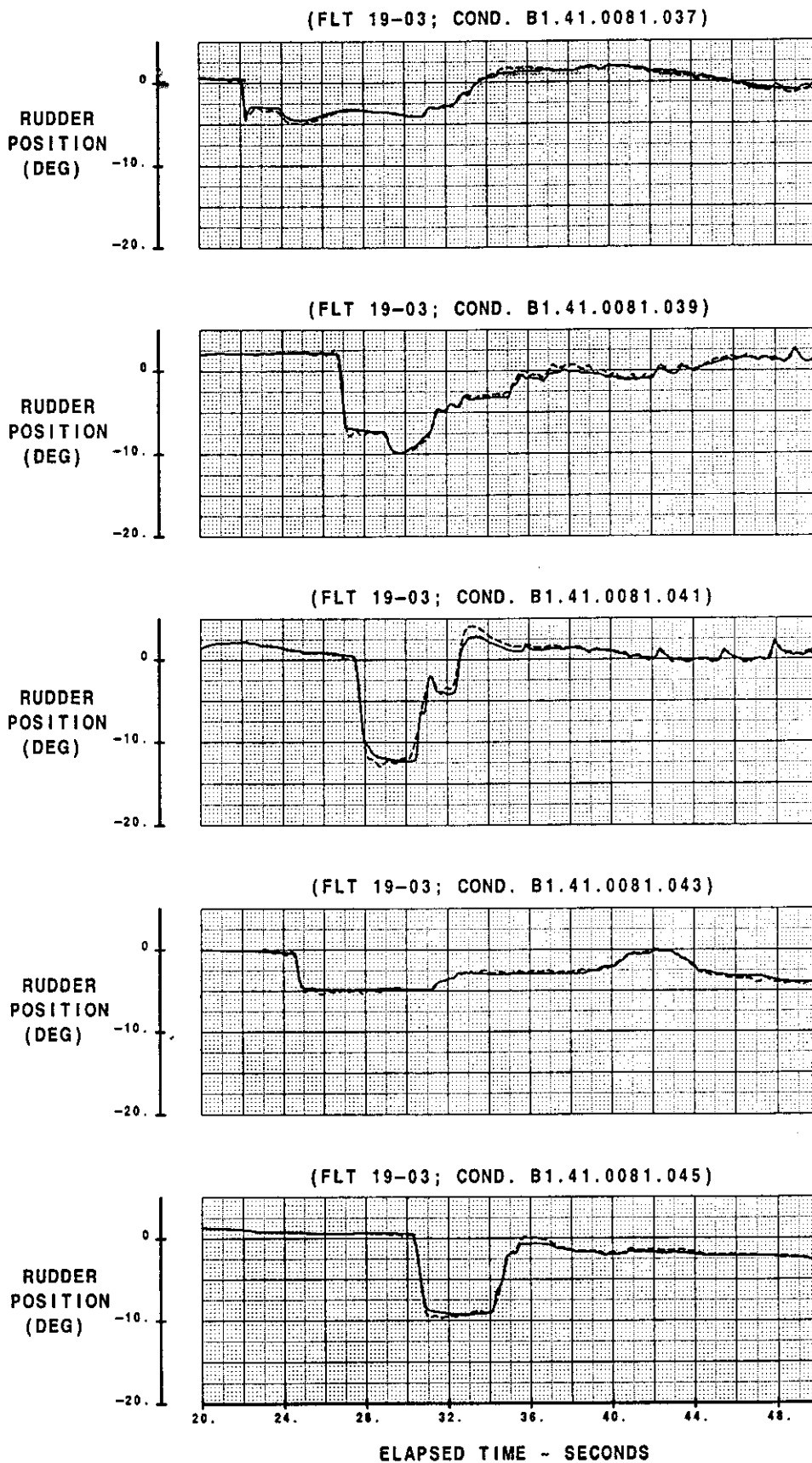


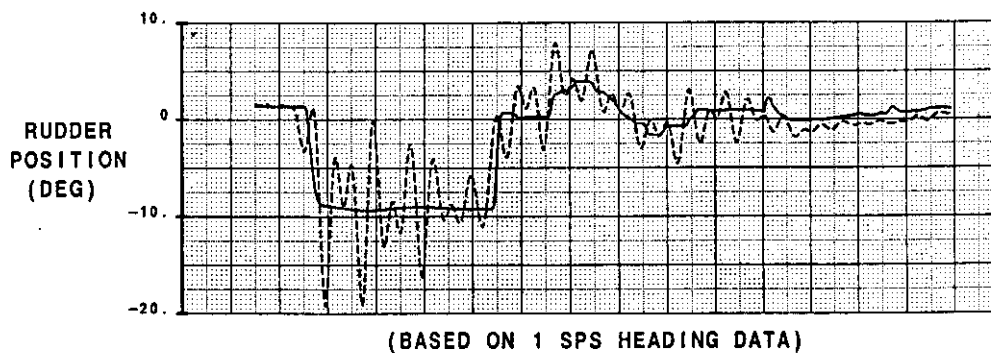
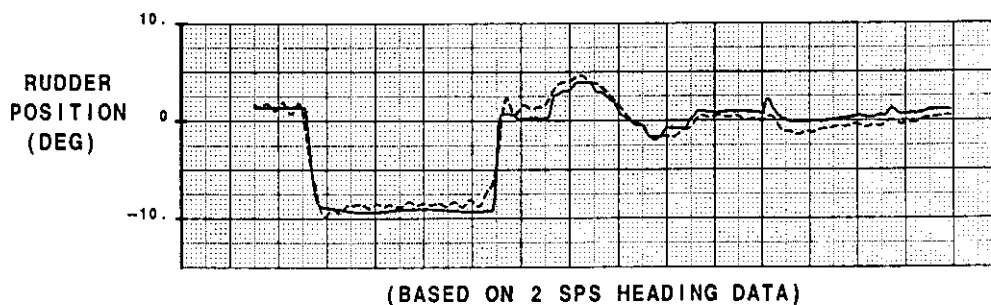
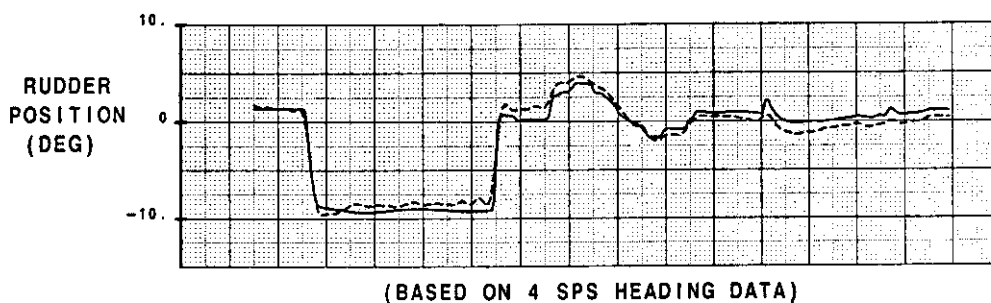
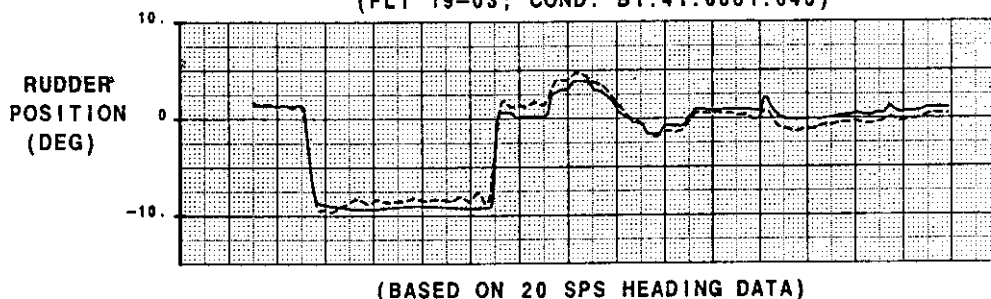
FIGURE E-1

CALC	REV	DATE	2/05/85
CHECK	REV	DATE	
APR	REV	DATE	
APR	REV	DATE	
Effect of Data Sample Rate on "Noise" in Rudder Position Predictions from Kinematic Analysis			
THE BOEING COMPANY			
PAGE			737-300

EFFECT OF DATA SAMPLE RATE ON "NOISE" IN RUDDER POSITION PREDICTIONS FROM KINEMATIC ANALYSIS

(FLT 19-03; COND. B1.41.0081.046)

— FDR DATA
- - - KINEMATIC ANALYSIS



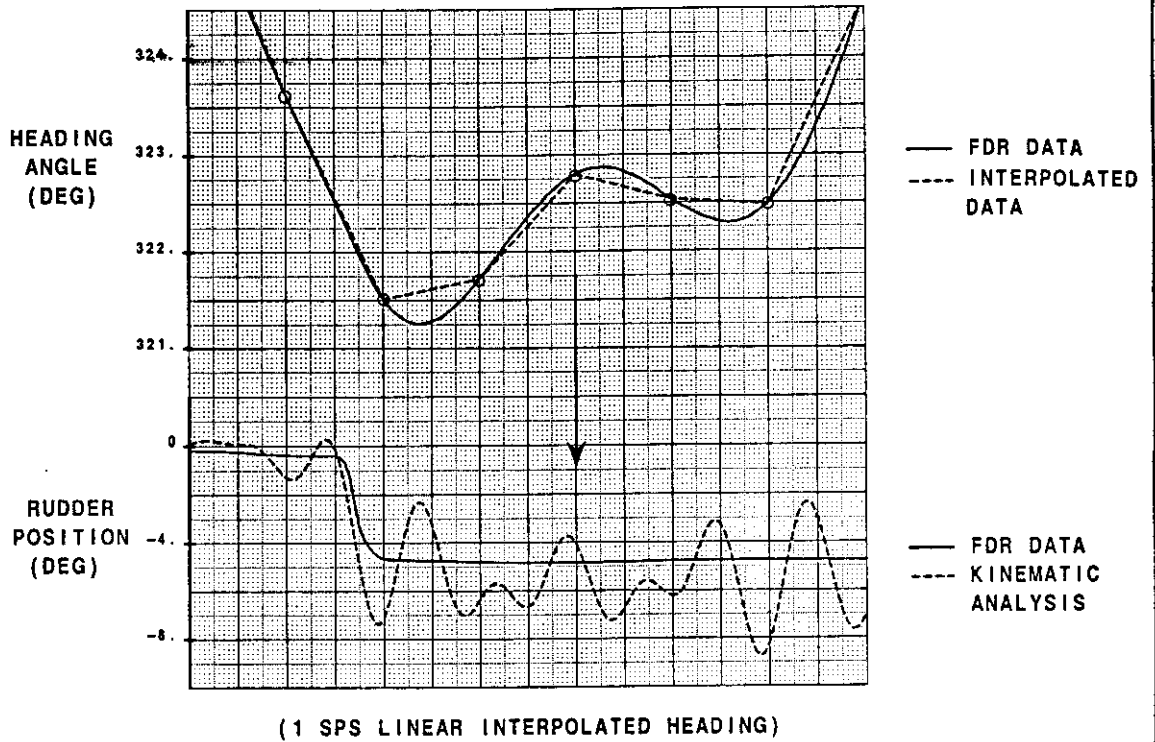
28. 32. 36. 40. 44. 48. 52. 56. 60.

ELAPSED TIME - SECONDS

CALC	H. Dillinger	2/10/78	REVISED	DATE	Demonstration of Enhancement Technique For Low Sample Rate Heading Data	717-300
CHECK						
APR						
MAY						
THE BOEING COMPANY					PAGE	

DEMONSTRATION OF ENHANCEMENT TECHNIQUE FOR LOW SAMPLE RATE HEADING DATA

(FLT 19-03; COND. B1.41.0081.043)



(ENHANCED, NON-LINEAR INTERPOLATED HEADING)

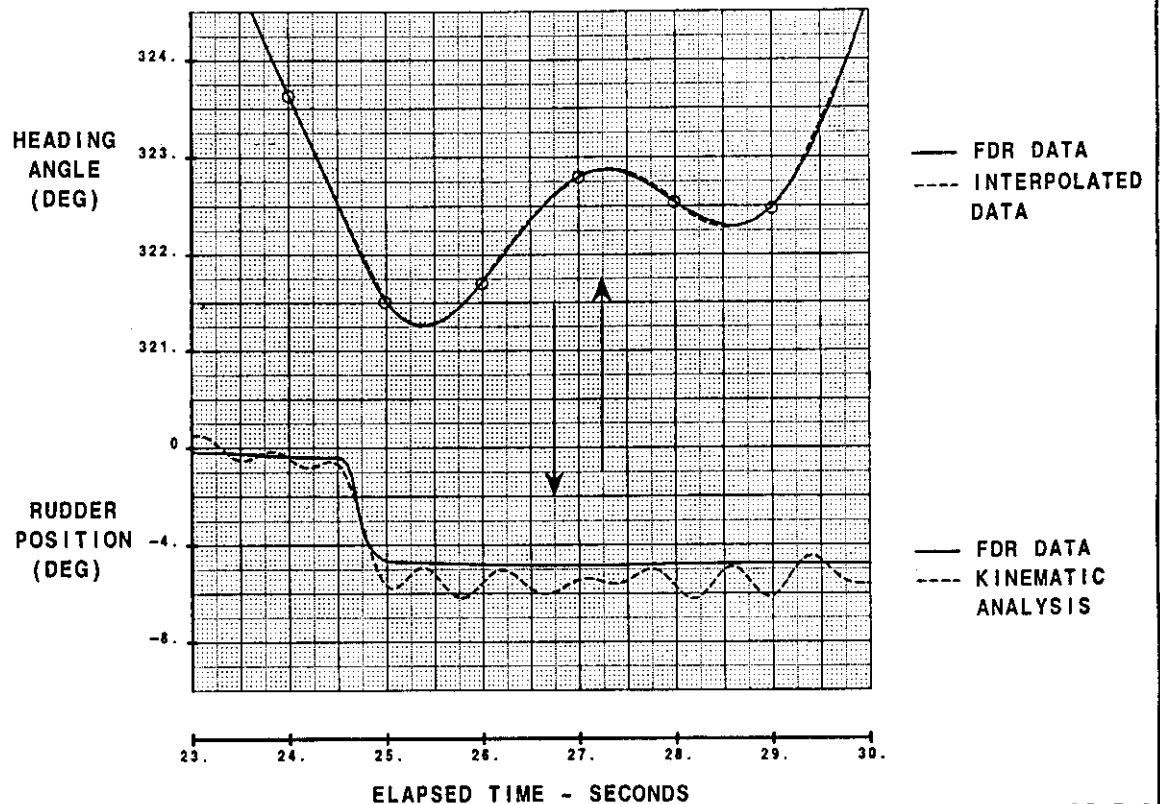


FIGURE E-3

CALC	DATE	2/20/78	REVISION		DATE	
CHECK	DATE					
APR						
APR						
Development of a Non-Linear Interp. of the USAir 427 Heading Data (Part 1)						777-309
THE BOEING COMPANY						PAGE

DEVELOPMENT OF A NON-LINEAR INTERPOLATION OF THE USAIR 427 HEADING DATA (PART 1)

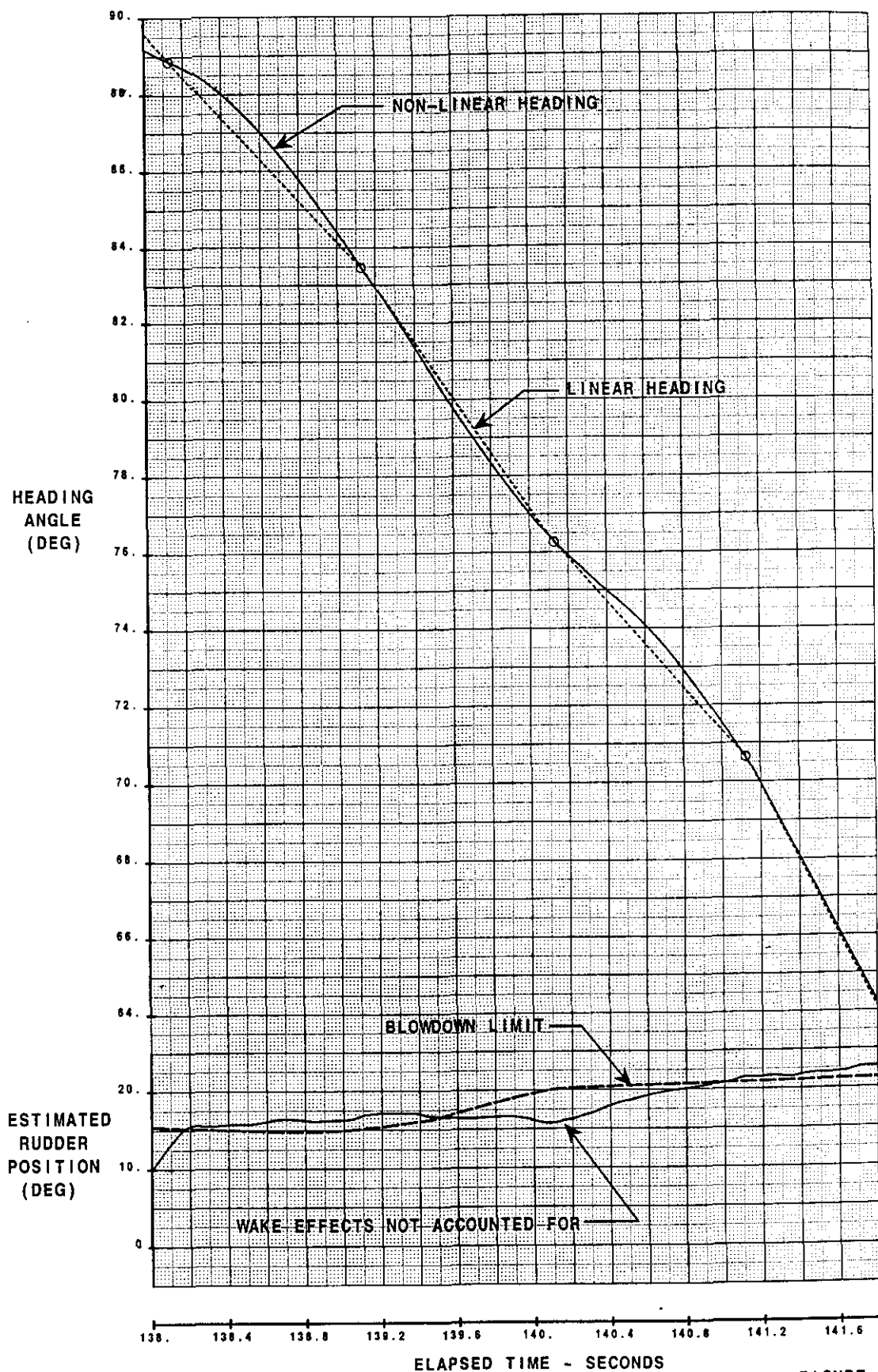


FIGURE E-4

DATE	10/18/78	REVISION	
CHECK		DATE	
APR			
APR			
Development of a Non-Linear Interp. of the USAir 427 Heading Data (Part 1b)			
THE BOEING COMPANY			
PAGE			737-500

DEVELOPMENT OF A NON-LINEAR INTERPOLATION OF THE USAIR 427 HEADING DATA (PART 1b)

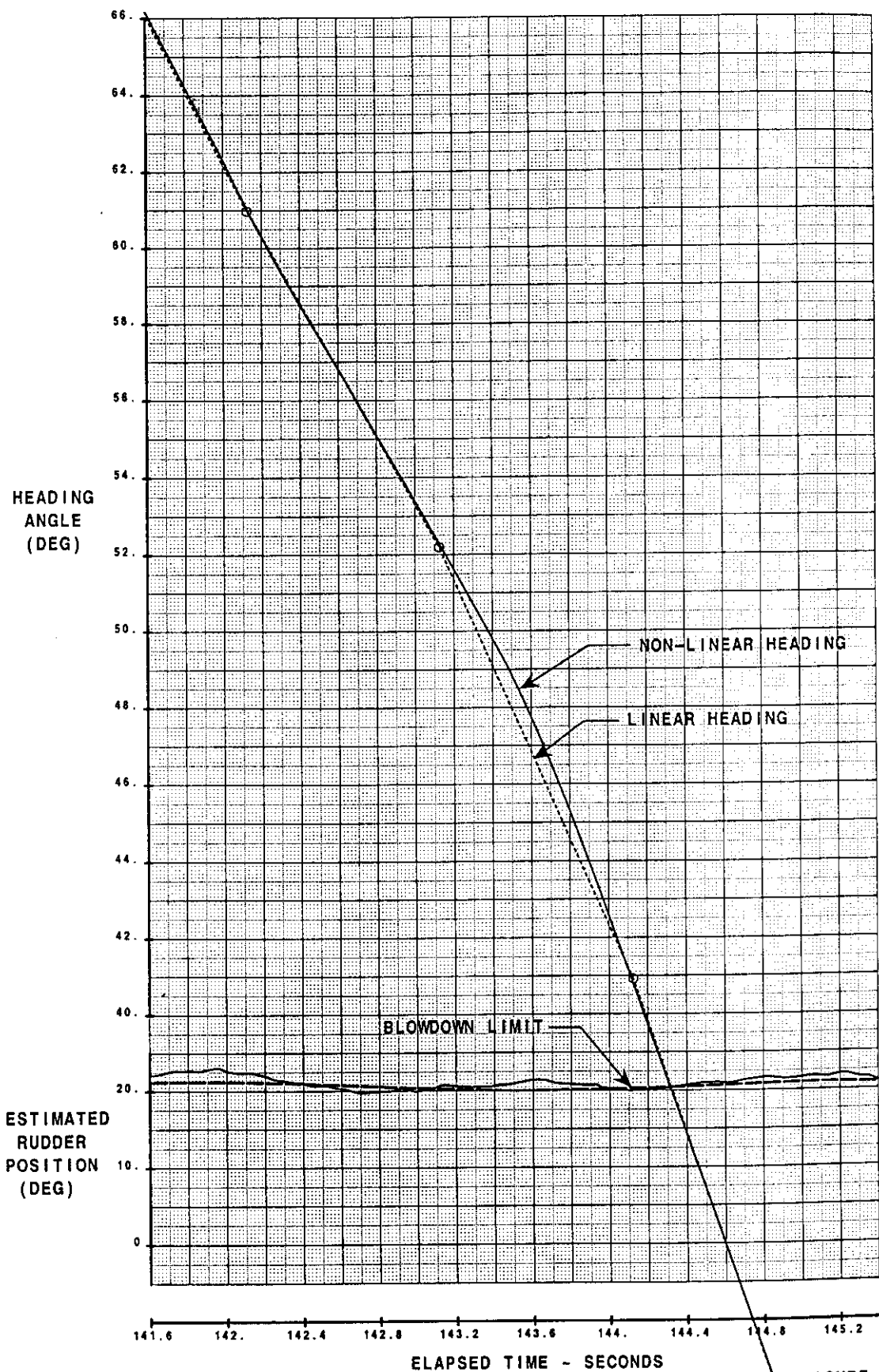


FIGURE E-5

CALC	H. Dattler	2/02/86	REVISION	DATE	Development of a Non-Linear Interp. of the USAir 427 Heading Data (Part 2)	737-300
CHECK						
APP						
APP						
THE BOEING COMPANY						PAGE

DEVELOPMENT OF A NON-LINEAR INTERPOLATION OF THE USAIR 427 HEADING DATA (PART 2)

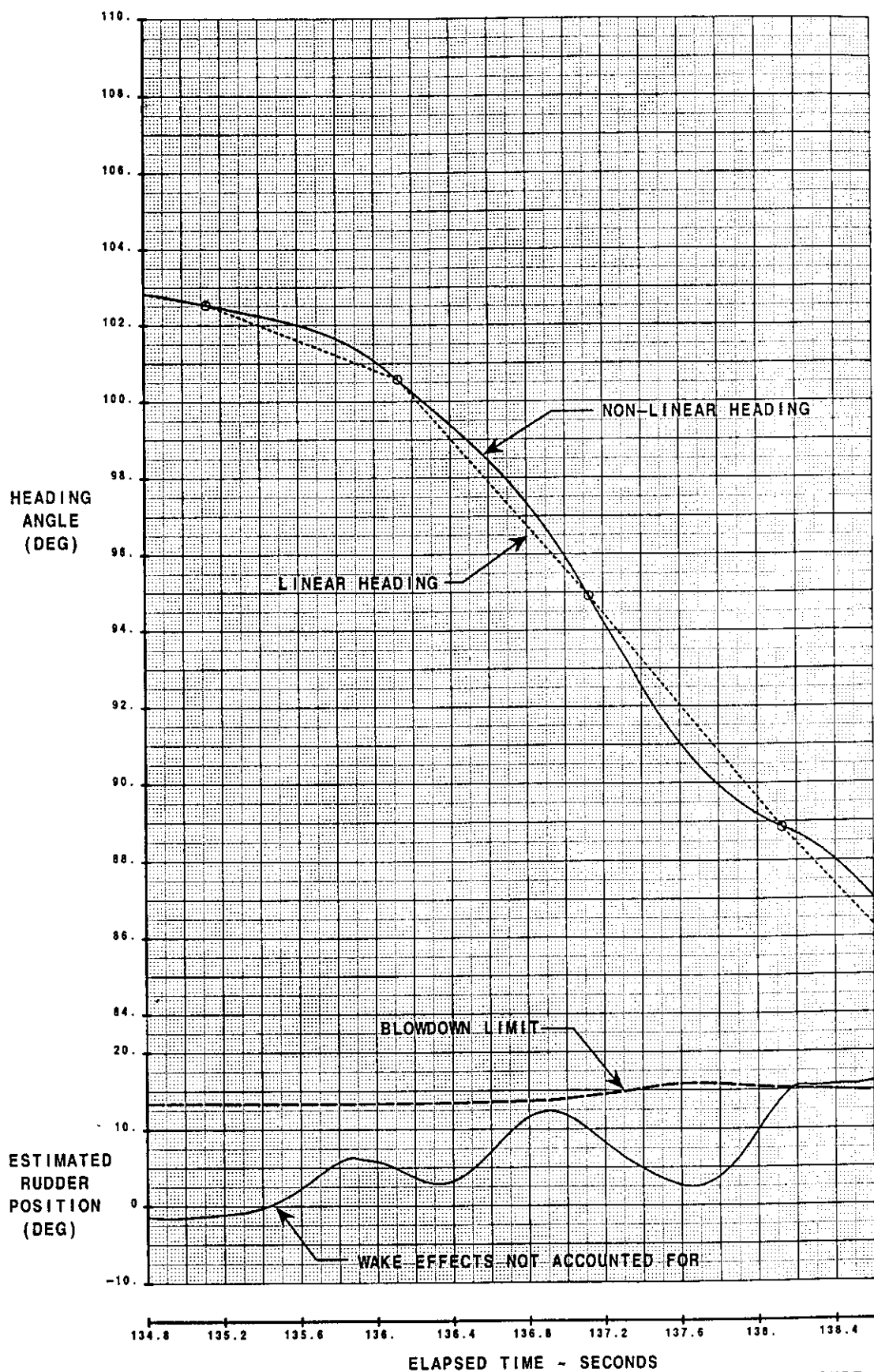
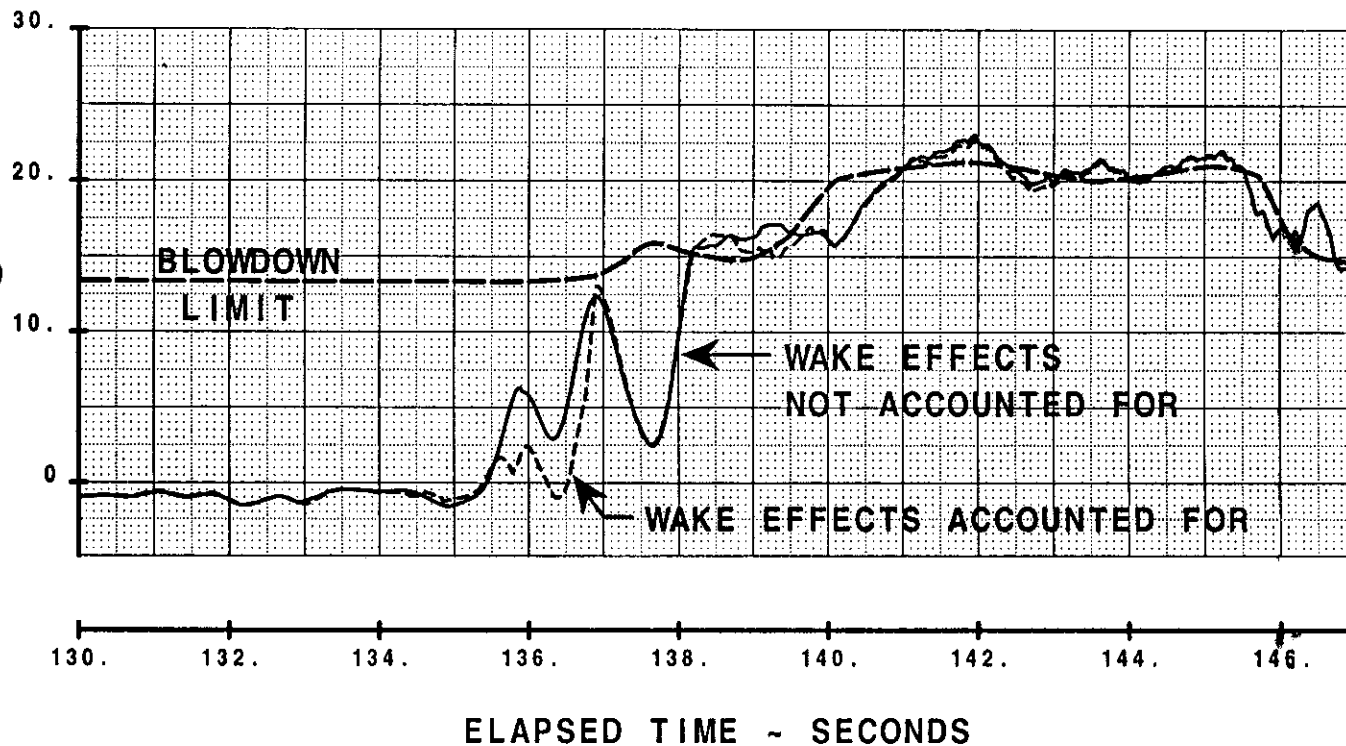


FIGURE E-6

EFFECT OF ESTIMATED WAKE INDUCED YAWING MOMENT ON USAir 427 ESTIMATED RUDDER POSITION

(BASED ON UPDATED AERO MODEL)
(NON-LINEAR HEADING INTERPOLATION)

ESTIMATED
RUDDER
POSITION
(DEG)



ELAPSED TIME ~ SECONDS

FIGURE E-7

CALC	H. Dellinger	2100T96	REVISED	DATE	THE BOEING COMPANY	Effect of Estimated Wake Induced Yawing Moment on USAir 427 Estimated Rudder	737-300	PAGE	USAir 427
CHECK									
APR									
APR									

Fig E-7

APPENDIX F. Parametric Study of Wake Position and Characteristics

The solutions for derived wheel and rudder position presented in Figure 17 of the main document represent those which give the best match of lift and pitching moment characteristics attributable to the wake. This solution also meets the boundary condition at time 135.2 in that the location of the wake impacts the fuselage of the aircraft as necessary to produce the “thump” heard on the USAir 427 CVR at that time.

A parametric study to observe the effects of changing the wake location and characteristics on the derived wheel and rudder positions is presented in this Appendix. In this study the wake was translated up to 15 ft in each direction from the nominal location presented in Figures 13 and 14 in the main document. In addition, wake circulation strength was varied from 500 ft^2/sec to 2400 ft^2/sec , and wake core radius was varied from 1 ft up to 10 ft.

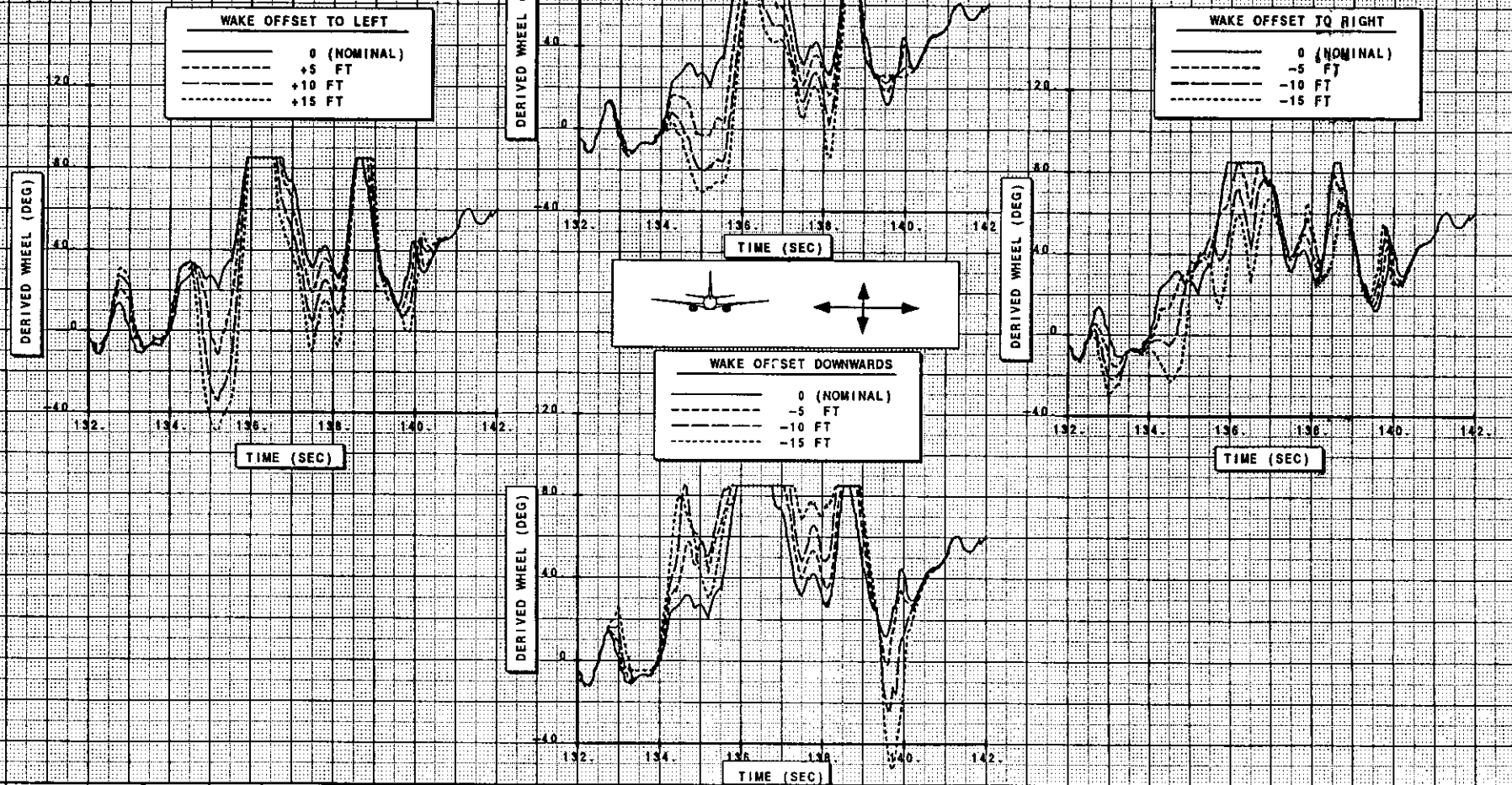
Figure F-1 presents the results of the study as pertains to the derived wheel. Because the wake-induced rolling moment is roughly equivalent to full wheel power for the 737, the variation of wake position can have a significant impact on the derived wheel position. However, in each case several characteristics are always present. Notably, in all cases a strong right wheel input is derived between times 136-137, and again at time 138.5. The largest variation between the cases occurs at time 135: derived wheel varies from nearly half left authority to full right authority. However, the solution at this time is constrained to be very close to the nominal solution in order to meet the boundary condition mentioned previously - the “thump” resulting from the wake impacting the fuselage.

Figure F-2 presents the results of the study as pertains to derived rudder. In this case the wake-induced yawing moment is much less than that which can be generated by full rudder on the 737. The result is that the rudder solution does not vary with position nearly as much as the wheel solution. The nature of the rudder solution in all cases contains an rapid input at time 137, followed by a rapid release at time 137.5, and the followed again by another rapid left input to blowdown at time 138.5. In the case where the wake is moved upwards, an additional release and input is derived from time 138.5 to 139.2. In some cases the small initial rudder input at time 136 is slightly amplified, and in others is slightly decreased; all are within the level of yawing moment that can be induced by the wake. The second spike and the step to blowdown that follow, however, are beyond the level of yawing moment that can be caused by the wake. Therefore, these characteristics are definite reflections of rudder movement.

Figure F-3 presents the root mean square (RMS) error for lift and pitching moment matches as a function of position. As the position of the wake was moved, the error in the match between lift and pitching moment increased from the nominal value. This is an indication that the nominal derived wake location is very close to that required to provide the best match of lift and pitching. This wake location would also result in the thump heard on the CVR at time 135.2. Significant movement of the wake from this position would not meet this boundary condition.

Figures F-4 and F-5 present the results of changing wake characteristics. In all cases the solution for rudder remains relatively unchanged, which again reflects that the wake yawing moment characteristics are minor compared to the magnitude of the rudder position. Derived wheel position is affected to a larger degree by changing circulation; in effect the change in circulation merely scales the level of wake rolling moment directly - the actual characteristics do not change significantly.

EFFECT OF WAKE POSITION ON DERIVED WHEEL POSITION



CALC	J. WILBORN	15OCT96	REVISED	DATE
CHECK				
APPD				
APPD				

EFFECT OF WAKE POSITION
ON DERIVED WHEEL POSITION

737-300

FIGURE

F1

PAGE

REV

EFFECT OF WAKE POSITION ON
DERIVED RUDDER POSITION

WAKE OFFSET UPWARDS

— 0 (NOMINAL)
- - - +5 FT
- - - +10 FT
- - - +15 FT

WAKE OFFSET TO LEFT

— 0 (NOMINAL)
- - - +5 FT
- - - +10 FT
- - - +15 FT

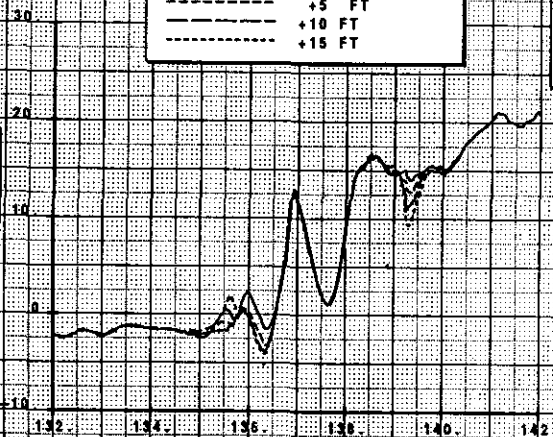
WAKE OFFSET TO RIGHT

— 0 (NOMINAL)
- - - -5 FT
- - - -10 FT
- - - -15 FT

WAKE OFFSET DOWNWARDS

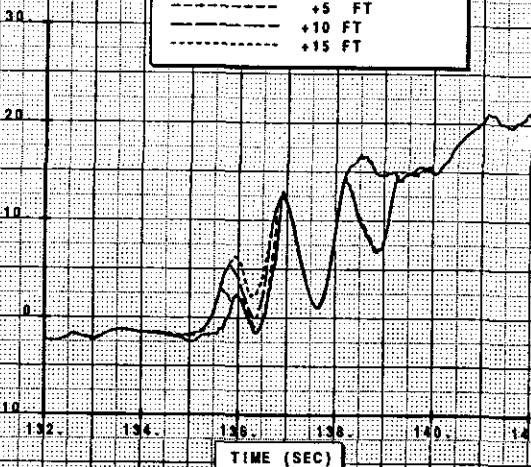
— 0 (NOMINAL)
- - - -5 FT
- - - -10 FT
- - - -15 FT

DERIVED RUDDER (DEG)

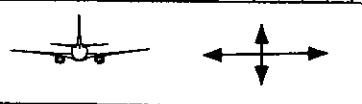


TIME (SEC)

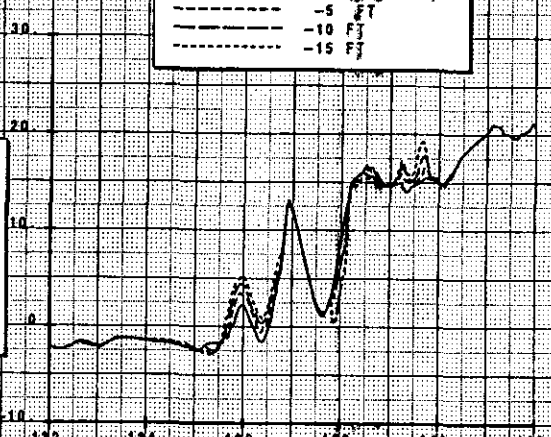
DERIVED RUDDER (DEG)



TIME (SEC)

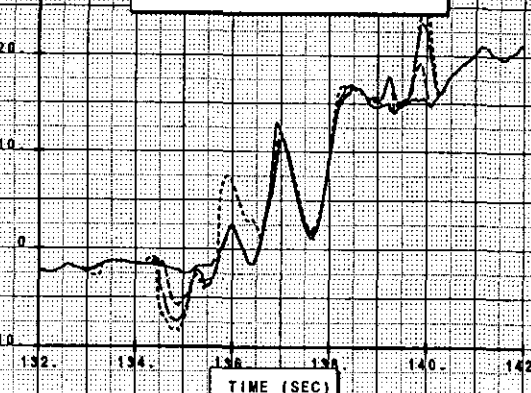


DERIVED RUDDER (DEG)



TIME (SEC)

DERIVED RUDDER (DEG)



TIME (SEC)

CALC	J. WILBORN	15OCT86	REVISED	DATE
CHECK				
APPD				
APPD				

EFFECT OF WAKE POSITION
ON DERIVED RUDDER POSITION

737-300

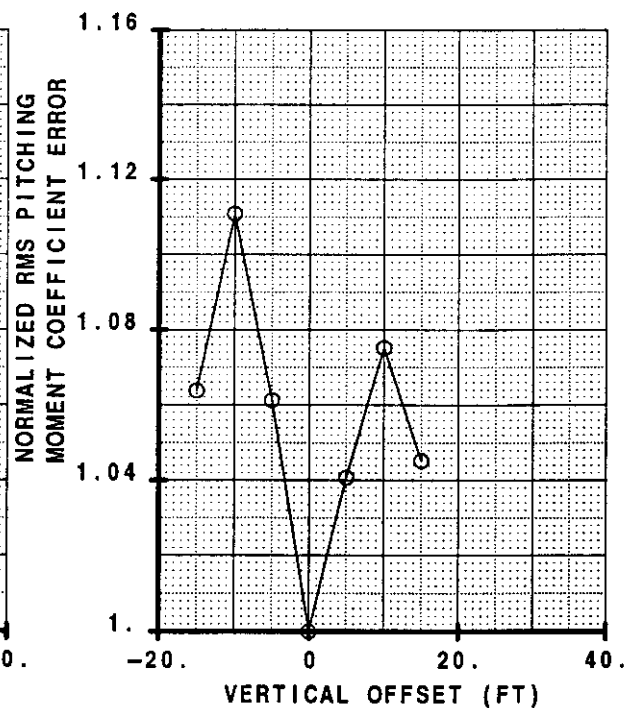
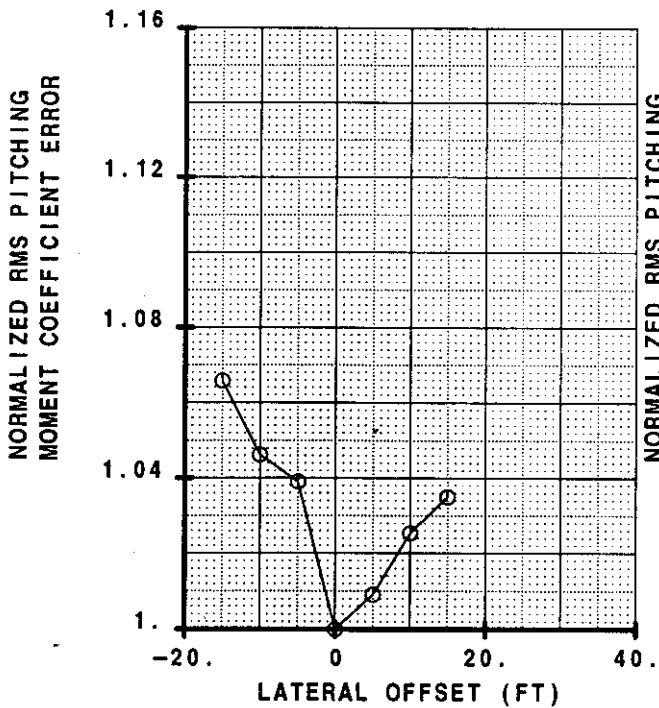
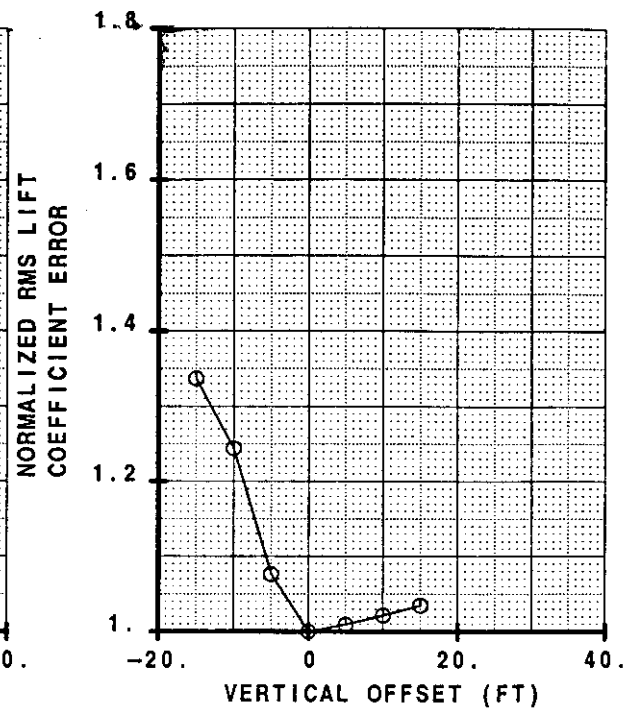
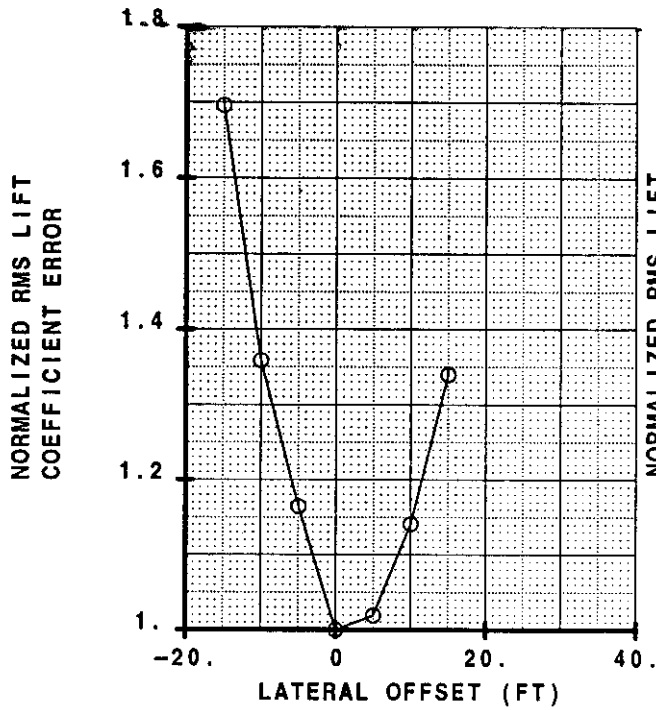
FIGURE

F2

PAGE

REV

**NORMALIZED ROOT MEAN SQUARE ERRORS
VARIATION WITH LATERAL AND VERTICAL
DISPLACEMENT OF WAKE FROM NOMINAL**



CALC	J. WILBORN	15OCT96	REVISED	DATE
CHECK				
APPD				
APPD				
REV				

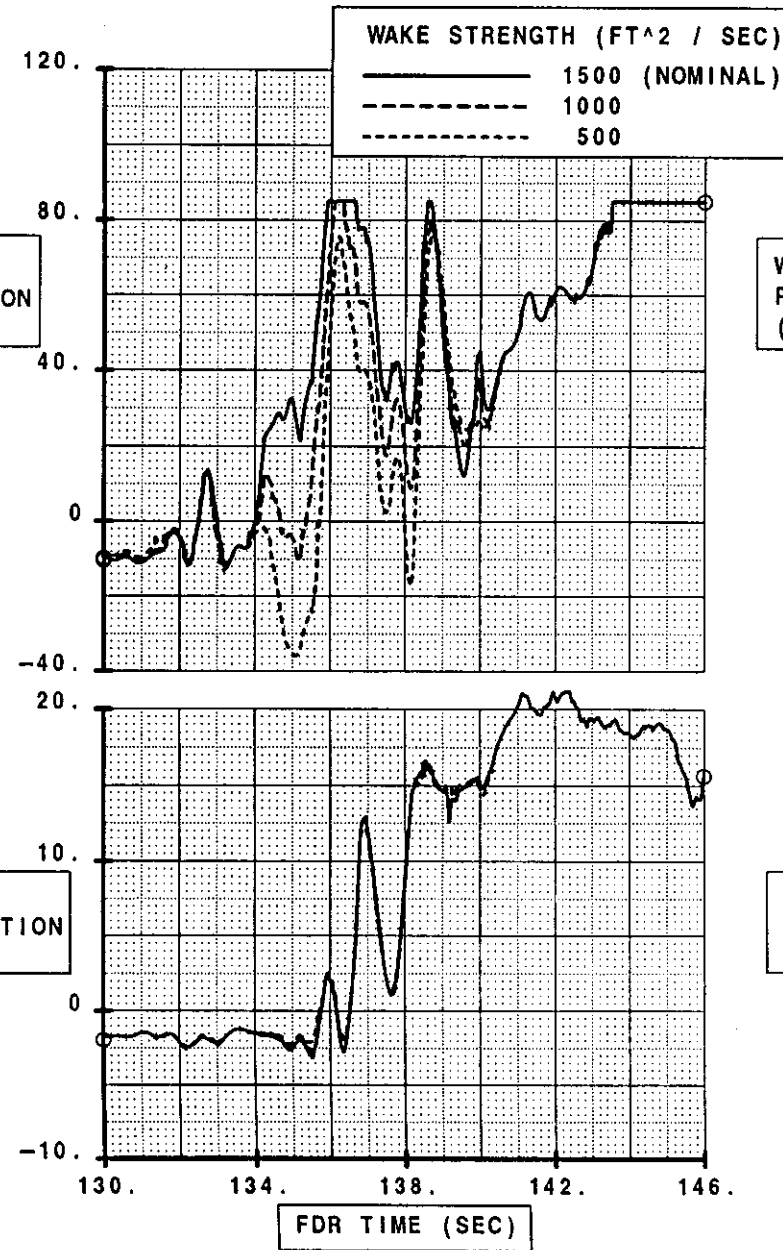
NORMALIZED RMS ERRORS IN LIFT AND
PITCHING MOMENT AS FUNCTIONS OF LATERAL
AND VERTICAL OFFSETS FROM NOMINAL

FIGURE
F3

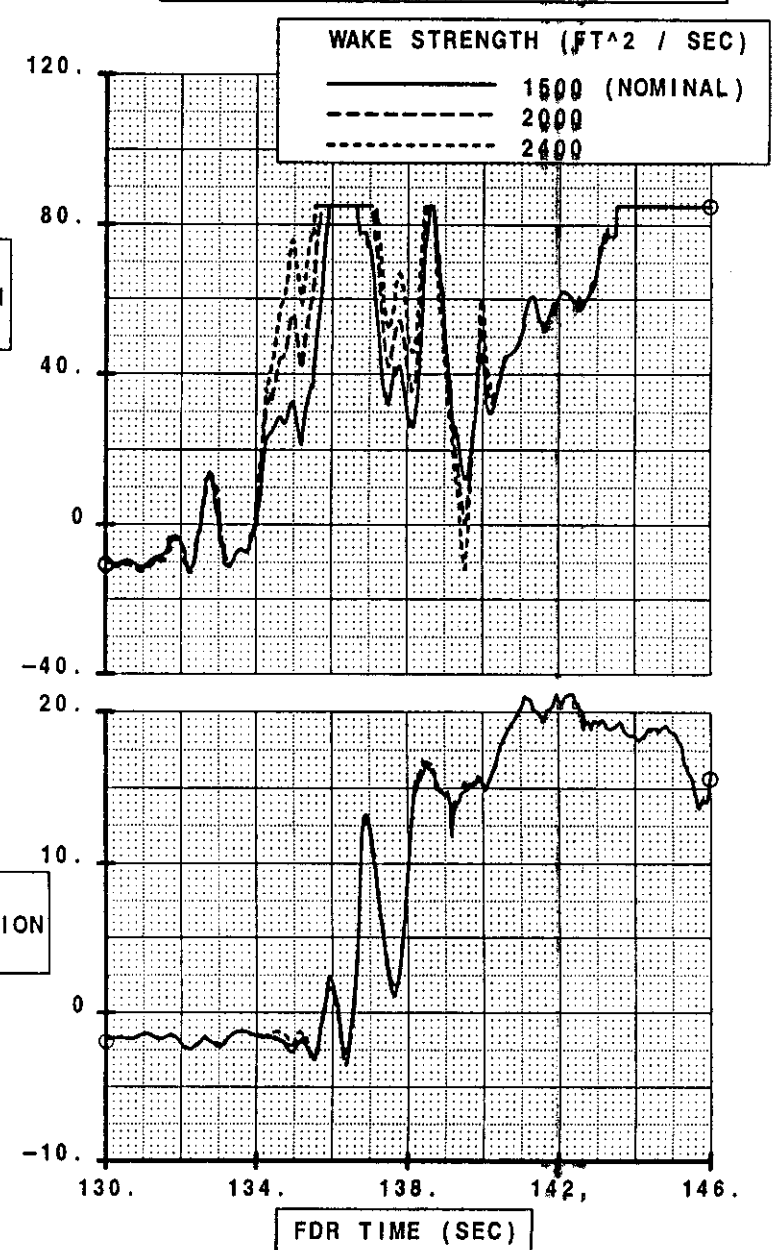
CALC	J. WILBORN	220C196	REVISED	DATE	EFFECT OF WAKE STRENGTH ON DERIVED WHEEL AND RUDDER POSITION
CHECK					
APPD					
APPD					

FIGURE
F4

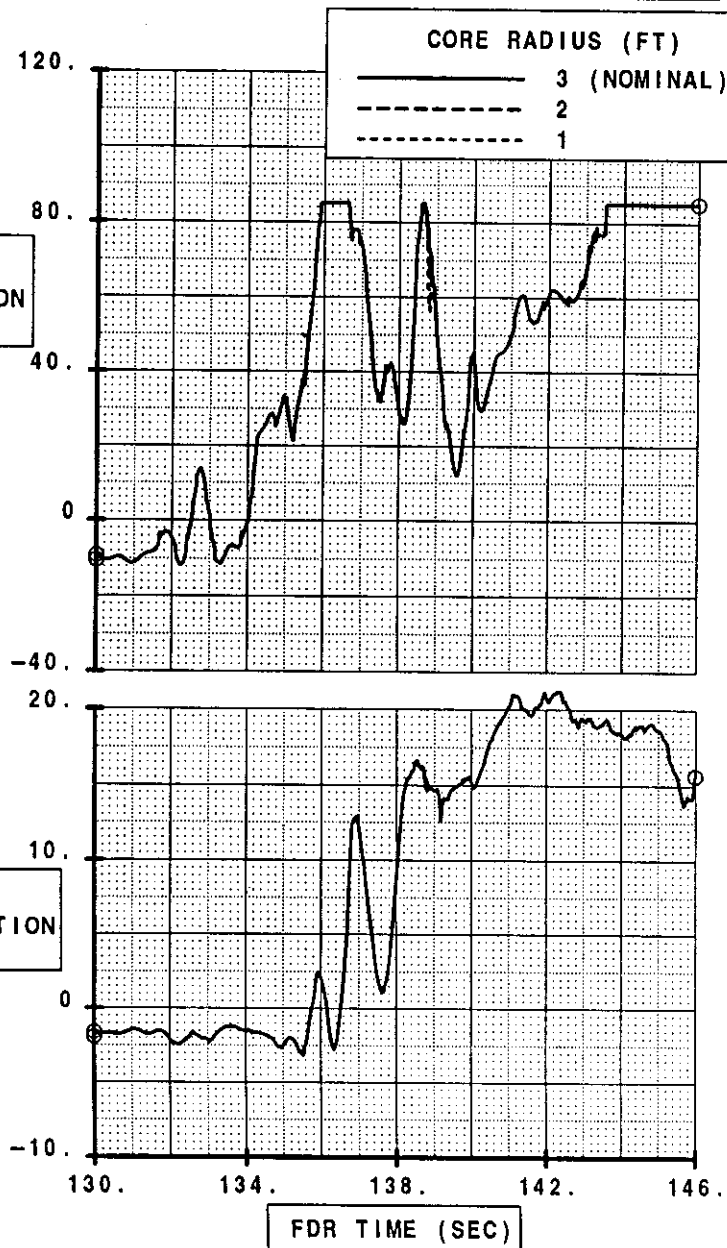
DECREASED WAKE STRENGTH



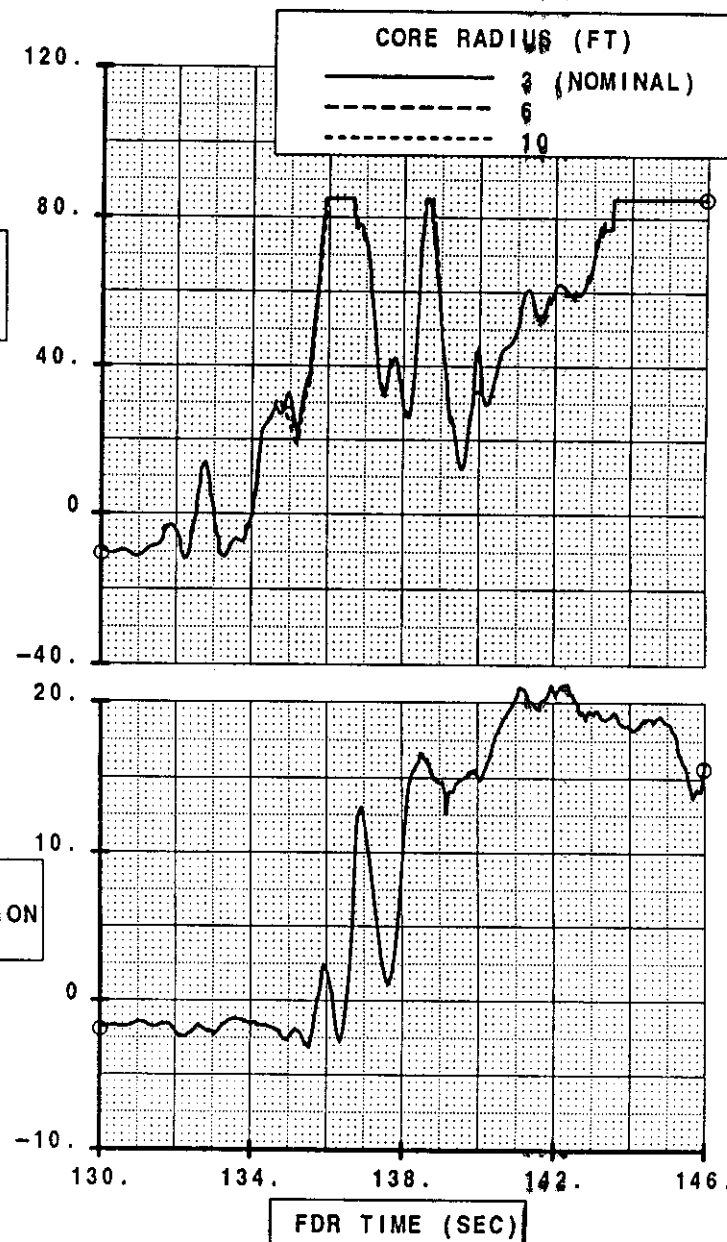
INCREASED WAKE STRENGTH



DECREASED CORE RADIUS



INCREASED CORE RADIUS



CALC J. WILBORN 22OCT96
 CHECK
 APPD
 APPD
 APPD

REVISED
 DATE

EFFECT OF WAKE CORE RADIUS ON DERIVED
 WHEEL AND RUDDER POSITION

FIGURE
 FS

APPENDIX G. Parametric Study of Derived Rudder Input

Data are presented in this section to quantify the effect of variations in the rudder position time-history for the USAir 427 scenario. Figure G-1 presents the rudder for best match of the FDR data as discussed in earlier sections of this document. Figures G-2 through G-7 present a series of arbitrary modifications to this derived rudder. Figures G-8 through G-16 present a series of simulated rudder PCU valve jams.

In all cases, the lateral control surfaces were driven to match the derived airplane roll acceleration to minimize deviation in roll attitude. The heading and pitch attitude parameters were allowed to respond freely to the rudder inputs.

The effects of these variations in rudder position are shown as incremental errors in airplane heading, pitch and roll attitude. The heading error is computed relative to the non-linear curve fit of the one-sample-per-second FDR data (See Appendix E). The time values of the actual FDR heading data points are indicated with symbols along the horizontal axis. The heading error should be evaluated at these time points in particular. The pitch and roll errors, which are of secondary interest only, are considered to be valid for all points along their respective curves because of the higher sample rate of the pitch and roll FDR data.

An IRU (Inertial Reference Unit) "Confidence Band" is also plotted along with the angular-error data to give proper perspective to the results. The indicated confidence level is based on a statistical survey of 737-300 flight test data. The survey covered all maneuver types, comprising 3328 flight conditions, for a total of 4.8 million data points. The outputs of the left and right IRU channels were compared after subtracting out any average offsets in the data. The remaining differences were then numerically ranked, point by point, showing that the left and right IRUs agree to within plus or minus 0.3 degrees for 99.96% of all surveyed data. Furthermore, 98% of the data points agree to within plus or minus 0.1 degree.

It may be reasonably stated, therefore, that failure of the heading error to stay within a plus or minus 0.3 degree confidence band, for any of the cases evaluated, constitutes a non-match of the FDR data. Judged on this basis, only the double-pulse rudder in Figure G-1 demonstrates an acceptable match. All other scenarios produce errors of at least one degree and, in most cases, much more.

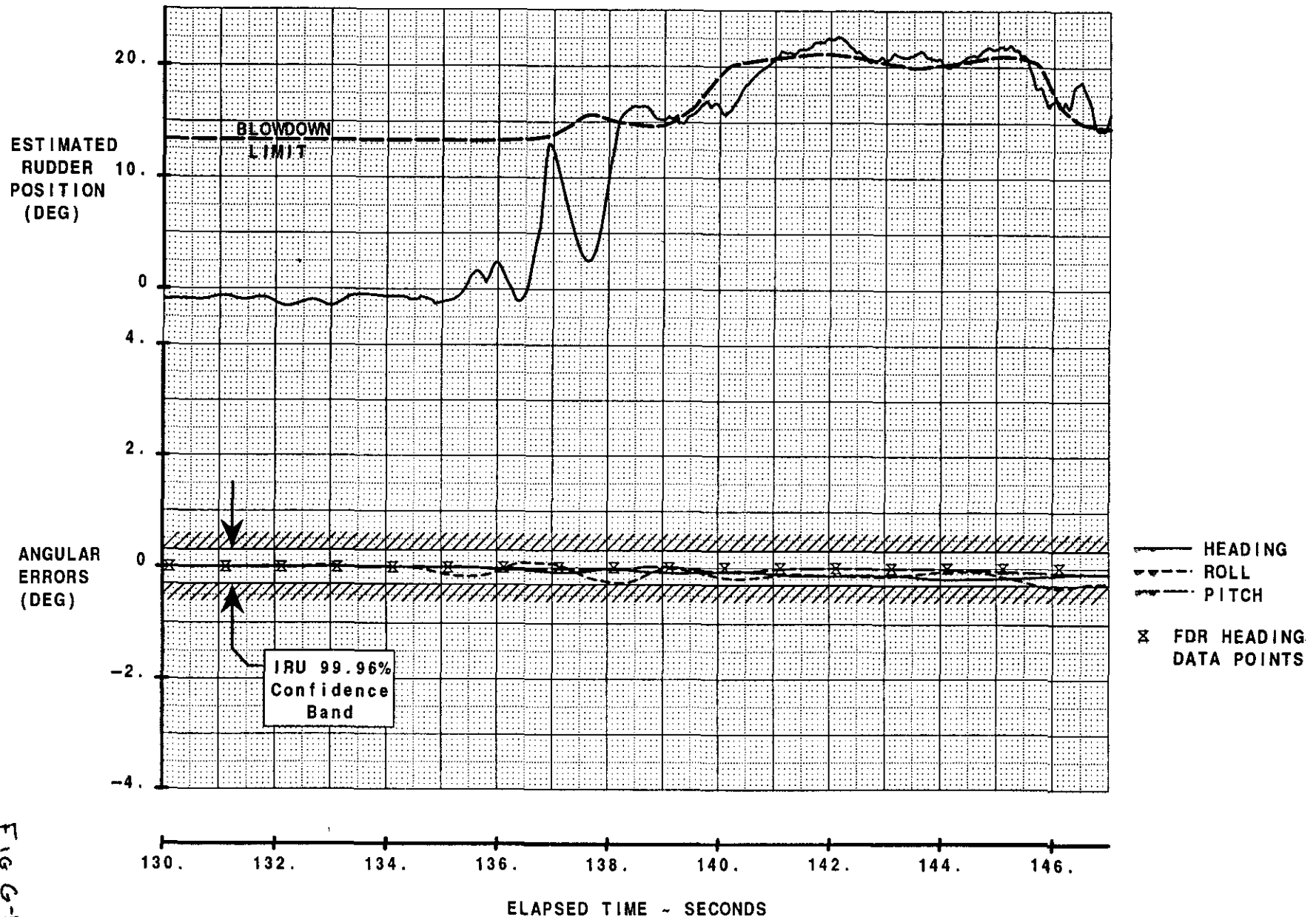
It should be noted here that the rudder derivations presented in References 1 and 2 also produced apparently acceptable matches of the FDR heading data. These early analyses were both lacking, however, in the following respects:

- The data in Reference 2 were based on a purely theoretical wake effects model. Subsequent wake-effects flight testing showed that the predicted nose-right, wake-induced yawing moment does not occur for an aircraft stationed above the right vortex core. Videotape evidence from the test suggests that the vortex core

dissipates rapidly as it passes beneath the aircraft in close proximity to the wing, thereby limiting its influence on the vertical tail. In addition, the current wake encounter scenario places the aircraft under the wake to achieve a substantially improved match of the wake-induced lift, compared to what was presented in May 1995. Placing the aircraft beneath the right vortex core can only result in a nose-left induced yaw. This completely invalidates the conclusions of Reference 2 with respect to the derived rudder position in the region where the aircraft is in the influence of the wake.

- The data in Reference 1 ignored the effect of the wake altogether and, most importantly, required periodic excursions of the rudder well beyond the rudder blowdown limit; a clearly impossible situation. Even so, that early derivation of the rudder showed much of the character of the initial double-pulse required to match the FDR data.

DOUBLE-PULSE RUDDER INPUT



ESTIMATED
RUDDER
POSITION
(DEG)

ANGULAR
ERRORS
(DEG)

IRU 99.96%
Confidence
Band

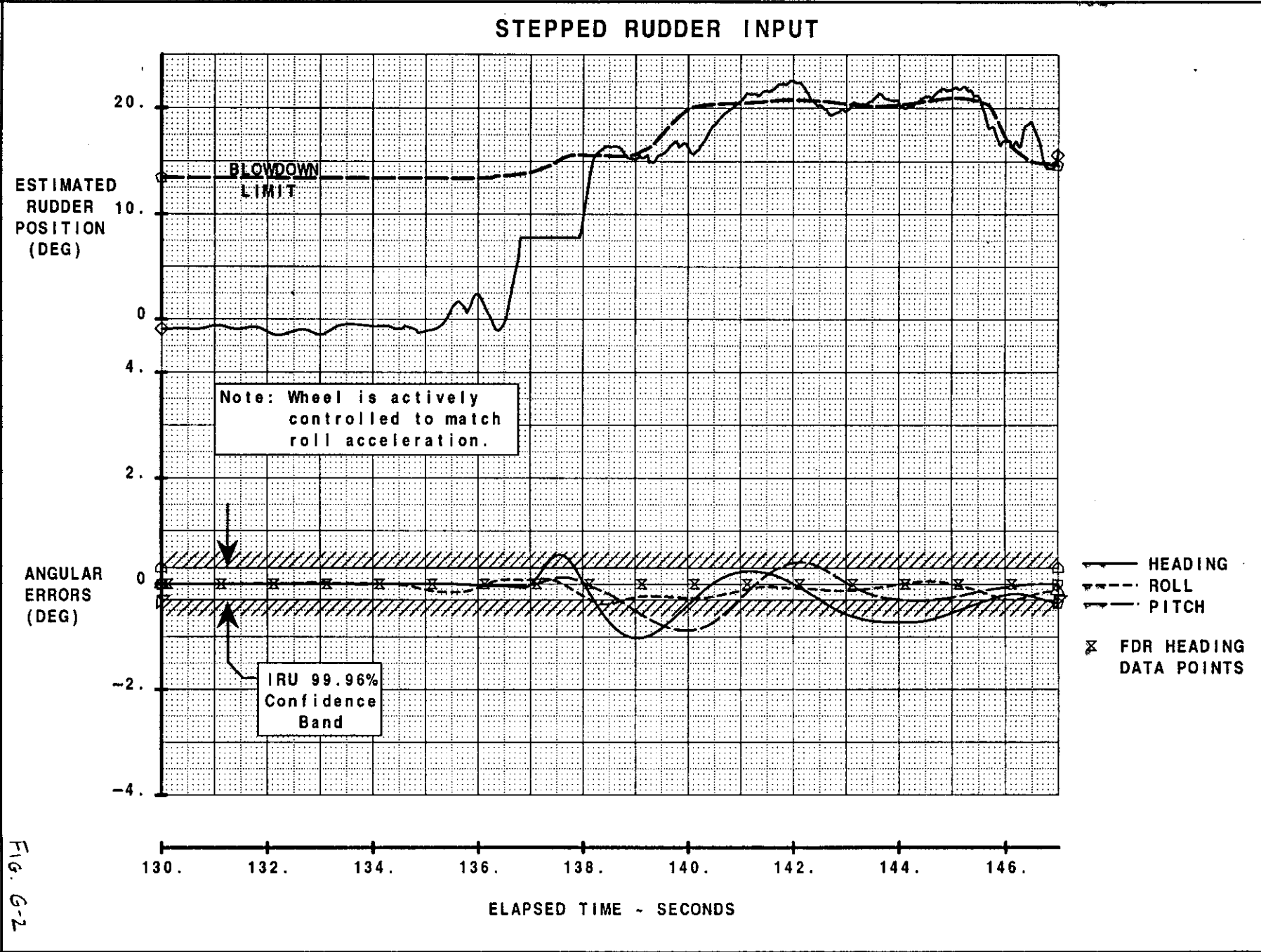
— HEADING
- - - ROLL
... PITCH
x FDR HEADING
DATA POINTS

ELAPSED TIME - SECONDS

FIG G-1

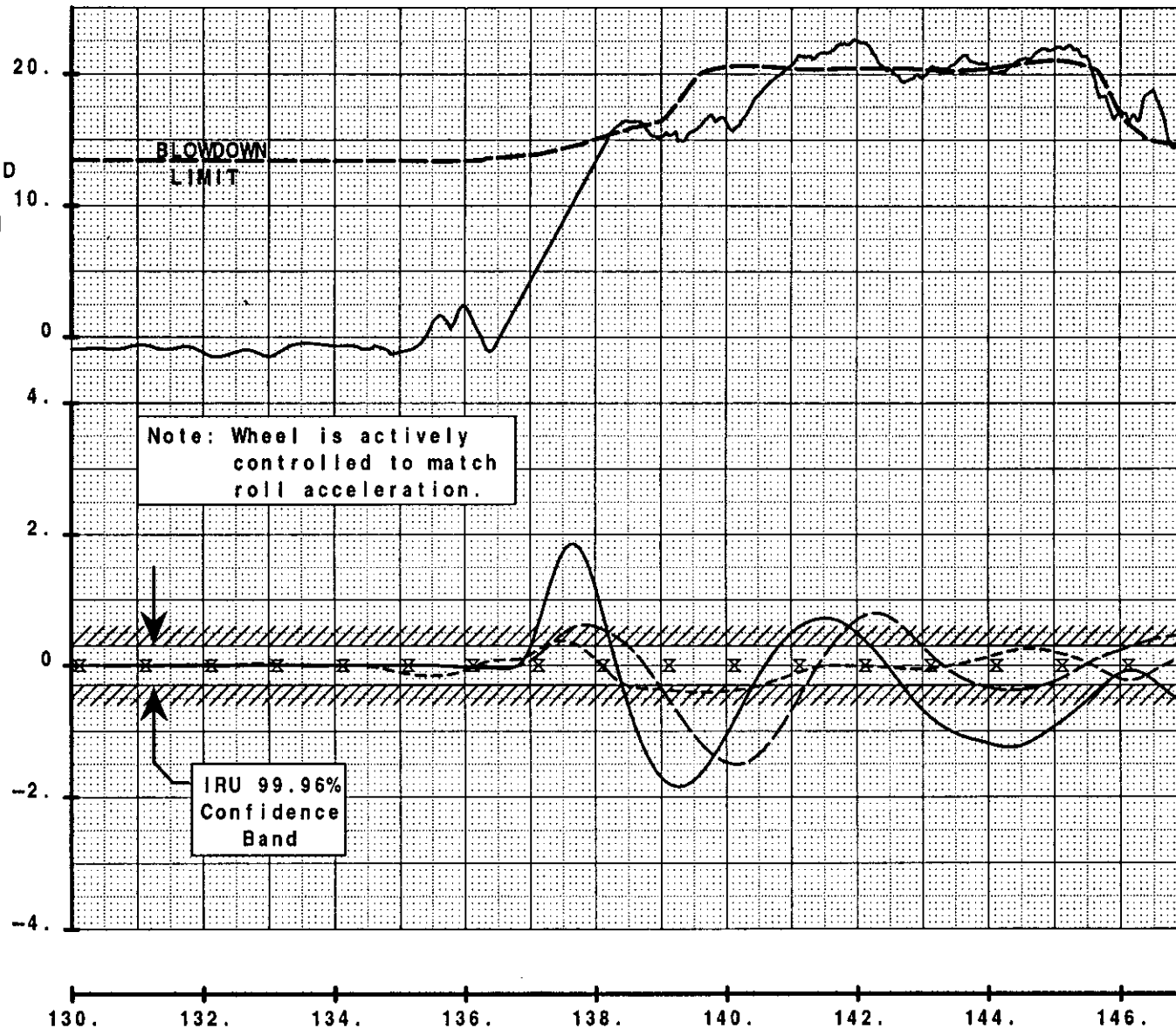
CALC	H. Dellicker	190CT96	REVISED	DATE	Effect of Modifications in Rudder Angle on Match of the USAir 427 FDR Data (Double Pulse Rudder Input)	
CHECK						
APR						
APR						
THE BOEING COMPANY					PAGE	737-300
						USAir 427

CALC	H. Dellinger	19OCT96	REVISED	DATE	Effect of Modifications in Rudder Angle on Match of the USAir 427 FDR Data (Stepped Rudder Input)	
CHECK						
APR						
APR						
THE BOEING COMPANY					USAir 427	PAGE



RAMPED RUDDER INPUT

ESTIMATED
RUDDER
POSITION
(DEG)



— HEADING
- - - ROLL
— PITCH
x FDR HEADING
DATA POINTS

FIG G-3

ELAPSED TIME - SECONDS

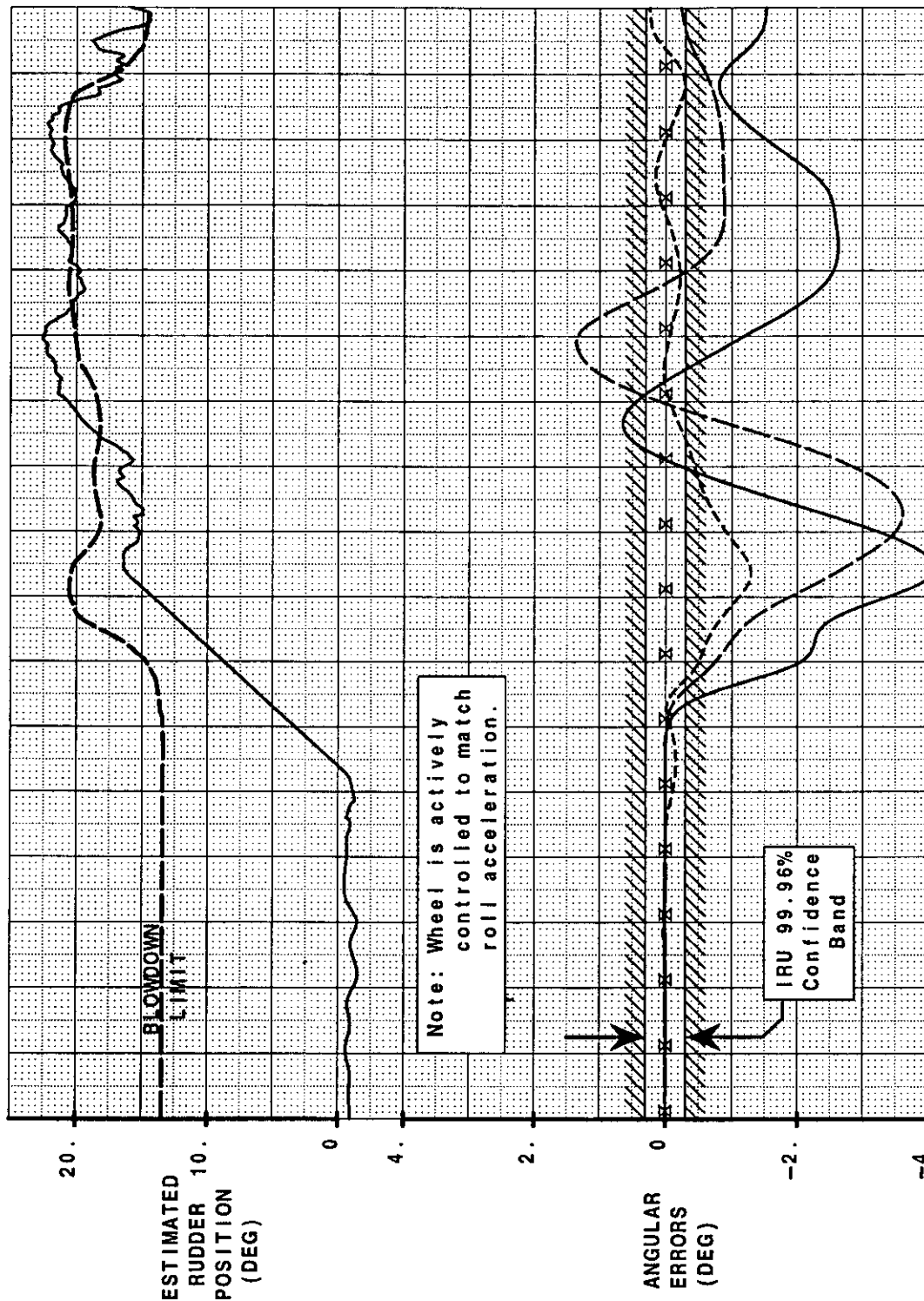
Effect of Modifications in Rudder Angle
on Match of the USAir 427 FDR Data
(Ramped Rudder Input)

THE BOEING COMPANY

737-300
USAir 427
PAGE

CALC H. Dellinger 190CT96
CHECK
APR
APR
APR
REVISED
DATE

SLOW RAMPED RUDDER INPUT



ELAPSED TIME - SECONDS

FIG. G-4

CALC	H. Dellicker	19OCT96	REVISED	DATE
CHECK				
APR				
APR				

Effect of Modifications in Rudder Angle
on Match of the USAir 427 FDR Data
(Slow Ramped Rudder Input)

THE BOEING COMPANY

737-300
USAir 427
PAGE

EARLY RAPID RUDDER INPUT

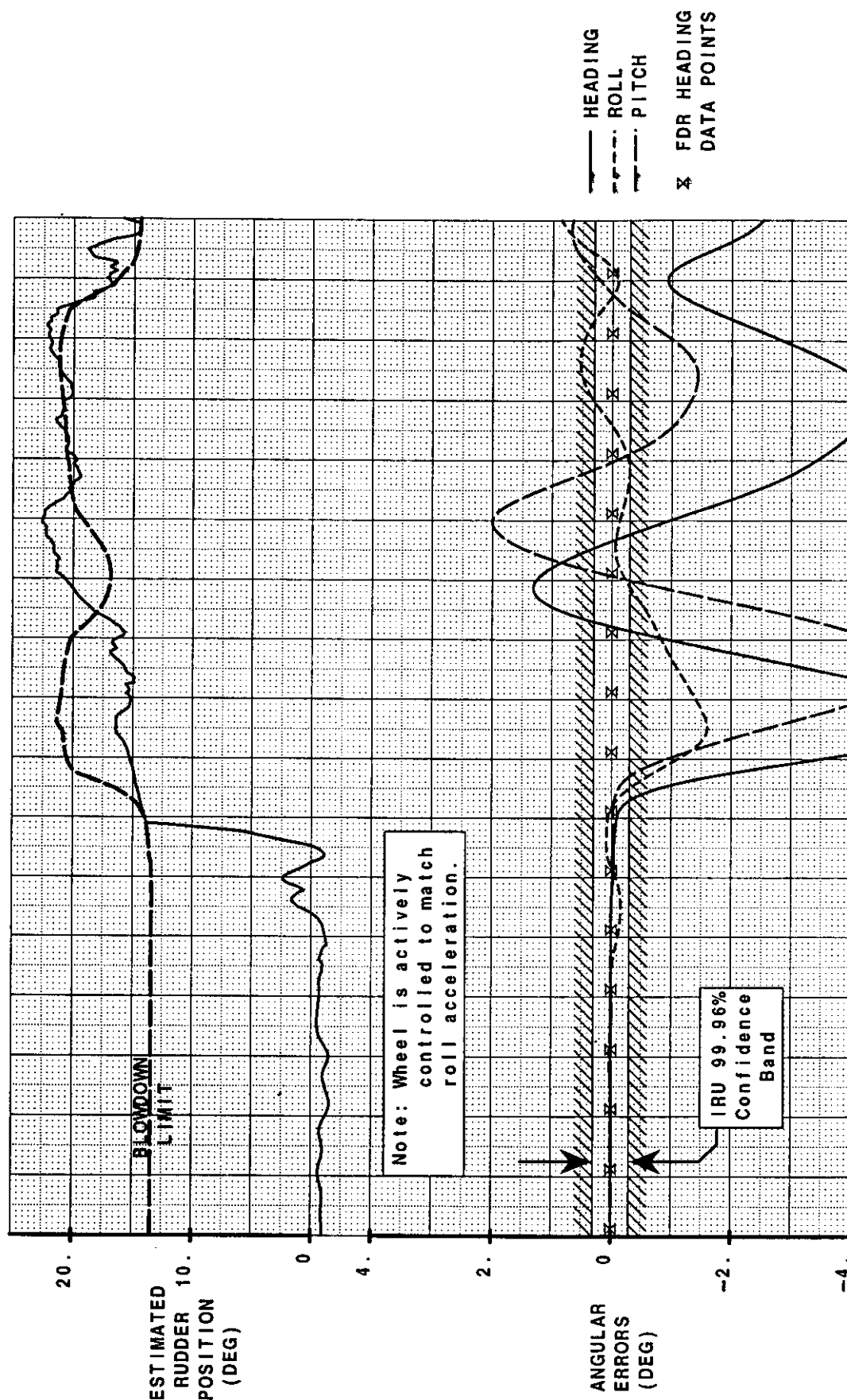


FIG. 6-5

CALC	H. Dellicker	19OCT96	REVISED	DATE	Effect of Modifications in Rudder Angle on Match of the USAir 427 FDR Data (Early Rapid Rudder Input)	737-300
CHECK						USAir 427
APR						
APR						
					THE BOEING COMPANY	PAGE

DELAYED RAPID RUDDER INPUT

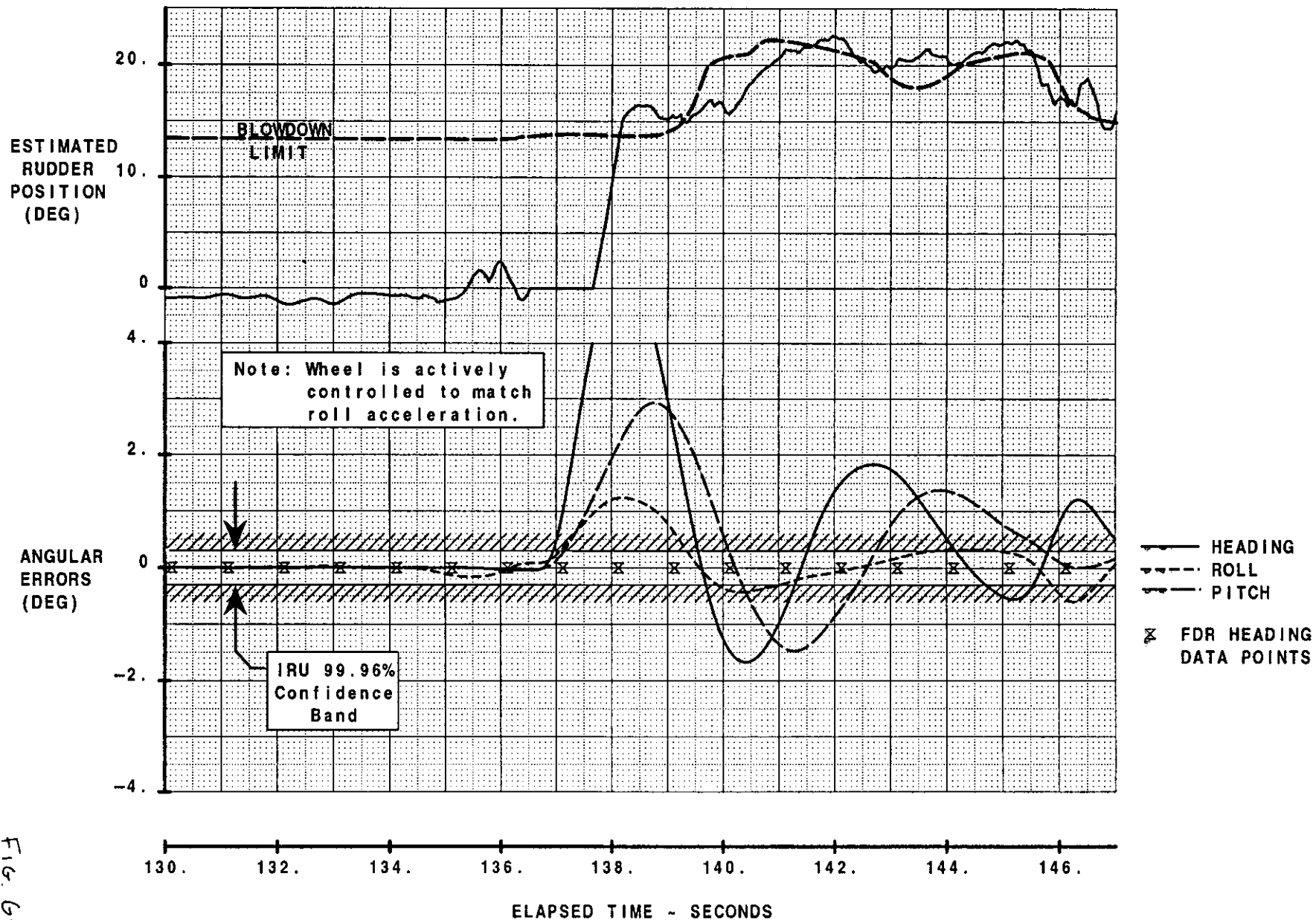


FIG. 6-6

Effect of Modifications in Rudder Angle
on Match of the USAir 427 FDR Data
(Delayed Rapid Rudder Input)

THE BOEING COMPANY

CALC	H. Dellinger	1900T96	REVISED	DATE
CHECK				
APR				
APR				

MID RAPID RUDDER INPUT

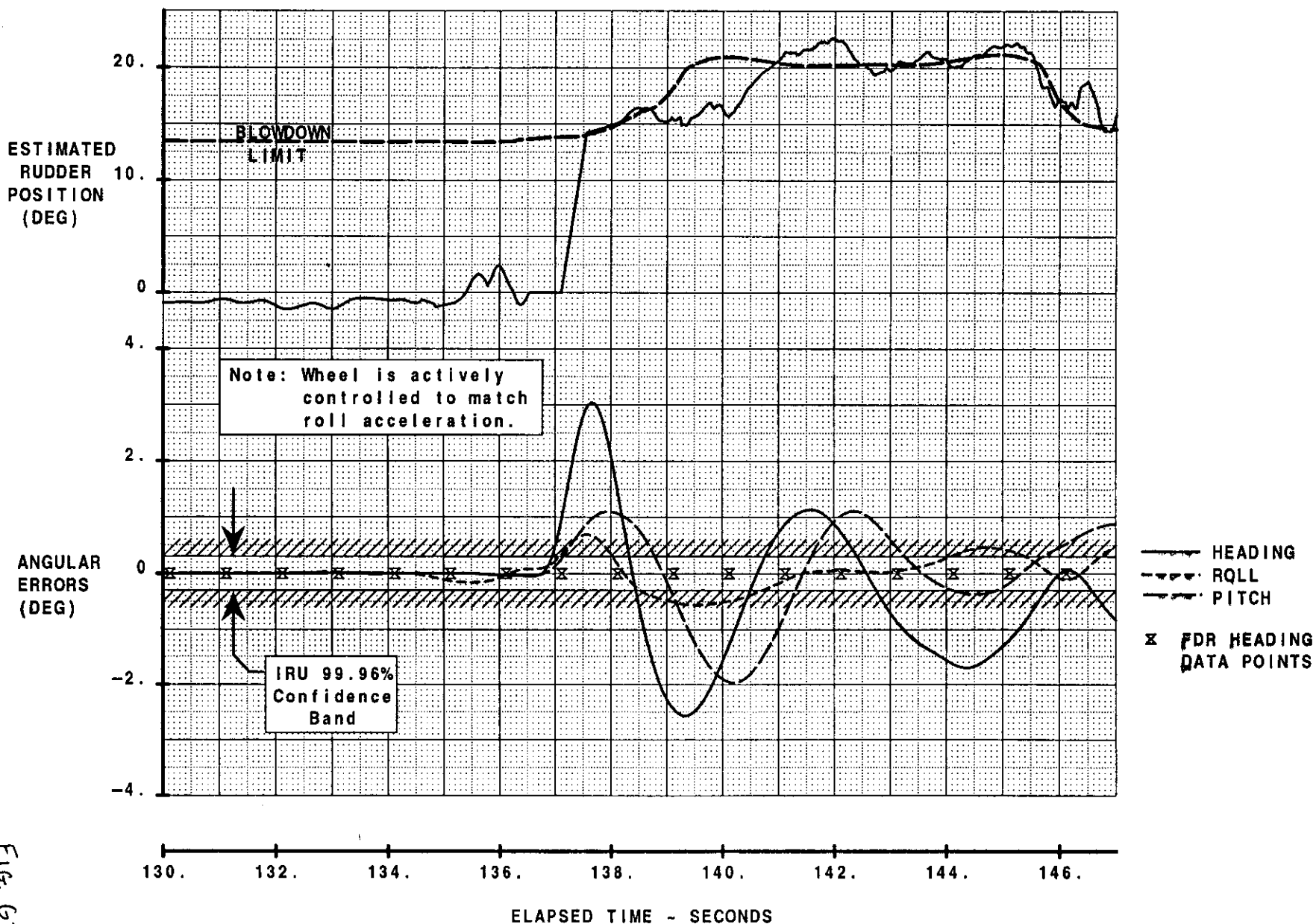
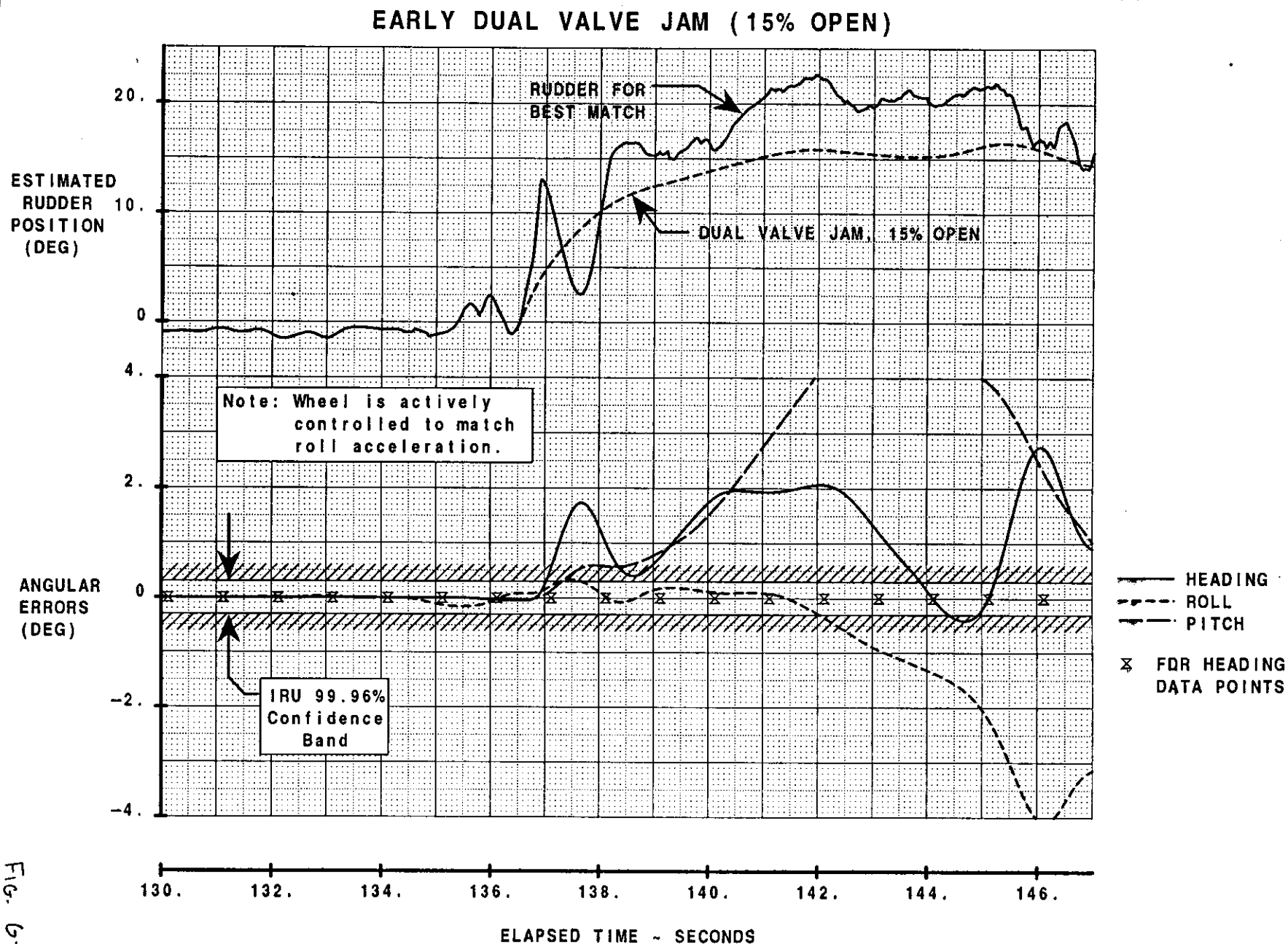


Fig. G-7

CALC	H. Dellicker	190CT96	REVISED	DATE	Effect of Modifications in Rudder Angle on Match of the USAir 427 FDR Data (Mid Rapid Rudder Input)		737-300
CHECK							
APR							USAir 427
APR							PAGE
THE BOEING COMPANY							

CALC	H. Dellinger	1906T96	REVISED	DATE	Effect of Modifications in Rudder Angle on Match of the USAir 427 FDR Data (Early Dual Valve Jam, 15% Open)	
CHECK						
APR						
APR						
THE BOEING COMPANY					PAGE	737-300
						USAir 427

FIG. 6-8



EARLY DUAL VALVE JAM (20% OPEN)

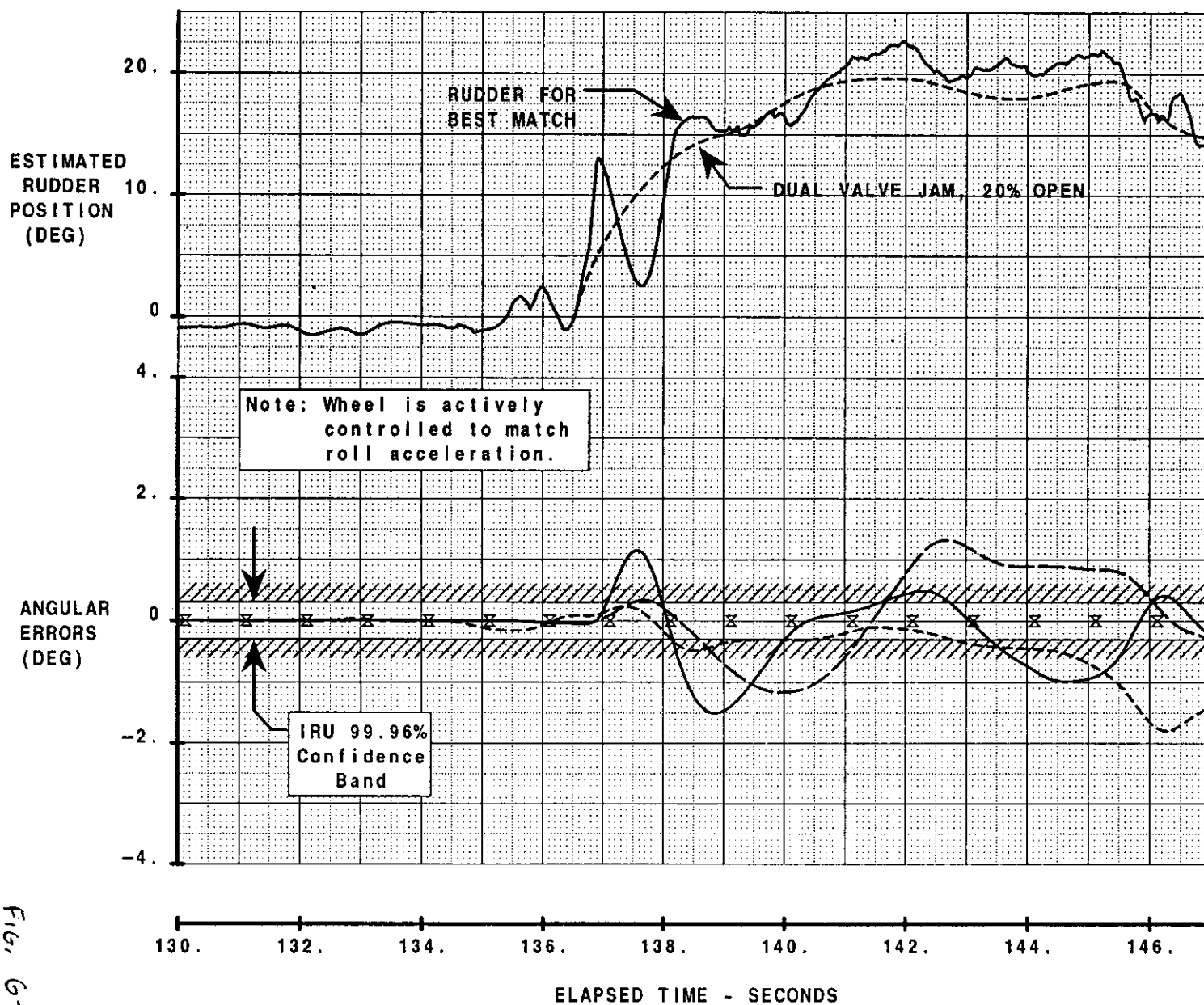


FIG. 6-9

CALC	H. Dellicker	190CT96	REVISED	DATE	Effect of Modifications in Rudder Angle on Match of the USAir 427 FDR Data (Early Dual Valve Jam; 20% Open)	
CHECK						
APR						
APR						
THE BOEING COMPANY					PAGE	737-300 USAir 427

EARLY DUAL VALVE JAM (50% OPEN)

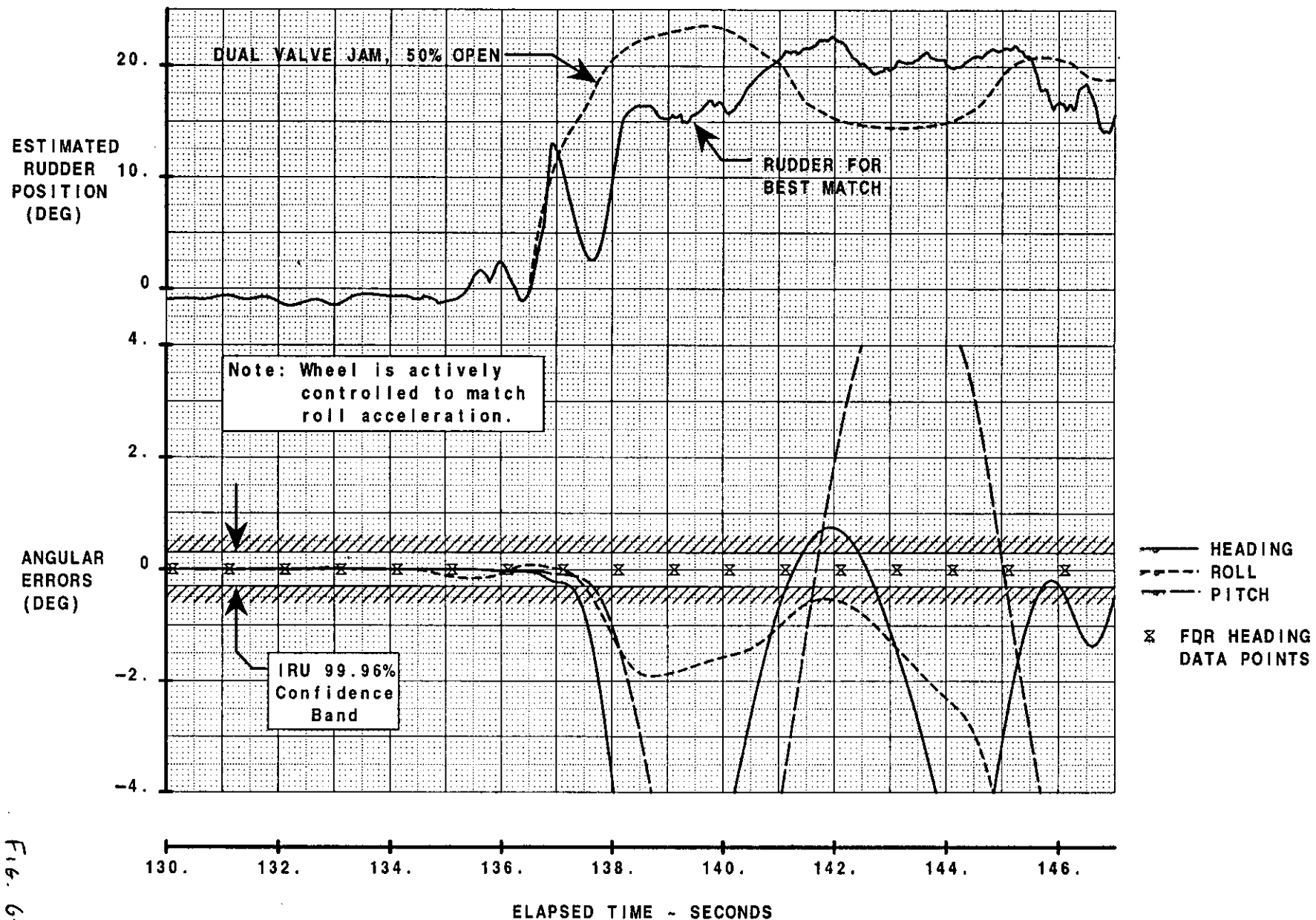


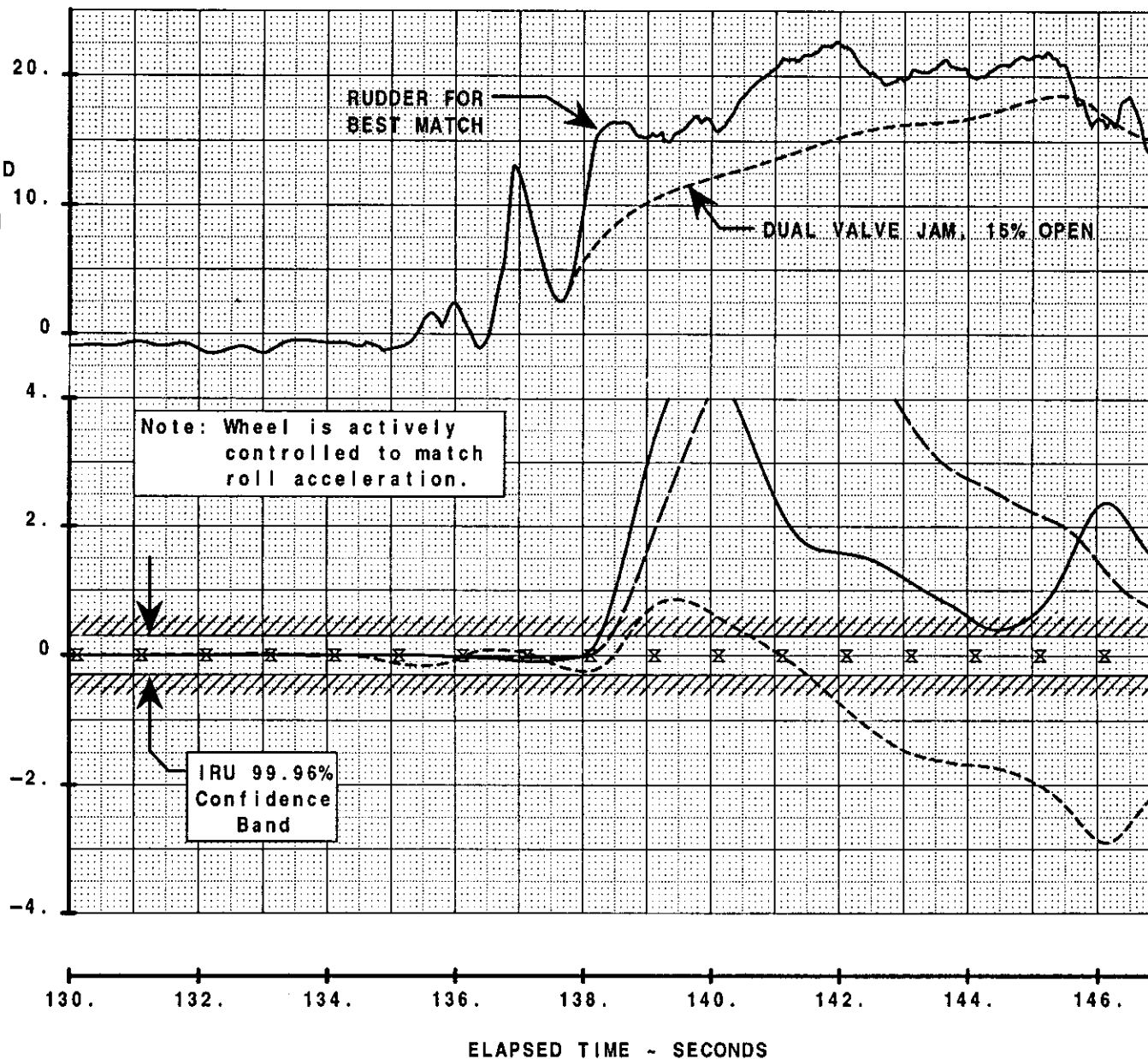
Fig. 6-11

CALC	H. Dellinger	190CT96	REVISED	DATE	Effect of Modifications in Rudder Angle on Match of the USAir 427 FDR Data (Early Dual Valve Jam; 50% Open)	
CHECK						
APR						
APR						
THE BOEING COMPANY					PAGE	737-300
						USAir 427

LATE DUAL VALVE JAM (15% OPEN)

ESTIMATED
RUDDER
POSITION
(DEG)

ANGULAR
ERRORS
(DEG)



— HEADING
- - - ROLL
... PITCH
x FDR HEADING
DATA POINTS

Fig 6-12

Effect of Modifications in Rudder Angle
on Match of the USAir 427 FDR Data
(Late Dual Valve Jam; 15% Open)

THE BOEING COMPANY

CALC H. Dellinger 190CT96
CHECK
APR
APR

REVISED
DATE

CALC	H. Dellicker	190CT96	REVISED	DATE	Effect of Modifications in Rudder Angle on Match of the USAir 427 FDR Data (Late Dual Valve Jam, 20% Open)	
CHECK						
APR						
APR						
THE BOEING COMPANY					PAGE	737-300
						USAir 427

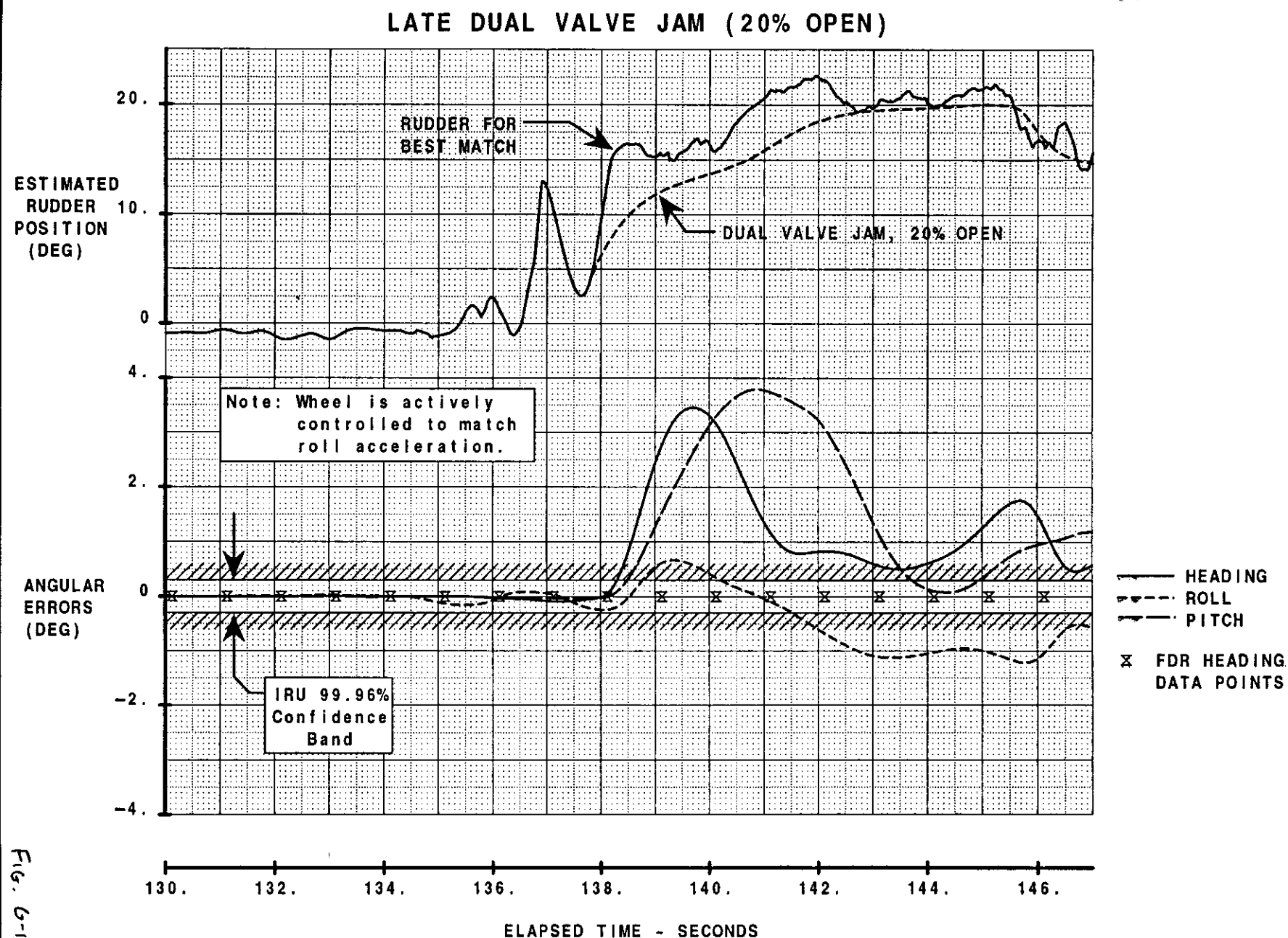


Fig. 6-13

LATE DUAL VALVE JAM (25% OPEN)

ESTIMATED
RUDDER
POSITION
(DEG)

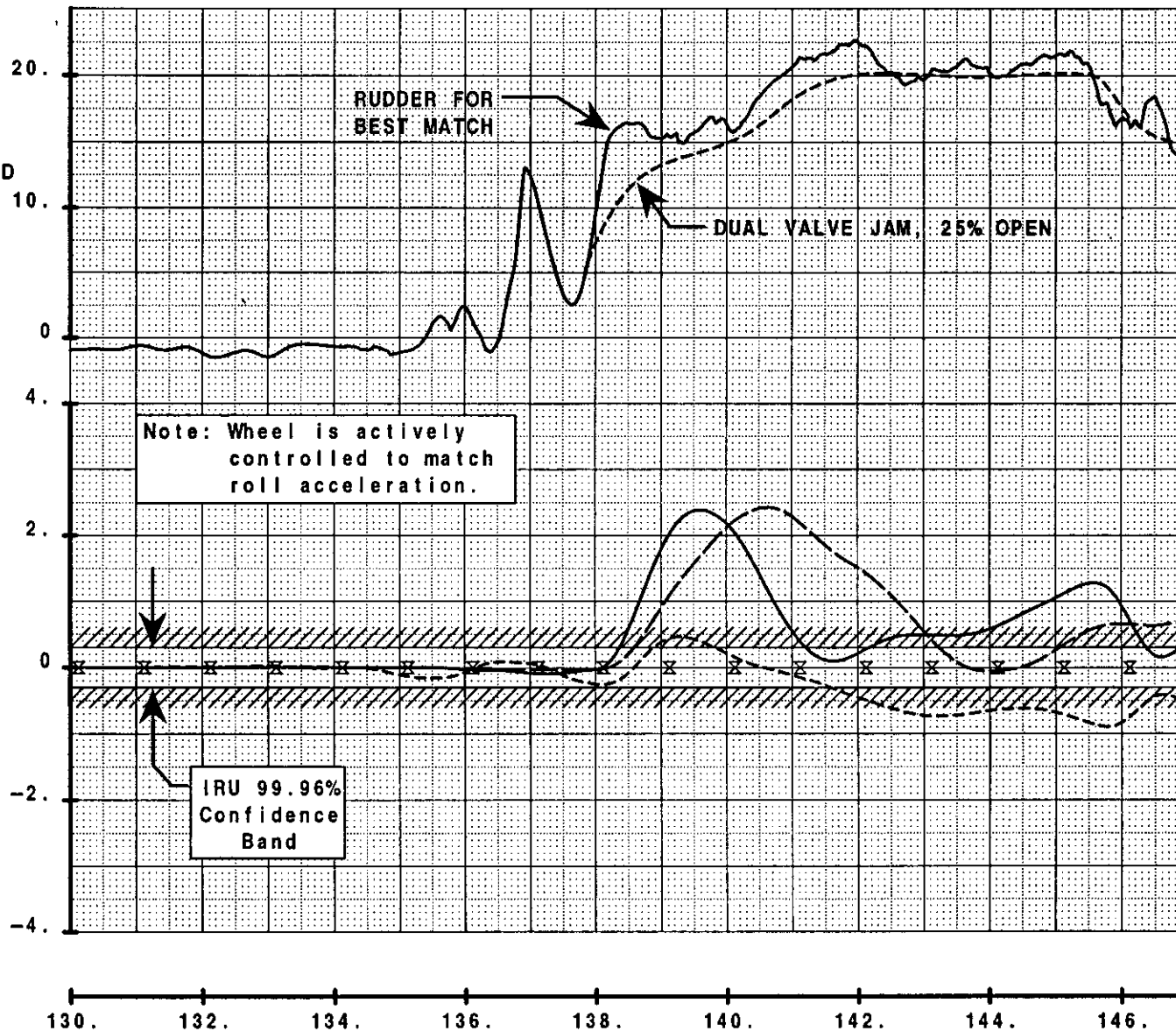


Fig. 6-14

Effect of Modifications in Rudder Angle

on Match of the USAir 427 FDR Data

(Late Dual Valve Jam, 25% Open)

THE BOEING COMPANY

737-300

USAir 427

PAGE

CALC H. Deilicker 190CT96

REVISED

DATE

CHECK

APR

APR

LATE DUAL VALVE JAM (35% OPEN)

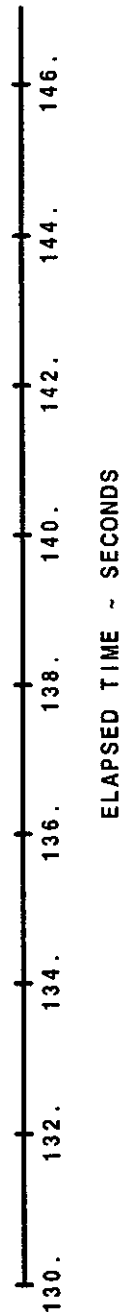
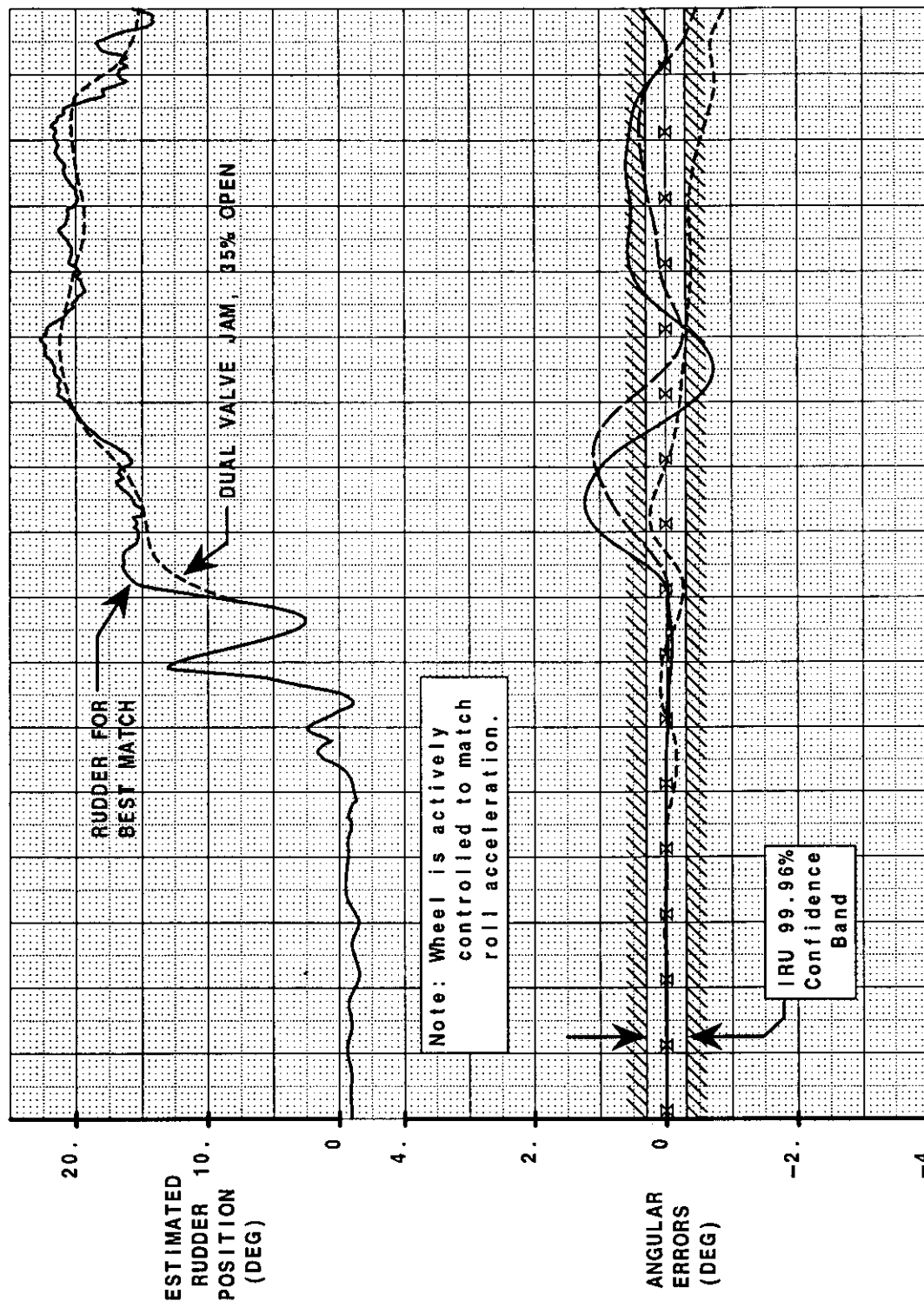


FIG G-15

CALC	H. Dellicker	19OCT96	REVISED	DATE
CHECK				
APR				
APR				

Effect of Modifications in Rudder Angle
on Match of the USAir 427 FDR Data
(Late Dual Valve Jam; 35% Open)

THE BOEING COMPANY

737-300
USAir 427
PAGE

LATE DUAL VALVE JAM (60% OPEN)

ESTIMATED
RUDDER
POSITION
(DEG)

ANGULAR
ERRORS
(DEG)

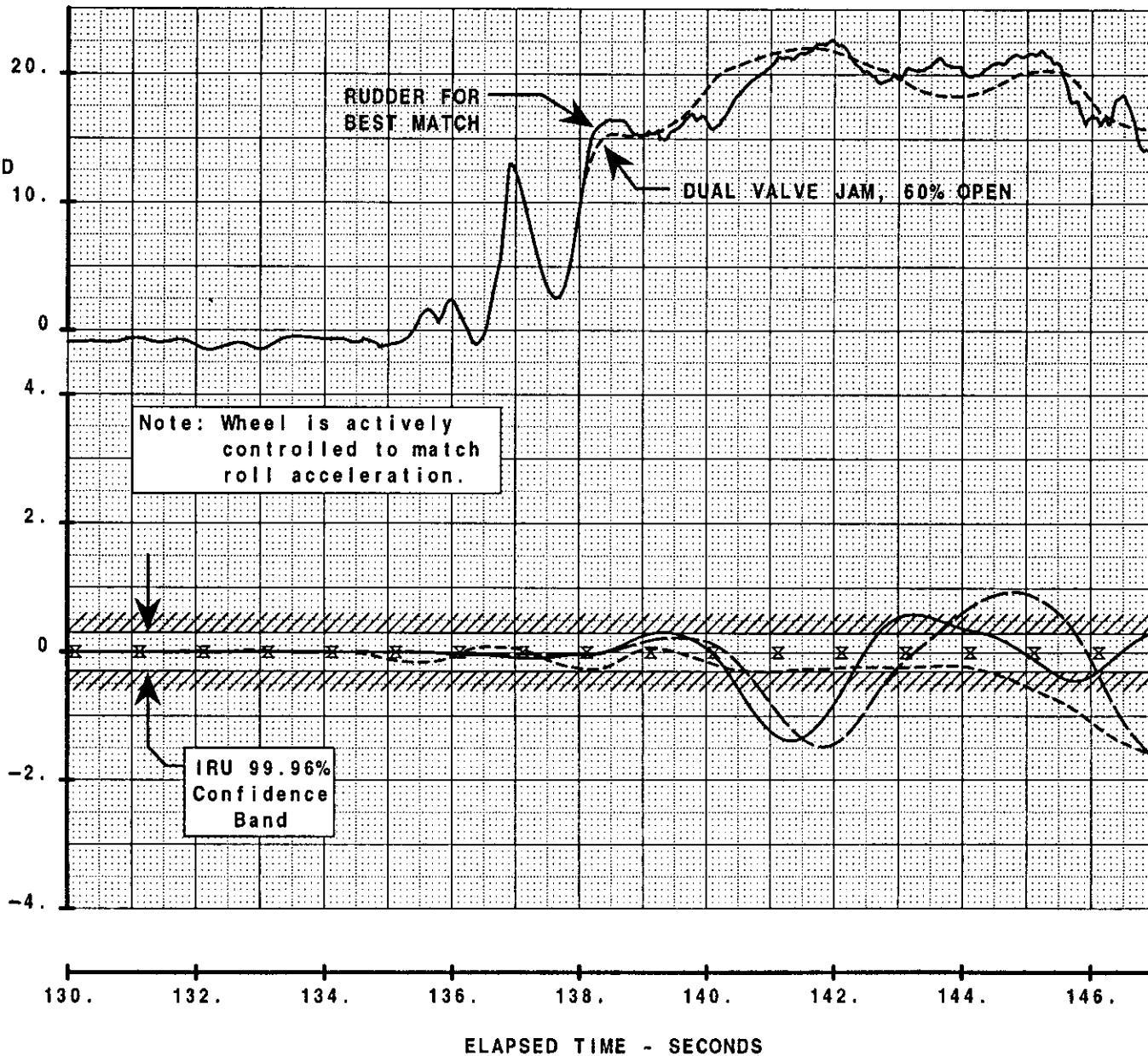


FIG. 6-16

CALC	H. Dellicker	190CT96	REVISED	DATE	Effect of Modifications in Rudder Angle on Match of the USAir 427 FDR Data (Late Dual Valve Jam; 60% Open)	THE BOEING COMPANY	737-300
CHECK							USAir 427
APR							
APR							
							PAGE